

Eli Enes, Åsmund Nordskog and Olav Torsvik

BESS (LiC) for regulation of wind and solar energy

Optimizing wind and solar energy with regard to power, voltage and frequency quality

Bachelor's thesis in Renewable Energy

Supervisor: Odne Stokke Burheim

Co-supervisor: Simon Birger Byremo Solberg

May 2022

Eli Enes, Åsmund Nordskog and Olav Torsvik

BESS (LiC) for regulation of wind and solar energy

Optimizing wind and solar energy with regard to power, voltage and frequency quality

Bachelor's thesis in Renewable Energy
Supervisor: Odne Stokke Burheim
Co-supervisor: Simon Birger Byremo Solberg
May 2022

Norwegian University of Science and Technology
Faculty of Engineering
Department of Energy and Process Engineering



NTNU

Kunnskap for en bedre verden



Department of Energy-
and Process Engineering

Bachelor thesis

Project title: BESS (LiC) for regulation of wind and solar energy	Given date: 13.01.2022
Prosjekttittel (NOR): BESS (LiC) for regulering av vind- og solenergi	Date to deliver: 20.05.2022
Group participants: Eli Enes Åsmund Nordskog Olav Torsvik	Number of pages/appendix: 61/9
Company: Beyonder	Supervisors: Odne Stokke Burheim Simon Birger Byremo Solberg
	Project number: 22BIFOREN-002
	Company contact: Anne Aspelund Pedersen Belissa Husanovic Omar Nahem Shagouri Øystein Tvedten

Freely available

Available after agreement with employer

Report released after

Eli Enes

Åsmund Nordskog

Olav Torsvik

Preface

The increasing implementation of intermittent renewable energy sources is causing disturbances in the grid which can lead to severe impacts on the power systems. Companies, such as Beyonder, are developing a technology capable of handling rapid power fluctuations and improving the power quality. Since the technology is relatively new, there is an imminent need for evaluating its performance before it is implemented in large scale applications.

This bachelor thesis is written by the three students; Eli Enes, Åsmund Nordskog and Olav Torsvik. It was conducted at the Department of Energy and Process Engineering at the Norwegian University of Science and Technology in the spring semester 2022 and concluded 20.05.2022. The project description was provided by Beyonder. The bachelor thesis is the final part of the three year study program *Bachelor in Engineering, Renewable Energy*.

Guidance and supervision have been provided by various people throughout the process of this bachelor thesis. In that regard we would like to extend our gratitude to our supervisors at NTNU, Odne Stokke Burheim and Simon Birger Byremo Solberg, for guidance and support throughout the process. We also want to thank our external supervisors from Beyonder, Anne Aspelund Pedersen, Øystein Tvedten, Belissa Husanovic and Omar Nahem Shagouri, for providing essential information and guidance through the whole of the thesis. In addition we wish to thank Stein Olav Kjerland at Agder Energi for providing relevant information and consultation during the project.



Abstract

With the increasing implementation of renewable energy sources in the grid, there is a clear need for a technology capable of handling the rapid power variations associated with these. Beyonder has developed a new high power lithium-ion capacitor produced in a sustainable manner. As the introduction of large scale intermittent renewable energy sources increases, the belonging power fluctuations can result in voltage and frequency deviations. Such deviations can have a severe impact on the power system and the security of delivery.

In order to investigate the lithium-ion capacitor, or LiC's, ability to improve the power quality associated with production from wind and solar power, three case studies were built. A system, consisting of several LiC cells connected in series and parallel, was tried implemented in a full scale wind power plant, a solar power plant, and in a solar power plant already containing a lithium-ion battery (LiB) used for energy shifting. In order to perform simulations of these systems, the software Simulink was used. The simulated systems was built up of constructions of a LiC and LiB, high resolution input signals, battery energy storage system (BESS) controllers and cycle counters. The capacity of the LiC for the different applications was determined by factors such as the energy demand, C-rate and the cycle life time.

All things considered the LiC had a beneficial impact on the wind and solar power cases. The results showed that if dimensioned and controlled properly, an improved power, voltage and frequency quality could be obtained. In these two cases it was found that the added benefits justified the investment cost. The implementation led to an improved utilization of the energy which furthermore led to the possibility of increased penetration of intermittent renewable energy systems, IRES. When assessing the integration of LiC in an energy shifting scenario, it was not evident that the beneficial impact would outweigh the investment cost. Even though the implementation contributed to a longer LiB lifetime, by presenting a more beneficial charge and discharge characteristic. However, the economical results from the two prior case studies pointed to the fact the the LiC technology is economically sustainable, with an investment cost corresponding to only 0.7% of that of a wind power plant. Additionally Beyonder's LiC has a low footprint considering that it is made using ecological materials and have a material production supported by a Norwegian power mix.

Sammendrag

På grunn av den økte implementeringen av fornybare energikilder i nettet, er det et klart behov for en teknologi som kan håndtere de assosierte effekt-svingningene. Beyonder har utviklet en høyeffekt lithium-ione kondensator som er produsert på en bærekraftig måte. Ettersom introduksjonen av storskala uregulerbare fornybare energikilder i nettet øker, kan de tilhørende effektsvingningene føre til spenning,- og frekvensavvik. Slike avvik kan ha betydelige innvirkninger på kraftsystemer og leveringssikkerheten.

Tre casestudier ble laget for å undersøke LiCens evne til å forbedre effektkvaliteten assosiert med produksjonen fra vind- og solenergi. Et system, konstruert av flere LiC-celler koblet sammen i serie og parallell, ble forsøkt implementert i en fullskala vind og solpark, i tillegg til en solpark som allerede inneholdt en LiB brukt til energiskifting. For å utføre simuleringer av de ulike systemene ble programvaren Simulink brukt. De simulerte systemene ble bygd opp av konstruksjoner av en LiC og en LiB, input signaler med høy oppløsning, batteri kontrollerer og syklustellerer. Kapasiteten til LiC-systemet for de ulike applikasjonene ble bestemt ut ifra faktorer som blandt annet energibehov, C-rate og levetid.

Alt i alt hadde implementeringen av LiCen en positiv effekt i vind,- og solparken. Resultatene viste at en forbedring i effekt,- spenning- og frekvenskvalitet kunne oppnås om LiCen ble dimensjonert og kontrollert på riktig måte. I disse to casene viste resultatene at investeringen kunne rettferdiggjøres. Implementeringen førte til et bedre energiforbruk og tilrettela for større implementering av fornybare energikilder i nettet. Med tanke på energiskifting senarioet var det usikkert om resultatene fra implementeringen av LiC var tilstrekkelige med tanke på investeringskostnaden, selv om LiB levetiden ble forbedret grunnet en mer hensiktsmessig ladingskarakterestikk. På den andre siden pekte resultatene fra de to andre casene på at investeringen var økonomisk bærekraftig, med en investeringskostnad på kun 0.7% sammenlignet med en hel vindpark. I tillegg er Beyonder sin LiC bærekraftig med tanke på at den produseres av økologiske materialer og at produksjonen skjer i Norge hvor vannkraft er dominerende.

Contents

- Preface** **i**

- Symbol List** **vii**

- Term List** **viii**

- Abbreviations** **ix**

- List of Figures** **x**

- List of Tables** **xii**

- 1 Introduction** **1**
 - 1.1 Problem to be addressed 2

- 2 Market Demand** **3**
 - 2.1 Energy demand and production 3
 - 2.2 The future situation 4
 - 2.3 The intermittent nature of wind and solar power 4
 - 2.3.1 Stabilizing power output 5
 - 2.3.2 Energy shifting 6
 - 2.4 Other applications for a lithium-ion capacitor 7
 - 2.5 Economy and sustainability 7

- 3 Case Study** **9**
 - 3.1 Case 1; Wind power plant 9
 - 3.2 Case 2; Solar power plant 11
 - 3.3 Case 3; Energy shifting-system in solar power plant 13

- 4 Theory** **14**
 - 4.1 Reliability of supply: power, voltage, and frequency 14
 - 4.1.1 Energy security and power quality 14
 - 4.1.2 Voltage quality 15
 - 4.1.3 Frequency 17
 - 4.1.4 The benefit of energy storage 19
 - 4.2 Lithium-ion capacitor generation 3 19
 - 4.2.1 Construction 20
 - 4.2.2 Performance 24
 - 4.3 Similar technologies 26
 - 4.3.1 Lithium-ion batteries 26
 - 4.3.2 Supercapacitor 27
 - 4.3.3 STATCOM 27
 - 4.3.4 Technical comparison 28
 - 4.4 Controlling and dimensioning of energy storage 30

5	Simulation Methodology	32
5.1	Software	32
5.2	Assumptions	32
5.3	Design of battery energy storage system	33
5.3.1	Lithium-ion capacitor	33
5.3.2	Lithium ion battery	35
5.3.3	High resolution power input signal	35
5.3.4	BESS controller	36
5.3.5	Cycle counter	37
5.4	LiC integrated in renewable energy production plant	39
5.5	LiC integrated in energy shifting-system for a solar power plant	39
5.5.1	Creating a reference system, LiB in solar	40
6	Results and Discussion	42
6.1	Design of BESS	42
6.1.1	Design and dimensioning process	42
6.2	LiC integrated in renewable energy production plant	44
6.2.1	Wind power plant	44
6.2.2	Solar power plant	47
6.2.3	Energy shifting-system (solar power plant)	50
6.3	Improving power quality	54
6.4	IRES penetration	55
6.5	Economical aspects	56
6.6	Sustainability and footprint	58
6.6.1	Exclusion of critical materials	58
6.6.2	Reduced CO ₂ emissions	58
6.6.3	Geographical production area	58
6.7	Limitations and future work	60
7	Conclusion	61
	Bibliography	62
	Appendix	I
A	Data from Beyond	I
A.1	Datasheet LiC Gen. 3	I
A.2	Excel spreadsheet for connecting cells	II
A.3	Excel spreadsheet for connecting cells w/ functions	III
B	MATLAB Scripts	IV
B.1	BESS-controller wind/solar power plant	IV
B.2	BESS-controller energy shifting-system	V
B.3	Cycle counter	VI
B.4	Calculation of reduction in fluctuations	VII

C Simulations in Simulink **VIII**

C.1 LiC integrated in wind/solar park **VIII**

C.2 LiC integrated in energy shifting-system **IX**

Symbol List

Symbol	Definition	Unit
C	Capacitance	[F]
I	Current	[A]
I_{SS}	Current from storage system	[A]
k	Window Size	[-]
P	Power	[W]
P_{avg}	Average power	[W]
P_{loss}	Loss of power	[W]
P_{SS}	Power from storage system	[W]
Q	Reactive power	[VAR]
Q	Capacity	[Ah]/[Wh]
R	Resistance	[Ω]
R_C	Ohmic resistance in a conductor	[Ω]
$R_{equivalent}$	Equivalent resistance	[Ω]
U	Voltage	[V]
U_G	Grid voltage	[V]
$U_{nominal}$	Nominal voltage	[V]
U_{PCC}	Voltage at the point of common coupling	[V]
V	Cell Potential	[V]
X	Reactance	[Ω]
Z	Impedance	[Ω]
Δ	Difference between end and start value	[-]
Σ	Summation	[-]

Term List

Term	Definition
Auxiliary power	Electric power supplied by alternating source.
Auxiliary transformer	Component used to supply low voltage for alternating current power systems.
Calendar ageing	All aging processes that lead to a degradation of a battery cell independent of charge-discharge cycling.
Capacitor	Component which has the ability to store energy in the form of an electrical charge.
Capacity factor	The actual energy production divided by the maximum possible energy output.
Charge transfer resistance	Measure of the difficulty encountered when an electron is shifted from one atom or compound to another atom or compound.
Coulomb counting	Technique used to track the State of Charge of a battery pack.
C-rate	The rate of time in which it takes to charge or discharge.
Cycle ageing	Degradation of a battery cell during charge and discharge cycles.
Cycle stability	The number of charging- or discharging cycles until its capacity is reduced to a certain amount.
Distribution grid	The final stage of the electrical grid which distributes electricity to homes, industry, and other end users.
Energy shifting	Shifting produced energy to match the grid demand.
Intercalation	Reversible inclusion or insertion of a molecule (or ion) into layered materials with layered structures
Kalman filtering	An algorithm that uses a series of measurements observed over time and produces estimates of unknown variables.
Operational security	Capacity of power supply system to withstand disturbances
Park pilot	Aggregates turbine controllers into one wind power plant controller, providing only one interface to the TSO.
Power quality	A set of boundaries that allows electrical systems to function in their intended manner. Power quality concerns the deviation of the voltage waveform from the ideal sinusoidal voltage of constant magnitude and constant frequency.
Solar irradiation	The power per unit area received from the Sun in the form of electromagnetic radiation.
Steady state	A state or condition of a system or process that does not change in time.
Thermal runaway	A phenomenon in which the lithium-ion cell enters an uncontrollable, self-heating state.
Viscosity	The resistance of a fluid to a change in shape or movement of neighbouring portions relative to one another.

Abbreviations

Abbreviation	Definition
AC	Activated Carbon
BESS	Battery Energy Storage System
BEV	Battery Electric Vehicle
CAES	Compressed Air Energy Storage
DOD	Depth Of Discharge
EDLC	Electric Double Layer Capacitor
ESD	Energy Storage Device
ESR	Equivalent Series Resistance
EU	European Union
EV	Electric Vehicle
HEV	Hybrid Electric Vehicle
IEEE	Institute of Electrical and Electronics Engineers
IRE	Intermittent Renewable Energy
IRES	Intermittent Renewable Energy Sources
LFP	Lithium Iron Phosphate battery
LiB	Lithium-Ion Battery
LiC	Lithium-Ion Capacitor
LTO	Lithium Titanium Oxide
NMC	Nickel Manganese Cobalt battery
OCV	Open-Circuit Voltage
PV	Photo Voltaic
RES	Renewable Energy System
SAC	Super Activated Carbon
SC	Supercapacitor
SEI	Solid Electrolyte Interphase
SMA	Simple Moving Average
SOC	State Of Charge
SOH	State Of Health
SRAM	Static Random-Access Memory
STATCOM	Static Synchronous Compensator
TCO	Total Cost of Ownership
TSO	Transmission System Operator

List of Figures

2.1	Forecast of the final energy demand divided into different energy carriers, up until 2050[10]	4
2.2	Energy transition outlook for electricity sources until the year of 2050 [11]	5
2.3	Time-shift benefits of energy storage, showing the possibility of energy shifting [13]	6
3.1	The setup at Lista renewable energy park containing 31 wind turbines divided into four groups. The electricity passes through a transformer before it enters the regional grid [20]	9
3.2	Wind speed and power production from a single 2.3 MW wind turbine during one day [20]	10
3.3	Wind speed and power production from a single 2.3 MW wind turbine during one hour [20]	10
3.4	Three-phase voltage amplitude during one day [20]	10
3.5	Frequency output from a single 2.3 MW wind turbine during one day [20]	11
3.6	Frequency output from a single 2.3 MW wind turbine during one hour [20]	11
3.7	Energy consumption and production from a PV facility in kWh [21]	11
3.8	Solar irradiation in Quebec, Canada between 7 am and 7 pm [22]	12
3.9	Solar power production and grid demand throughout a time period of one day[22]	13
4.1	Registered under,- and over-voltage incidents for respectively 12.02.21 and 26.02.21 [21]	16
4.2	Equivalent circuit of IRES generation and the power grid [30]	16
4.3	Example of frequency response after frequency event, containing initial response, secondary control and tertiary control [31]	18
4.4	Ragone plot containing different battery energy storage devices rated by energy density and power density [38]	20
4.5	Chemical composition of supercapacitor, lithium-ion battery and lithium-ion capacitor, where the LiC is a composition of the two other technologies [38]	21
4.6	Structure of lithium-ion capacitor including electrolyte, separator and anode and cathode materials [47]	23
4.7	Different effects of ageing mechanisms for a lithium-ion capacitor[51]	25
4.8	Snapshot of the performance of a LFP battery [70]	29
4.9	Snapshot of the performance of a NMC battery [70]	29
4.10	Snapshot of the performance of a LTO battery [70]	29
5.1	Simulink illustration; Complete construction of lithium-ion capacitor in Simulink containing a battery, controlled current source, current sensor and voltage sensor	34
5.2	Wind power production and a moving average for one hour from Lista	36
5.3	Solar power production combined with a moving average during one day in Qubec	36
5.4	Flow chart illustrating a BESS controller with power, average power and SoC as inputs, and current as output.	37
5.5	Flowchart illustrating the cycle counter based on ΔSoC for grid tide BESS subject to microcycles.[73]	38

5.6	Simulink illustration; The complete construction of a lithium-ion capacitor integrated in a wind power plant in Simulink containing a signal builder, cycle counter and BESS controller. The figure is simplified for visual purposes	39
5.7	Simulink illustration; LiC and LiB systems integrated in an energy shifting-system for a solar power plant. The system is simplified for visual purposes	40
5.8	Solar power production, calculated average with a \pm constant, estimated grid demand and base production	41
6.1	Wind power output and power output in MW after implementing the LiC-system during one hour	44
6.2	Numbers of cycles for LiC due to micro cycles at three different capacities while stabilizing one hour wind production	45
6.3	C-rate for two different LiC capacities during stabilizing of one hour wind production	45
6.4	Solar power and power out after stabilizing with LiC at two different capacities .	47
6.5	Solar power and power output after stabilizing with LiC at two different capacities, magnified	48
6.6	SoC for LiC while stabilizing solar power at two different capacities	48
6.7	Numbers of cycles for LiC due to micro cycles at three different capacities	48
6.8	C-rate for two different LiC capacities during stabilizing of solar production . . .	48
6.9	Power assigned to LiC and LiB respectively for the entire day	50
6.10	Power assigned to LiC and LiB respectively, magnified	50
6.11	Power output from LiB with solar output power and grid demand	51
6.12	Power output from LiC and LiB with solar output power and grid demand	51
6.13	Number of cycles for LiB at two different capacities during energy shifting	51
6.14	C-rate for LiB at two different capacities during energy shifting	51
6.15	Carbon Intensity, share of low carbon power production and share of renewable power production in southeast Norway [82]	59
6.16	Carbon Intensity, share of low carbon power production and share of renewable power production in Kansai, Japan [82]	59

List of Tables

4.1	Comparison of key performance parameters of commercial and proposed energy storage devices	28
5.1	The complete data for a single LiC cell including the capacity and voltage values. The values are obtained from the excel-spreadsheet sent from Beyonder, shown in appendix A.2	35
5.2	The complete data for a single NMC cell including the capacity and voltage values [71, 72]	35
6.1	Design parameters of LiC integrated in different systems, including values for the resistance, capacity and open cell voltage at different state of charge-values . . .	42
6.2	Installed capacity, price and weight of LiC-system for three different applications	56

1 Introduction

The world is facing the biggest environmental crisis of its history. By 2021 the emitted amount of greenhouse gasses has exceeded 60 gigatonnes precipitating global warming, an increase in extreme weather and rising of sea levels [1]. In accordance with the UN Climate Change Conference, COP26, and the Paris agreement, the participants are to join in on a common effort to reduce and reverse the ongoing crisis. This can to some degree be achieved by the ongoing electrification of the society and the implementation of more renewable energy. It is in accordance to the UN's Sustainable Development Goals, in particular goal 7; *Affordable and clean energy*, 11; *sustainable cities and communities* and 13 *climate action*[2]. However a process such as this requires different innovative solutions to be implemented.

The need for green and affordable energy is ever rising. It is predicted that by 2050, 2/3 of the energy used will originate from renewable sources [3]. However, such a transition may cause problems. By introducing a higher penetration of intermittent renewable energy in the power system, problems like poor power quality, insufficient utilization and reliability caused by an unstable and non constant production will be more prominent.

These problems can to some degree be solved by introducing energy storage devices. Research on the topic have suggested that it is only necessary to store 8% of a production plant's capacity in order to remove 90% of the variations in the energy production [4]. Lithium-ion batteries have for a long time been the dominant storage device due to its impeccable specific energy. However, what the LiB has in energy density it lacks in power density, creating a demand for storage devices capable of delivering high power. Beyonder is a Norwegian based company which specializes in solving this problem, i.e. high power batteries or lithium-ion capacitors produced in a sustainable manner. Able to handle rapid power variations as found in intermittent renewable energy production, the lithium-ion capacitor could better the utilization and power quality from this production. Lithium-ion capacitors can be used for a wide range of applications. They are best suited for applications which require a moderate energy density combined with a high power density, in addition to excellent durability. The lithium-ion capacitor is also capable of integration with power electronic devices at a much higher frequency then that of similar technologies. Possible applications include electric grid, renewable energy sources, electric vehicles and transportation [5]. This paper looks to further investigate the implementation of Beyonder's lithium-ion capacitor in wind and solar power for energy generation optimization purposes.

1.1 Problem to be addressed

Can the implementation of lithium-ion capacitors be a possible solution in order to optimize wind and solar power with regards to power, voltage and frequency quality. Is the LiC in combination with a LiB a viable solution in energy shifting if the focus area is to prolong the LiB's lifetime. Could the implementation of LiC enable higher penetration of intermittent renewable energy sources?

This paper is limited to only consider LiC integration in a large scale wind and solar power production plant. For that reason, energy storage for domestic usage will not fall into the scope of this paper. It is set to only consider the effect LiC implementation has on a system compared to a system without. The paper will consider the market demand and several simulations based on different case studies. These will only consider simplified systems based on power in and power out in Simulink in order to address the effect of LiC implementation. The paper will not consider in-depth economical and sustainable analyses, however both aspects will be acknowledged.

2 Market Demand

The world's energy usage has rapidly increased since the 1950s. The growth is due to several factors including economic development, a rising population and advances in technology. As countries become more developed there is an increase in living standards. A higher demand for food, rapid industrialisation and urbanisation and increased purchases of cars and domestic appliances which all contribute to a higher energy demand [6].

The world's electric demand has also grown considerably in keeping with the rising energy demand. Electricity is a central aspect in modern life and the society is becoming progressively more electricity-based. The increasing global demand is pushing prices, creating strains in major markets and putting pressure on the electric grid. The rising use of both energy and electricity have shown themselves to negatively impact the climate. Solutions on how to cover the increasing demand in a sustainable manner is essential in order to slow down the climate changes the world are experiencing [7].

Humanity's increased use of fossil fuels, deforestation and increasingly intensive agriculture have led to higher concentrations of greenhouse gases which has caused global warming. Many countries have built their economies on burning fossil fuels in order to provide electricity, power the transport sector and develop industries. All of these demands and future demands can be covered by sustainable solutions such as the use of renewable energy sources. A transition from fossil fuels to renewable energy will generate a demand for power and voltage-regulation, which can be covered by technologies such as lithium-ion capacitors [8, 9].

2.1 Energy demand and production

Increasingly more of the world's energy demand is covered by electricity, where continuity of supply and voltage quality are important factors in today's energy market. The electricity used today is produced in sync with the consumption, meaning that the production is adjusted to match the demand, leading to a close correlation between the two. Hydropower plants or other large fossil driven turbines are ramped up during peak-hours to cover the demand. The electricity is then transported through the power distribution network to the consumer. While this process is adequate when both the production and demand are predictable and stable, it can cause problems when intermittent energy sources and a higher, unpredictable, demand breaks down the symbiotic relationship between production and demand. A problem which can in time disrupt the supply continuity. Not only is the continuity of supply important, but also the quality of the power delivered which is regulated by several injunctions. These regulations dictate an acceptable voltage quality range. If the power supplier fails to comply with the regulations it can affect the consumer and their appliances by irregular performance and in worst case breakdown and malfunction. The implementation of renewable energy sources, RES, and an overall increase in consumption makes it harder to uphold the regulations. When the production is too high it must be exported, often at a negative price. If the demand exceeds the production it could result in poor voltage quality and discontinuity of supply.

2.2 The future situation

The worlds electricity demand is predicted to double by 2050, although the total energy demand is anticipated to stay approximately equal to today's usage. Due to increased electrification of the transport and industry section, the electricity demand is predicted to increase in sync with the decrease in carbon based energy carriers as shown in figure 2.1. Electrification poses as part of the solution to the climate crisis, however the current distribution grid is not capable to handle the predicted electrification. This is particularly if the energy stems from intermittent energy sources, which often creates difficulties for the grid.

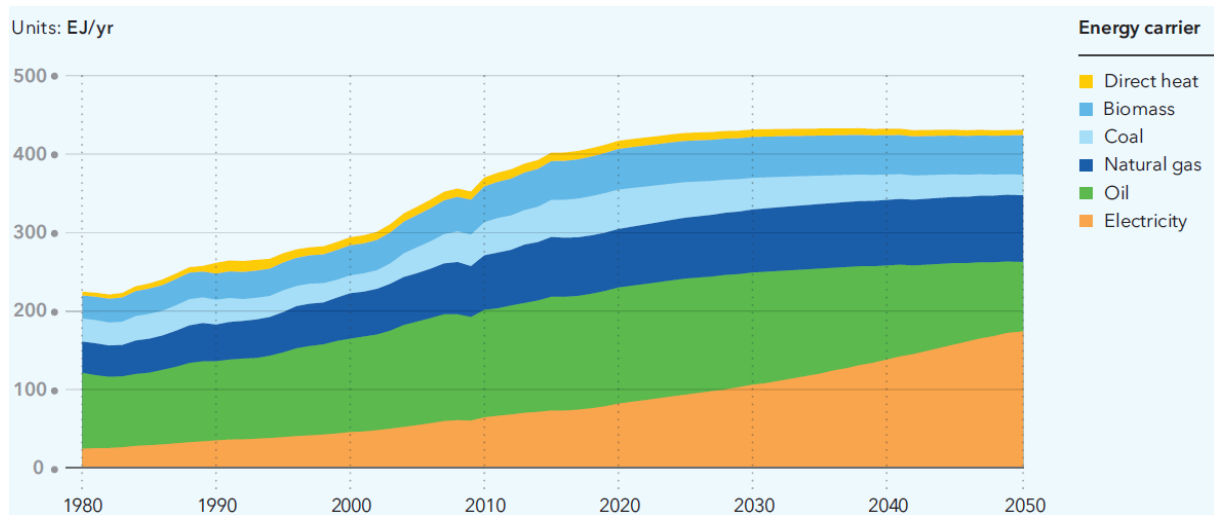


Figure 2.1: Forecast of the final energy demand divided into different energy carriers, up until 2050[10]

2.3 The intermittent nature of wind and solar power

The potential of wind and solar power is ever growing due to their low carbon footprint and overall decreasing investment cost. However, despite the many advantages, several major obstructions hinders an unmitigated growth of implementation for grid-tied PV-plants and wind power. One being the intermittent nature of wind and solar power, which varies not only from day to day and season to season, but also from one second to the next. The strong dependency of local weather conditions, changes the dynamics of the energy supply.

The introduction of intermittent energy sources combined with an increase in electrification, can cause reliability and quality problems for the power grid. A problem which only increases with an enhanced penetration level of intermittent energy as well as the degree of electrification. Figure 2.2 shows the worlds grid-connected electricity generation by power station type, both historically and future predictions. This graphically illustrates the predicted increase in generation from PV-plants and wind power, divided into onshore and offshore wind. It also shows the decrease in coal, oil and gas-fired power plants.

This prospect might look promising with regard to the ongoing climate crisis, however the development can cause issues for the distributing grid and its power quality. Issues like sag,

swell, flicker, harmonic, interruptions and voltage imbalance. These issues only increases with increased dispersion of intermittent renewable energy sources, IRES. To be able to utilize the energy to its full potential, technologies which improves the power, voltage and frequency quality are highly needed. One way to achieve this is by stabilizing the power output.

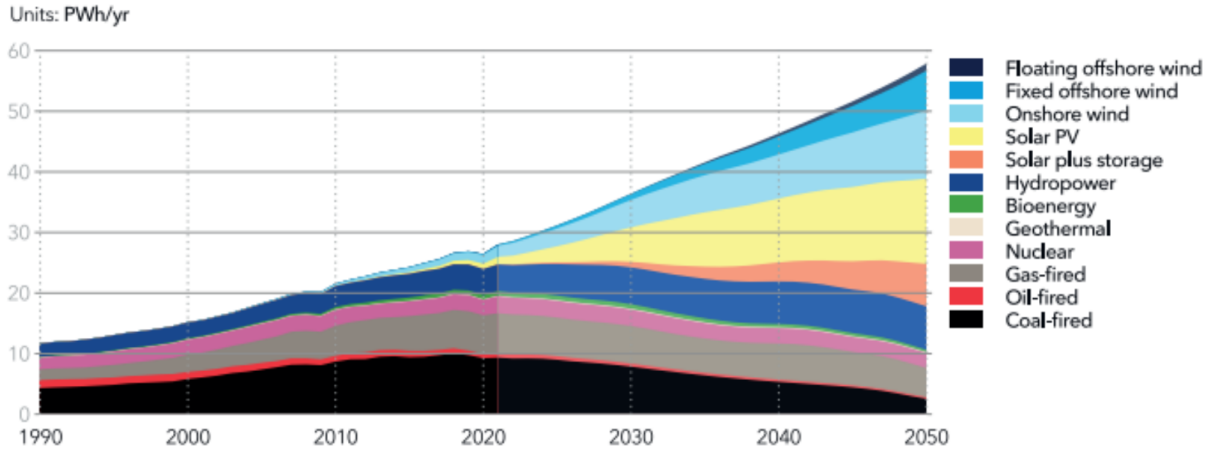


Figure 2.2: *Energy transition outlook for electricity sources until the year of 2050 [11]*

2.3.1 Stabilizing power output

In the case of large scale applications of IRES, power fluctuations can result in voltage and frequency deviations, later explained in depth in section 4.1. Voltage-flicker is an important power quality aspect that should be reduced in order to enable the quality of electric power. Additionally, deviations in frequency can cause protective relay equipment to trip as later explained in section 4.1.3. This may have a severe impact on the power system and can cause power outages. The uncertainty of wind and solar also accompanies difficulties regarding operation planning, optimal scheduling and unit commitment. There have also been set many requirements, by different utility companies, that have to be met in order to connect such intermittent energy sources to the grid. With regards to all these problems, companies like Beyonder are developing new technologies that can offer a solution to the issues regarding the variable power output from wind and solar energy [12].

A lithium-ion capacitor, with its high power capacity compared to conventional batteries, is such a solution. It has the capability to handle both the rapid power variations from wind power in addition to the more sluggish, energy demanding solar power. By storing surplus energy which can be released during low production periods one can obtain a more stable power output characteristics, less prone to problems.

2.3.2 Energy shifting

The sun is subject to seasonal, daily and hourly variations which seldom corresponds with the demand. This substantiates the need for a type of energy storage system that can store the surplus energy and shift it to a time of day where the demand is higher. This is shown in Figure 2.3, where the solar supply peaks at the time of day when the grid demand is at its lowest. Wind power on the other hand can produce electricity at all hours, which also means that there might be production when the demand is at its highest. This is also shown in the same figure where the production is steady, but at a lower level.

It is only in the middle of the day the solar supply exceeds the demand, however the surplus is significant. If the production from both the solar and wind supply could be distributed throughout the day, it would help covering the peaks of the grid demand. Storing the surplus from the solar supply at midday for the upcoming peak in demand is called energy shifting, which is shown in Figure 2.3. For these types of applications, a high energy density provided by a lithium-ion battery is needed. For LiBs used in energy shifting, the so-called 4 hour rule is applicable. This rule states that the storage device should have the ability to operate for a minimum of four consecutive hours at maximum power output. The variations in solar irradiation substantiates a need for something that can stabilize the production. A LiC would be able to satisfy this need, where implementing it would reduce battery stress and possibly extend its lifetime. An extended lifetime would be environmentally beneficial, since it would result in the LiB not having to be replaced as frequently.

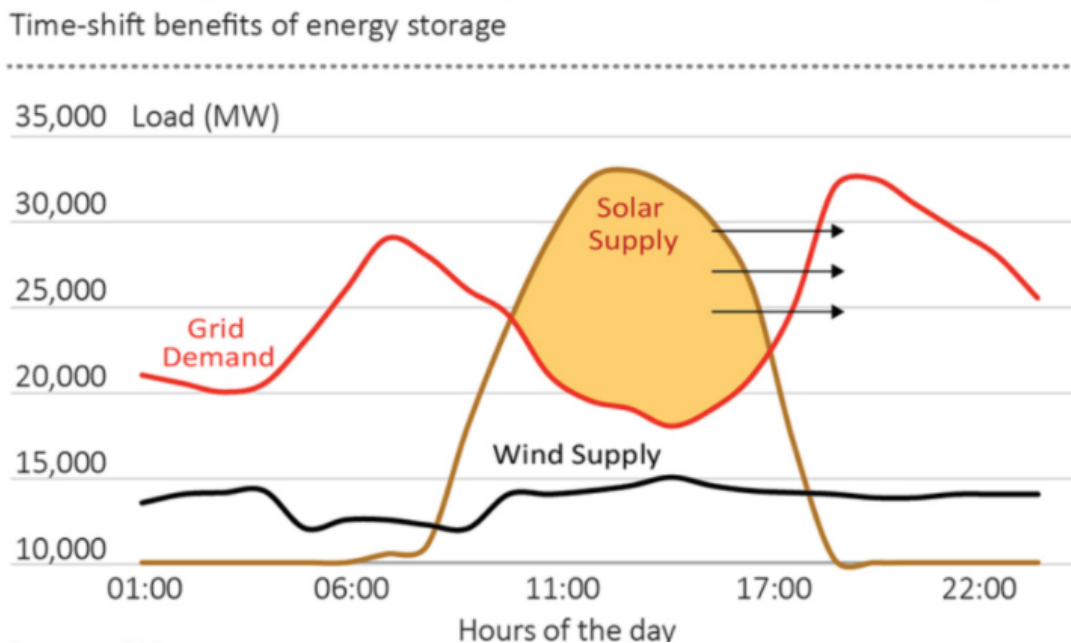


Figure 2.3: Time-shift benefits of energy storage, showing the possibility of energy shifting [13]

2.4 Other applications for a lithium-ion capacitor

There are several other applications where the introduction of LiCs could improve the existing systems. These vary from applications in the electricity grid to the transport sector.

Electricity grid

In addition to applications in renewable energy a LiC can also be implemented in the electric grid. The increasing electricity consumption and renewable energy production causes high fluctuations in power, voltage and frequency in the grid. These fluctuations leads to losses which again leads to higher costs for power producers. Implementing LiCs would be favourable in these situations since they have the ability to stabilize the fluctuations.

Charging infrastructure

Another application suitable for LiCs is charging of electric vehicles (EVs). Due to environmental concerns and increasing gas prices, Battery Electric Vehicles (BEVs) and hybrid electric vehicles (HEVs) have become an attractive transportation option. The EV market is a fast growing market where the battery capacity are becoming increasingly bigger. The current electric grid is not dimensioned to allow for charging of many EVs simultaneously. LiCs can be implemented to shave power peaks in order to reduce the load on the grid. That way energy is used more efficiently and further expansion of the electric grid can be avoided [14].

Transport sector

LiCs can also be used in the transportation sector, with applications both in larger electric transportation devices and smaller ones. The current battery technologies in these vehicles have limited power, lifetime and safety in combination with long charge times. They are also heavy and occupy a lot of space. LiCs in combination with LiBs can be a favorable choice in these situations, especially during driving in urban areas. Acceleration and regeneration leads to a rapid degradation of a LiB. Introducing a LiC which can handle the peaks and regeneration would increase the lifetime of the LiB considerably which again leads to reduced costs [14].

2.5 Economy and sustainability

As the grid demand varies throughout the day, peaks will form when the demand is at its highest. If the peaks could be covered by storing the surplus produced energy, large financial burdens can be circumvented. The CCO of Energi Norge stated that the power grid will be the key to the electrification and the climate control the world needs [15]. According to The Way Forward report, an increased integration of intermittent renewable energy sources is one of the biggest driving forces for the current billion dollar investment in the power grid [16].

An increased penetration of IRES could also lead to higher operational costs and ancillary service cost in conventional power plants. As auxiliary power plants are expected to provide for the variability of IRES, a higher penetration results in higher stress on these power systems. R. Ford and D. Milborrow approximated that a reserve power production of 4-8% of the installed wind capacity was needed for 20% wind penetration. A reserve which increased with higher IRE

penetration, resulting in high balancing and operational costs [17]. Another issue with IRES, is the occasionally poor power quality. An energy storage device could help stabilizing the production by improving the power quality. This would make it easier to meet the grid demand with less need for auxiliary power generation and more efficient utilization of the renewable resources. This means that the power producers would increase their incomes, in addition to a possible decrease in consumers electricity prices. Investing in an energy storage device that can help to solve these issues, would therefore be economically beneficial on multiple levels. Stabilizing the power production, can also lead to reduced losses in the grid and less downtime and interruptions. This again leads to a lower costs of not delivered power. This cost is what the distributor has to pay for not delivering the power they originally should. A more steady production could therefore lead to a substantial decrease in these expenses for the distributors [18].

If power producers easily can sell their surplus energy back to the grid, as a result of a more flexible grid, this opens up for a brand new market. Being able to store the surplus energy means that it can be stored when prices are low, and sold when they are high. Utilizing the possibility of producing, storing and trading power, makes for a market where it is possible to make a significant profit. This could also reduce the curtailment rate of renewable energy as excess production can be stored. In the years between 2019 and 2022 Agder Energi have, together with several partners including Statnett, tested different technological solutions to redeem more flexibility in the grid. This pilot called Norflex looked into how large scale consumers could benefit from reducing their consumption during peak load hours, and making their capacity at the disposal of the grid [19]. This differs from implementing storage technology, but is also a viable solution for obtaining a more robust power grid by focusing at the consumers and not the producers.

The transition from fossil to renewable energy drives the development of a technology that can provide both a high specific power and energy. A technology like this will be crucial to reduce both expenses and emissions. Beyond's LiC is such a technology and has the potential to optimize wind and solar power.

3 Case Study

In order to evaluate the LiC's performance, several case studies need to be built. The LiC will be implemented for stabilisation purposes in a wind power plant, a solar power plant and in an energy shifting-system. The cases will focus on the LiC's ability to improve the power, voltage and frequency quality. In an effort to realistically simulate a working wind and solar power plant, high resolution datasets from actual renewable energy production plants are needed. Such datasets were collected from Lista renewable energy park and a solar research facility in Quebec, Canada. These datasets were then plotted as seen in Figure 3.2 to 3.9.

3.1 Case 1; Wind power plant

To illustrate a working wind power plant, and obtain an input signal to be used in the simulations, actual data from Lista renewable energy park was collected [20]. Lista has a wind power plant consisting of 31 Siemens SWT-2.3-93 turbines, each at 2.3 MW. The turbines have a rotor diameter of 93 m and a tower height of 80 m. Lista has a total installed power of 71.3 MW. For the power plant, the expected yearly energy production is 220 GWh which is enough to cover the energy consumption of around 12 000 households. The wind turbines are divided into 4 groups with an inverter, which produces the correct frequency in each turbine. This is also where the voltage quality is constructed. Everything is controlled by a park pilot which aggregates turbine controllers into one wind power plant controller, providing only one interface to the transmission system operator (TSO). The plant controller ensures flexibility and enables increased adaptability. The setup at Lista is demonstrated in Figure 3.1.

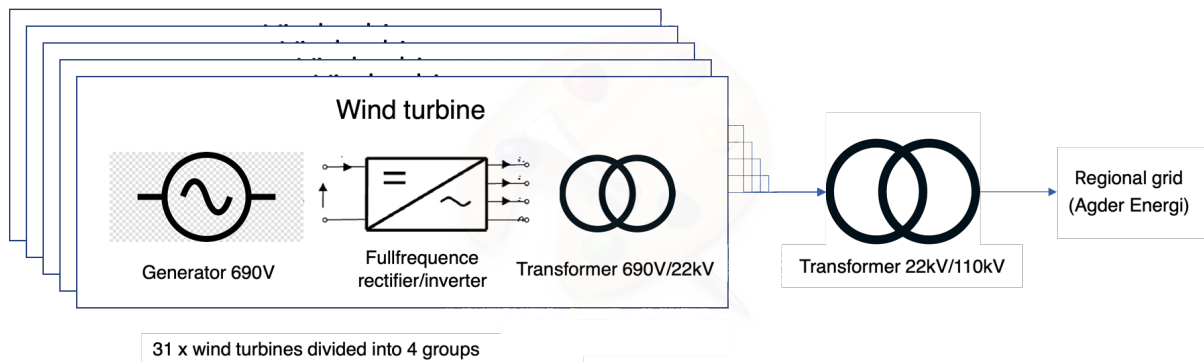


Figure 3.1: The setup at Lista renewable energy park containing 31 wind turbines divided into four groups. The electricity passes through a transformer before it enters the regional grid [20]

The collected data from Lista is extracted from one wind turbine and shows power, voltage and frequency on an hourly and daily basis on the first of January 2022. Considerable amounts of the collected data are illustrated in different plots below.

Figure 3.2 shows that the wind speed varies a lot during the day from almost 0 m/s to 17 m/s. This goes to show that wind is a unreliable energy source. The figure also shows that the produced active power correlates to the current wind speed. The wind power plant does not produce power when the wind speed is below 3 m/s. At the same time the power never exceeds

2300 kW during high wind speeds, due to the wind turbine's rated power which reach its limit at approximately 13 m/s. Figure 3.3 shows the same values as Figure 3.2, but zoomed in at only one hour. The figure shows a more accurate representation of the wind speed and active power, at a higher resolution with more data points.

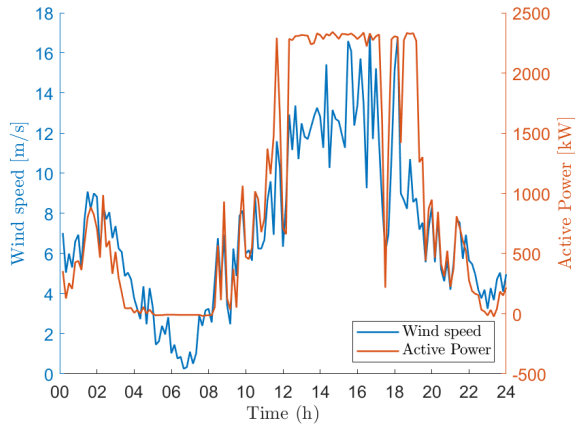


Figure 3.2: *Wind speed and power production from a single 2.3 MW wind turbine during one day [20]*

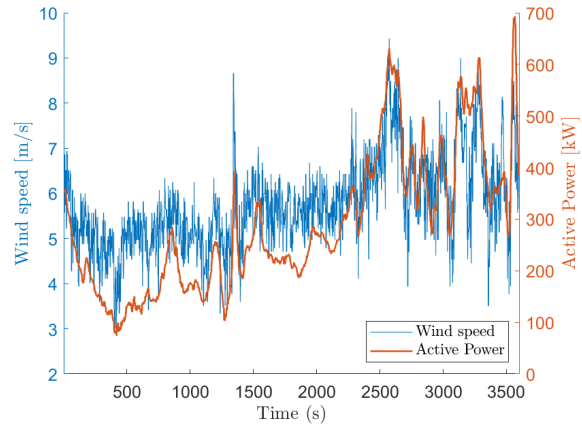


Figure 3.3: *Wind speed and power production from a single 2.3 MW wind turbine during one hour [20]*

Figure 3.4 shows the three different voltage phases for one day. All three phases stays between 106.8 kV and 108 kV. The voltage at Lista is set to be 107 kV due to requirements from the distribution network operator. By comparing Figure 3.4 to the active power in Figure 3.2 it can be seen that the voltage and power correlates to each other. For that reason stabilizing the power output could contribute to stabilizing the voltage output as well.

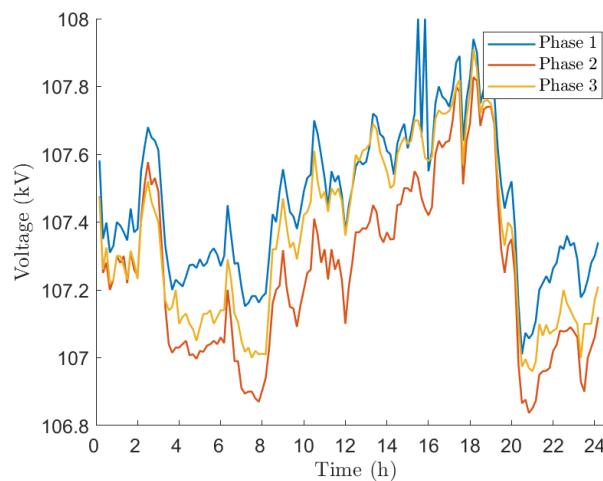


Figure 3.4: *Three-phase voltage amplitude during one day [20]*

Figure 3.5 illustrates the fundamental variations in frequency from the wind power plant, whilst Figure 3.6 shows a more detailed illustration. The frequency is supposed to be at 50 Hz in Norway with a normal variation between 49.9 and 50.1. As the figures show, the frequency lies between the normal variation at large proportions of the time. Nevertheless there are some exceptions where the frequency exceeds 50.1 Hz or dips below 49.9 Hz. The deviations are most likely due to sudden changes in the power production. Such variations are common in wind power, as can be seen in Figure 3.2 and 3.3, since wind is a unreliable energy source.

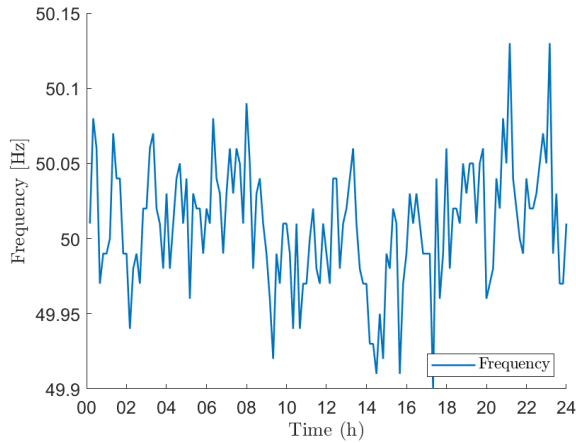


Figure 3.5: *Frequency output from a single 2.3 MW wind turbine during one day [20]*

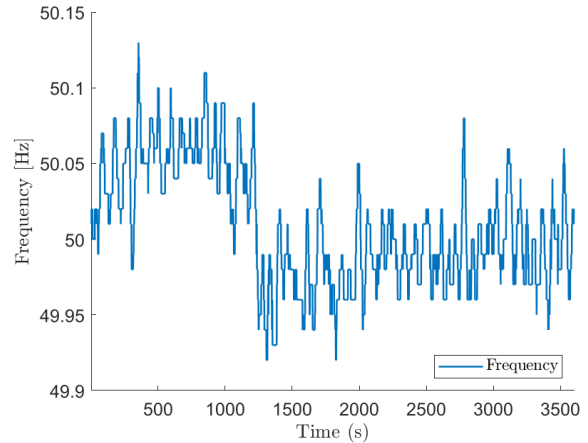


Figure 3.6: *Frequency output from a single 2.3 MW wind turbine during one hour [20]*

3.2 Case 2; Solar power plant

In order to illustrate a working solar power plant, and obtain an input signal to be used in the simulations, actual data was collected from a solar power plant at a school and sport facility in the south of Norway as well as irradiation data from a cite in Canada. The school alone is capable of producing 680 MWh per year with east-west facing PV panels. In addition, this facility have storage capability to increase the utilization of the irradiation. Figure 3.7 shows data collected from the school where the production is shown in orange and the schools consumption in blue, over a period of one year. From this it is evident that the production does not correspond with the consumption.

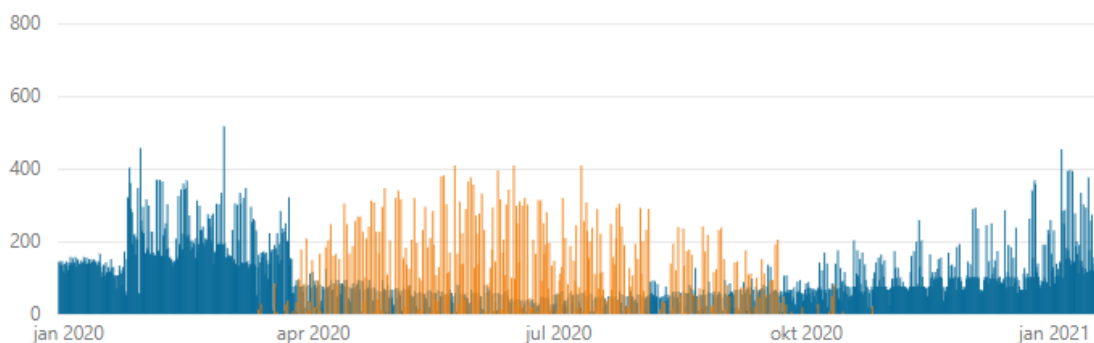


Figure 3.7: *Energy consumption and production from a PV facility in kWh [21]*

Figure 3.8 shows the daily solar irradiation from a cite in Quebec, Canada, with recorded data points every half second. The data is issued by the Canadian government to help simulate solar photo-voltaic system operation and study the short-term impact of irradiance fluctuations on the energy production [22]. From this it is evident that the irradiance varies over time, depending on time of day and cloud coverage. Here the variations are not as radical and frequent as in the wind power example, however there are still severe variations during daytime, and of course no production during night time. Integration of an intermittent energy source like this can cause reliability problems for the distribution grid if not well regulated. In addition, the utilization of the produced energy will not reach its full potential if the production does not correspond with the consumption. In other words, by introducing energy storage to regulate solar energy, a higher degree of utilization can be reached and it can reduce the amount of problems for the distribution grid.

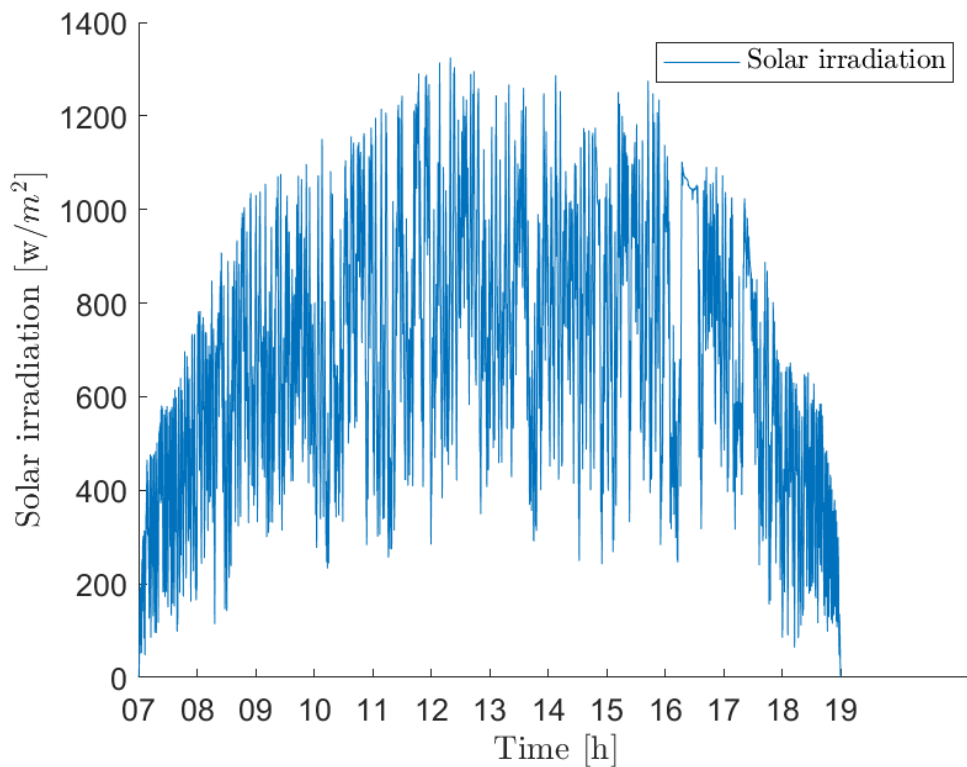


Figure 3.8: *Solar irradiation in Quebec, Canada between 7 am and 7 pm [22]*

3.3 Case 3; Energy shifting-system in solar power plant

For the final case, the same solar irradiation data as in the previous case was used. The grid demand was retrieved from Figure 2.3 for illustrative purposes. How the grid demand varies, combined with the solar irradiation throughout a day is shown in Figure 3.9. It is clear that there is a mismatch between the peaks in the grid demand and the solar power production. From around 8am to 6pm, the production exceeds the demand. However for the hours before and after this, the sun does not shine to produce enough power to cover the grid demand. The difference between production and consumption is highlighted in Figure 3.7. This substantiates the need for a technology that can both stabilize the production and store the surplus solar energy.

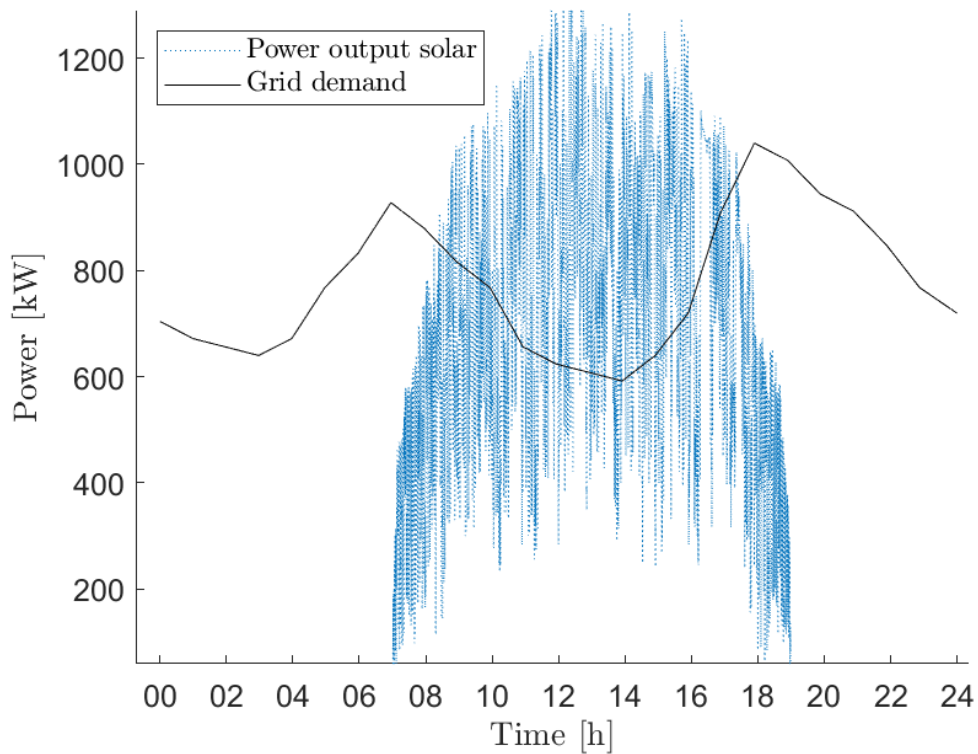


Figure 3.9: *Solar power production and grid demand throughout a time period of one day[22]*

The case studies presented above will later be used for simulation purposes. In order to evaluate the LiC's performance in different applications a simulation methodology will be manufactured, however firstly a theoretical foundation will be established.

4 Theory

The above section enlightens the increasing problem with grid connected intermittent energy sources, however it also introduces a solution. This section exhibits how LiCs can be integrated in combination with IRES to create a viable and sustainable solution both for the present but also the future. By understanding the market demand explained earlier it is evident that innovative solutions are needed. This section seek to present the theory behind the transmission system and the importance of reliability and power quality, in addition to introducing the lithium-ion capacitor (LiC) and its applications.

4.1 Reliability of supply: power, voltage, and frequency

Energy production is often located far from where it is consumed. This requires a well developed electricity grid which can transport the power to where it is needed. The grid consist of two main components; the transmission grid and the distribution system composed of the distribution and regional grid. In Norway, the transmission grid is a nationwide, high voltage (300-420 kV) system, connecting the producer to the costumer. It is also responsible for the power exchange between nations. The distribution system links the transmission grid to the end user, with a high voltage part (22 kV) and a low voltage segment carrying 230-400 V. The transmission system is critical infrastructure and needs to be operational and reliable [23].

The reliability of supply is an important aspect of the distribution grid. Increase in electrification and an overall higher demand can leave the grid crumbled during peak demand hours. Reliability is divided into the power grids ability to deliver energy and power at a certain time with adequate frequency and voltage quality. The transmission system operator (TSO) is responsible for the operational security, meaning the capacity of the power supply system to withstand disturbance. Disturbances which can lead to power outages or frequency and voltage deviations with potential serious consequences for the consumer. A problem that arises when there are imbalances between production and demand [24].

4.1.1 Energy security and power quality

Energy security is defined as the power systems ability to meet the electricity demand by corresponding production. In times where shortage of primary energy supplies as water, gas and coal is prominent and the demand exceeds the production, energy shortages and insecurity can arise. Reservoir of primary energy sources and transnational trading in combination with adequate transmission capacity is essential to maintain a high energy security. The power system is not only required to meet the overall electricity demand, but also the instantaneous demand. A demand which fluctuates from season to season but also from hour to hour, and a demand predicted to increase in time, with the introduction of more power demanding technology. This introduces the adequacy of the power supply system, which is the capacity the power supply system has to meet the instantaneous load and is important for the overall security of supply. At high consumption hours, if the demand exceeds the adequacy of the power system, a capacity shortage can arise. The security of supply depends on a power grid with adequate transmission capacity, and the ability to handle both short- and long-term fluctuations in pro-

duction and consumption. At high consumption hours, the grid is also subject to high losses [24].

As a power provider it is desirable to have power quality components in your system. Power conditioning equipment ensures that the produced power matches the voltage and frequency of the energy flowing through the grid. Such measures are desirable for several reasons. The first being to comply with national guidelines for equipment manufacture, operation and installation. Examples of such guidelines are IEEE 1547-2003 which provides technical requirements and tests for grid-connected operations, and UL 1741 which certifies inverters, converters, charge controllers and output controllers for grid-connected renewable energy systems. Secondly, by implementing power conditioning equipment in renewable energy production plants, losses will be reduced and thereby improving the power, voltage and frequency quality [25].

The power grid is subject to losses, and it is estimated that around 10% of the produced energy is lost in transmission. The losses is proportional with the ohmic resistance of the conductor which is dependent on the overall distance. They are also proportional to the square of the current transmitted, and since the power is the product between voltage and ampere, the losses are the greatest during high power peaks and increases with the square of the power. As shown in equation 4.1 where P_{loss} is the power loss, R_c is the ohmic resistance in the conductor and I is the current.

$$P_{loss} = R_c \cdot I^2 \quad (4.1)$$

The losses is on the other hand proportional to the inverse of the voltage squared, as a higher voltage equals an equivalent lower current, thus the high voltage on the transmission grid. The transmission losses could be decreased by stabilizing the consumption and the production crating an overall lower power demand. In addition to this, local production can shorten the transport distance and also reduce transmission losses [26].

As the fraction of production based on IRES is increasing, as well as an increase in the peak load demand, the requirement of a flexible power grid is ever rising. Changes in production and consumption patterns can have extensive influence on the future operation of the power grid as well as the investments needed in the sector and the power quality [27]. The power quality can be defined as the ability the bus voltage has to maintain a sinusoidal waveform at rated voltage and frequency. Voltage quality and frequency is thus closely related to power quality [28].

4.1.2 Voltage quality

Voltage quality is closely related to the production and consumption, but also the transmission capacity. The applicability of the energy is dependent on the voltage quality, therefore it is important to withhold a nominal operational voltage so that electrical appliances have an intended performance. The voltage amplitude needs to be at an acceptable level and is for that reason closely regulated and monitored. An acceptable voltage usually ranges between $\pm 10\%$ of the nominal value and is restricted by several legislations. When the production is uneven and not in

sync with the demand, significant voltage variations will be prominent. An increasing problem with deeper penetration of IRES and electrification of rural areas. This problem is illustrated by Figure 4.1 where the yellow warning triangles represent registered under-voltage and the red triangles shows registered over-voltage. In this case, locations where the voltage variation exceeds the $\pm 10\%$ limitation. Both images are from the same area in Norway, but at different dates. Data for the left image was collected 12.02.21 at 09:30 where as the right one represents a warmer day two weeks later. This portray a close correlation between the temperature and registered voltage incidents. The data was accumulated from Power BI's ADMS system and is directly connected to the advanced metering infrastructure at the costumers location. A tool which can make grid operation simpler and more effective. Figure 4.1 shows the magnitude of the imminent problem, which is only predicted to increase with the increase of electrification and implementation of IRES [29].

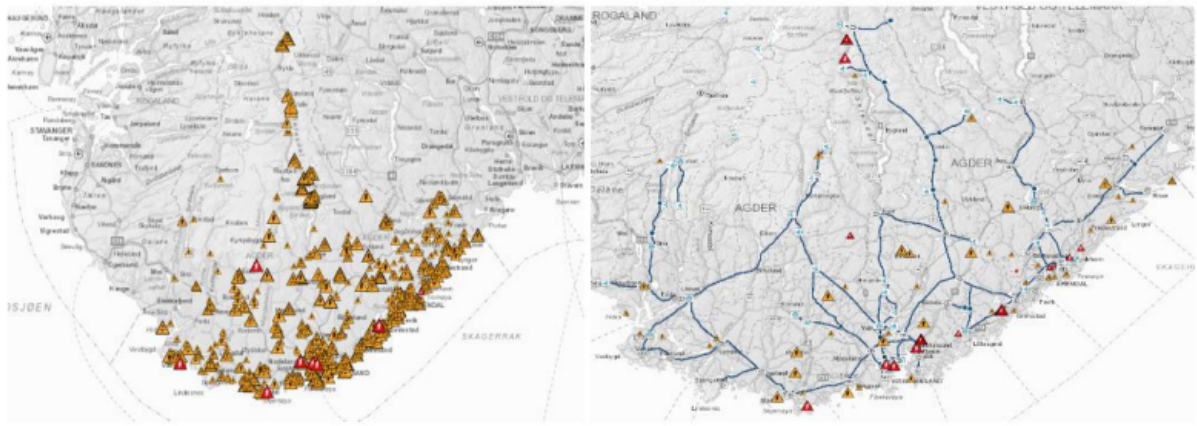


Figure 4.1: Registered under,- and over-voltage incidents for respectively 12.02.21 and 26.02.21 [21]

Voltage fluctuations and disturbance are closely related to the production of active and reactive power. If the available power varies with time, which is the case with IRES, so does the voltage. Figure 4.2 shows an equivalent circuit for IRE production connected to the utility grid.

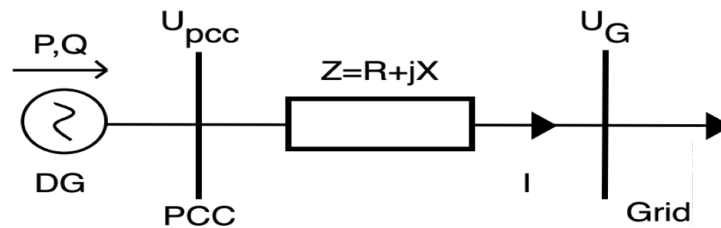


Figure 4.2: Equivalent circuit of IRES generation and the power grid [30]

The current can be expressed as below, where P and Q is the generated active and reactive power and U_{PCC} is the voltage at the point of common coupling.

$$I = \frac{P - jQ}{U_{PCC}} \quad (4.2)$$

The voltage between U_{PCC} and U_G is equal to the voltage over the impedance Z given by equation 4.3, where U_G is the grid voltage, X is the line reactance and R is the line resistance.

$$\Delta U = U_G - U_{PCC} = I \cdot Z = I(R + jX) \quad (4.3)$$

Substituting I in equation 4.3 by equation 4.2, gives equation 4.4

$$\Delta U = \frac{RP + XQ}{U_{PCC}} + j \frac{PX + QR}{U_{PCC}} \quad (4.4)$$

From this it is evident that the variation in active and reactive power production induces voltage fluctuations. Both solar and wind power are subject to highly fluctuating power output and can have a significant impact on the power system at high penetration levels [30].

4.1.3 Frequency

An electric power system is characterized by two main parameters: voltage and frequency, where frequency is a measure of the instantaneous balance. The most common nominal frequency in power systems is 50 Hz in Europe and Asia and 60 Hz in North-America. The basis for this choice are technical compromises and historical situations. A normal variation range of the frequency is ± 0.1 Hz. Variations outside this range are called an emergency condition and can cause system failure. Such variations occur because of an imbalance between generation and load. This imbalance can be caused by faults, sudden changes in electricity production or imbalances related to changes in flow along interconnectors. Frequency deviations can lead to a whole range of problems so it is important to ensure that the instantaneous balance is maintained. Especially since many countries are part of the same synchronous area, which means that one country's choices or faults affects all the others. In order to maintain the instantaneous balance, the transmission system operator (TSO) needs to have power reserves available. Such reserves are often provided by hydropower plants which have the ability to regulate the production in order to stabilize the system. Simultaneously new technological and market solutions can help to maintain the instantaneous balance and make the power supply system more resilient to such deviations in the future [24, 31].

However if the frequency value in the power system reaches the emergency condition, a frequency control strategy is initiated. The strategy consists of three levels which are primary, secondary and tertiary control. Primary control is the fastest, and commences when there is an imbalance between generation and load which affects the frequency. The energy needed to compensate for such changes are provided by generation units. These units are generally able to generate the required power within 30 seconds and take the system to a stable condition. The continuous

growth of renewable energy sources (RES) generates consequent difficulties to perform frequency regulation. Generators must be able to modulate their power according to the frequency value which is manageable in the case of over-frequency. In the case of under-frequency, which requires a power increase, the operation is a lot more complex and sometimes not even possible. However there are already several solutions under analysis to address the problems associated with the deployment of RES. Battery energy storage systems (BESS) are one of the most promising technologies thus far [31].

Once the primary regulation have accomplished its target, the secondary control sets in. After the primary control the frequency value is still different from the nominal one, the reserve margins of the generators are fully or partially used up and the power exchange between the interconnected power systems are different. The purpose of the secondary control is to restore all these values. In order to complete this task, a reserve power consisting of dedicated generators are used. If the frequency value is less than nominal, additional capacity is started and if it is higher, capacity is stopped or the load is increased. The primary and secondary control after a frequency event is demonstrated in Figure 4.3 where the green and red-dashed line shows two different responses according to the inertia level of the system [31].

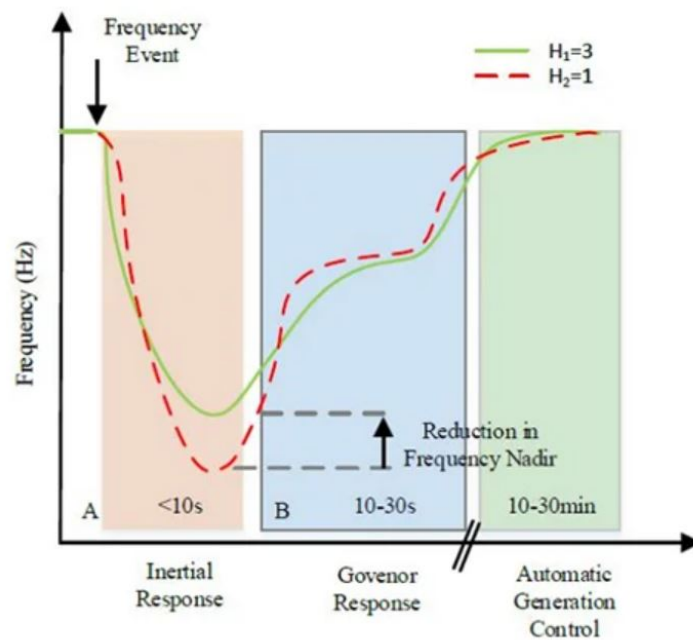


Figure 4.3: *Example of frequency response after frequency event, containing initial response, secondary control and tertiary control [31]*

At last, after the secondary control, the reserve margin used for that phase has to be restored which is the purpose of the tertiary control. In order to do so, the tertiary reserve is determined and activated for both upward and downward regulation. Tertiary reserve can be provided by both spinning- and non-spinning generators [32].

4.1.4 The benefit of energy storage

As presented in the section above, the requirement for a reliable and secure transmission grid is fundamental. The introduction of more IRES and an overall higher degree of electrification creates a higher demand on the grid. A demand the grid needs to cope with as the future is predicted to be electric with a high share of IRES. A more robust grid could be obtained by introducing storage technologies. The development of new and innovative technologies for energy storage could allow for an even fuller use of intermittent energy production and a greater control over the power grid. The existing capacity in the grid could be used to its fullest, and reduce or at least postpone the need for grid updates.

At present, there are few energy sources that can compete in terms of price and efficiency with flexible hydropower. However, by introducing wide scale energy storage that has the capability to stabilize the production from wind and solar power, the potential of intermittent production increases. The next section introduces the lithium-ion capacitor and its application areas in addition to a comparison to similar technologies.

4.2 Lithium-ion capacitor generation 3

Renewable energy have been predicted to be the prominent solution for the ongoing climate crisis. Wind and solar power in particular have experienced extraordinary growth the last decade and is predicted to surpass fossil fuels. However, due to its intermittent nature and a non-constant and unpredictable energy generation, energy storage devices (ESD) is fundamental for sustaining a flexible and trustworthy energy grid.

Energy can be stored by utilizing several storage technologies. Some of them being pumped hydro-power, compressed air energy storage, flywheel, and solid state batteries [33, 34]. Lithium-ion batteries and supercapacitors (SC) are also components frequently used in consumer electronics and other energy storage applications. LiB production have increased massively the last decade and due to its high energy density (150-200Wh/kg) it reaches a wide range of applications [35]. From BEV's to smartphones and intermediate storage in power grids. On the other hand the supercapacitor has a high power density (10kW/kg) and excessive longevity (100 000 cycles). Although it is limited by its insufficient energy density (5-10Wh/kg) [36].

Both LiB and SC are mature technologies although there are still improvement potentials. Such as trying to improve the power densities of a battery by optimizing micro-structure to enhance the kinetics at the interface between the electrode and electrolyte. Or the attempt to enhance the energy density of a SC by extensive research on high surface area carbon materials. There are applications where both these technologies are inadequate, applications were both high power and energy density are demanded, as well as extensive longevity. Applications suitable for a lithium-ion capacitor. LiC is a hybrid energy storage device which operates in the gap between a LiB and SC. With the power characteristics of a SC with an Electric Double Layer Capacitor (EDLC) type cathode and a superior energy density compared to a common SC with

a battery type anode. This, in combination with a better cycle stability, makes it an appealing solution for multiple applications. Especially when considering that the LiC generally consists of materials originating from areas free of geopolitical conflicts and environmental unfriendly excavation, which can not be said about the LiB. This aspect is covered in depth in section 6.6 "Sustainability and footprint" [37]. A Ragone plot, which combines the energy and power density of the different storage technologies, is shown in Figure 4.4.

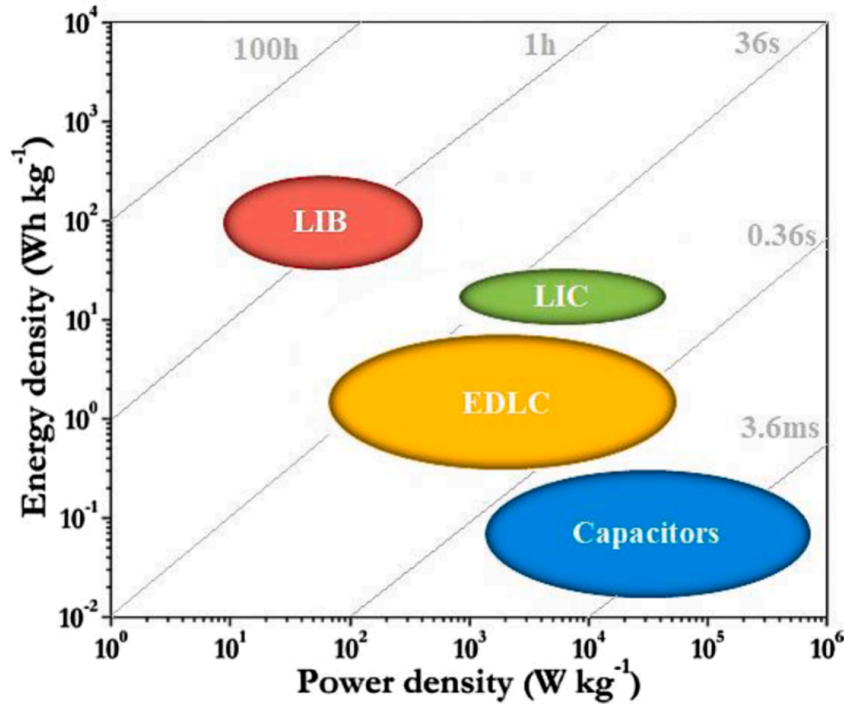


Figure 4.4: Ragone plot containing different battery energy storage devices rated by energy density and power density [38]

4.2.1 Construction

A LiC combines the pre-lithiated LiB anode and the EDLC cathode together with either an aqueous or a non-aqueous (organic) electrolyte containing lithium ions [39]. The anode and cathode materials dictates the electro-chemical performance in addition to the pre-lithiation process at the anode and the electrodes configuration. Yang and Amatucci was one of the first to construct and evaluate a LiC with an activated carbon (AC) cathode and a nano-structure $Li_4Ti_5O_{12}$ (LTO) anode [40]. Later, several different chemical compositions have been tested. To understand the composition of a LiC one must first comprehend the workings of both the LiB and SC. A schematic illustration of the composition is shown in Figure 4.5.

Lib is an energy storing devise with high energy density. By relying on electrochemical reactions and intercalation and deintercalation of lithium ions on the electrode, the energy density is unmatched by any other battery chemistry to date. It can deliver and absorb power at unity

C-rate and has a medium to low power density. The cathode is composed of materials such as lithium iron phosphate, lithium cobalt oxide or lithium manganese oxide which are all commonly used. All with their own attributes but also their own drawbacks. Where the anode is usually graphite, lithium titanate or carbon-silicon composite which in the electro-chemical process receives the lithium ions [41].

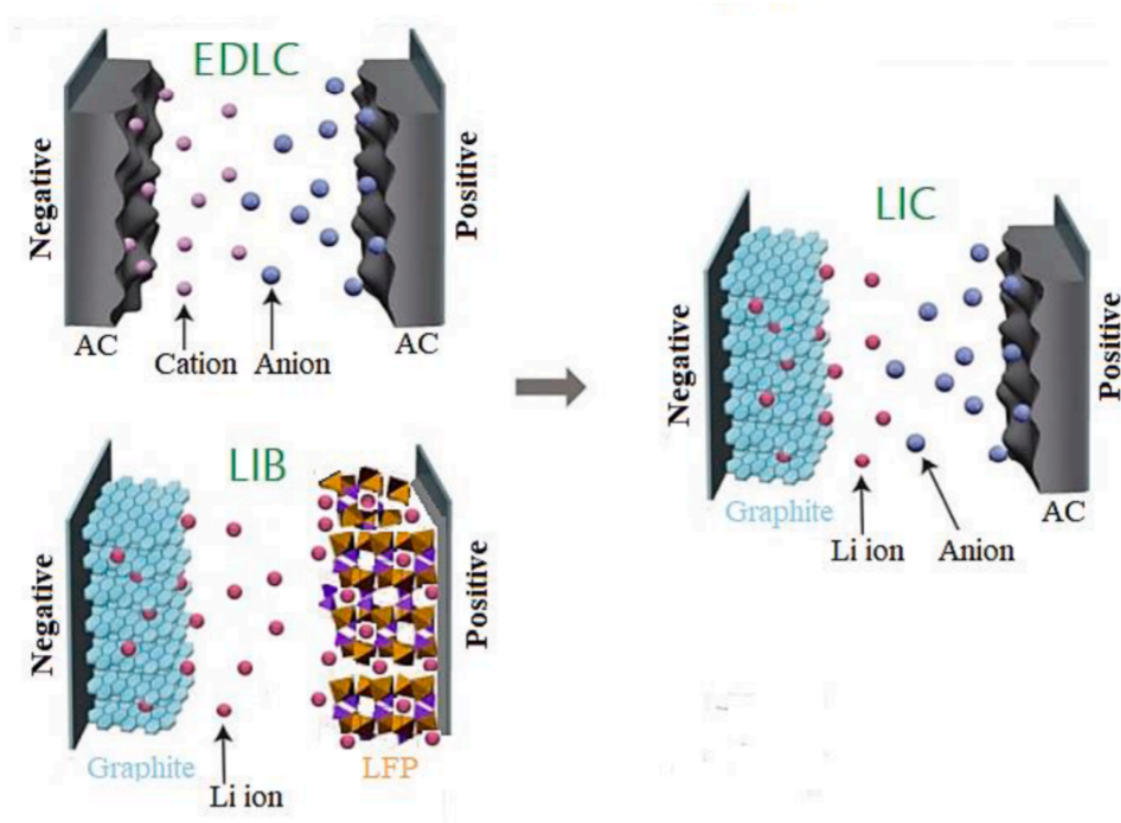


Figure 4.5: Chemical composition of supercapacitor, lithium-ion battery and lithium-ion capacitor, where the LiC is a composition of the two other technologies [38]

In contrast to a LiB, the SC has a higher power density and C-rate. The C-rate is a measurement on the rate at which a storage device is being charged or discharged. During charging, the porous active carbon physically absorbs positive and negative charges on the respective electrodes, which can then be released without sluggish kinetics resulting in a formidable power characteristic. Electrodes usually consists of graphene, activated carbon and carbon nano-tubes [42].

By combining the anode from the LiB and the cathode from an EDLC, a LiC with both satisfactory power and energy densities can be obtained. LiC is categorized as a class of hybrid capacitors composed of a high power positive electrode similar to an EDLC and a highly energetic lithium based negative electrode similar to that of a LiB, with an organic lithium based electrolyte. During charging and discharging, the ions are either absorbed or desorbed at the positive electrode which has a large surface area. At the negative electrode lithium ions inter- or de-intercalates. A process which is sluggish compared to the reaction on the positive

electrode, and dictates the cells power performance as this is the limiting factor.

A combination of the faradic intercalation and the non-faradic surface reaction increases both the specific energy and power of the cell. For a LiC the energy and power can be expressed respectively as:

$$E = \frac{1}{2}CV^2 \quad (4.5)$$

$$P = \frac{V^2}{4R} \quad (4.6)$$

Where V is the cell potential (V), R is the equivalent series resistance (Ω) and C is the capacitance (F) [43].

As shown, both the energy and power is proportional to the voltage squared. This implies that these properties are significantly improved by increasing the cell voltage. The cell voltage of the LiC's electrodes differs due to the different electrochemical mechanisms which leads to a higher achievable voltage potential. If compared with the voltage of an EDLC cell which is limited to 2.7 V, the LiC can achieve up to 4.0 V which in turn can improve the specific energy more than three times. The above equations also indicates the influence of the series resistance and the capacitance as this also affects the performance of the LiC. The specific capacitance is again affected by several factors including the specific surface area, pore-size distribution of the active material and conductivity of the electrolyte and the active material. A higher specific capacitance would increase the specific energy. The equivalent series resistance is dictated by the conductivity of the electrode and the electrolyte materials as well as the contact resistance between the current collector and the electrode. This series resistance negatively impacts the specific power and can be reduced by improving the surface area, using an aqueous electrolyte and increasing the conductivity of the electrode [43, 44].

Anode and cathode materials

There are several desired properties that the anode and cathode materials must obtain. The electrode potential of the anode is an important parameter where LTO and graphite is most commonly used. LTO has a higher lithiation potential, 1.55V greater than graphite [45]. This causes a safe potential and high capacity electrodes with an operating window in the range of 3.8-4.0 V. The carbon on the anode side is lithium-doped which drastically increases the energy density compared to the EDLC. Beyond utilizes a technology with a silicon anode which further increases the energy and power density. A silicon-carbon composite could also slow the rate of active lithium consumption when long-term cycling by providing a surplus of lithium which could give the LiC over 95% capacitance retention after 10,000 cycles [46]. This concept is further explained in section 4.2.2. The potential for silicon as anode material is huge due to its high theoretical capacity, low overpotential and low cost. However it is subject to large volumetric change during lithiation and delithiation [47, 48].

The most commonly used cathode material is active carbon, which displays power characteristics to that of an EDLC by utilizing the absorbing and desorbing electrode. In addition to pore size distribution and pore volume, the dominant attribute of active carbon is its surface area which exceeds $1000 \text{ m}^2/\text{g}$. These qualities are determined by the activation process and the post-activation treatment and dictates the performance of the LiC. Beyonder has a patented production process to create what is called super activated carbon (SAC). Based on forest residue, it poses as a sustainable alternative for cathode manufacturing. Without the use of heavy metals and a reduction of chemicals in production, this production method has an overall low environmental footprint. This technology boosts the specific capacitance through pore size optimization and reaches a specific surface area of $3000 \text{ m}^2/\text{g}$ [37].

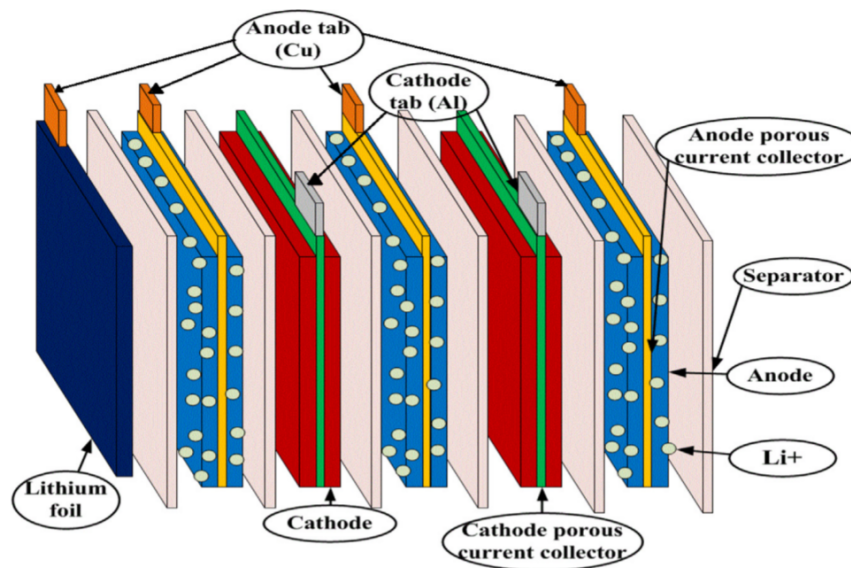


Figure 4.6: Structure of lithium-ion capacitor including electrolyte, separator and anode and cathode materials [47]

Electrolyte

The electrolyte is, as in similar chemical energy storage systems, responsible for the charge transfer in the cell. It is composed of three main components which can vary in concentration to obtain desired attributes and is usually a mixture of lithium salt dissolved in carbonate-based solvents. Lithium salt is the main charge carrier due to its polarity and its lithium-ion separability. The additives can modify the features of the composition and improves the ionic conductivity and the solid electrolyte interface (SEI). The solvent dissolves the lithium salt and has a low viscosity for good ion transport. Depending on the desired property of the electrolyte it can either be composed of an aqueous or non-aqueous solution. The aqueous has a lower viscosity, resulting in a high ion mobility. On the other hand it has a lower operating voltage compared to the non-aqueous electrolyte. The non-aqueous has a higher viscosity, resulting in a lower ionic conductivity. To summarize, the aqueous electrolyte results in a higher power density

due to its superior ionic conductivity, in contrast to its contribution for lower energy density as a result of its lower cell potential. The non-aqueous electrolyte is not subject for thermal runaway and therefore a safer option, combined with its high energy density, the non-aqueous is most commonly used in commercial products [38].

Separator

The separator, usually consisting of polymer or paper for organic electrolytes and ceramic or glass fiber for aqueous electrolytes, prevents electrical contact between the electrodes, while still remaining ion-permeable. The LiC performance is proportional to the ionic conductance, electrical resistance and the thickness of the separator. Separators such as microporous membrane coated polypropylene and cellulose-based TF40-30 are commonly used [38]. A complete structural composition of the LiC is shown in Figure 4.6.

4.2.2 Performance

The performance of a LiC can be divided into several sub-categories and is important to determine the LiC's application areas. C-rate, energy and power density and lifetime are all important parameters. In this section the main focus will be on Beyonder's LiC cell and its performance

C-rate and power density

The C-rate is an important tool to compare ESDs, especially when high power characteristics are desirable. The C-rate dictates the rate at which a battery is charged or discharged relative to its maximum capacity. A C-rate of 1C refers to a discharge current that will deplete the battery in 1 hour. This will, in a battery of 1000 mAh correspond to a discharge current at 1000 mA. Where as 4C corresponds to a 4000 mA discharge current and depletion within $\frac{1}{4}$ hour. For reference, Beyonder's LiC can deliver power at a C-rate of 20. In contexts where large amounts of energy is needed fast, a storage device with a high C-rate is crucial. This also dictates the charging time and how fast the storage device can absorb energy. In applications like fast charging, regenerative braking, grid connection, or regulation of IRES, the C-rate is one of the limiting factors for implementation.

The power density of the LiC is one of its most appealing attributes, and is together with its cycle stability the reason for its huge potential within several markets. As can be seen in the data sheet in appendix A.1, the LiC have a power density of 10 kW/kg which makes it ideal for high power applications. This is, as mentioned earlier, what distinguishes the LiC from a traditional LiB. On the other hand the relatively high energy density of 80 Wh/kg is what separates it from a supercapacitor.

Aging mechanisms and life time

The estimation of ageing and degradation of any storage device is evidently an important factor to determine the estimated capacity degradation over time and overall lifetime. In contrast to pumped hydro, compressed air energy storage (CAES) and thermal energy storage, which have little to non degradation, electrochemical storage do. Both, when the storage device is charged

and discharged (cycle ageing), and when the device is not in use (calendar ageing). The LiC has an estimated lifespan of 15 years or 100 000 cycles, despite the fact that several variables affects the electrochemical stability and capacity performance [49]. This includes temperature, state of charge (SOC), anode and cathode composition, electrode potential range and degree of pre-lithiation [50].

The irreversible degradation of the capacity when stored is called calendar ageing, which is mostly associated with the altering of material characteristics and parasitic reaction between the electrolyte and the electrode. This is mainly dependent on the SOC, temperature and storage time. All of these ageing mechanisms also occurs when the system is in use, in addition to the effects of cycle ageing. An overview of the different ageing mechanisms can be seen inn Figure 4.7.

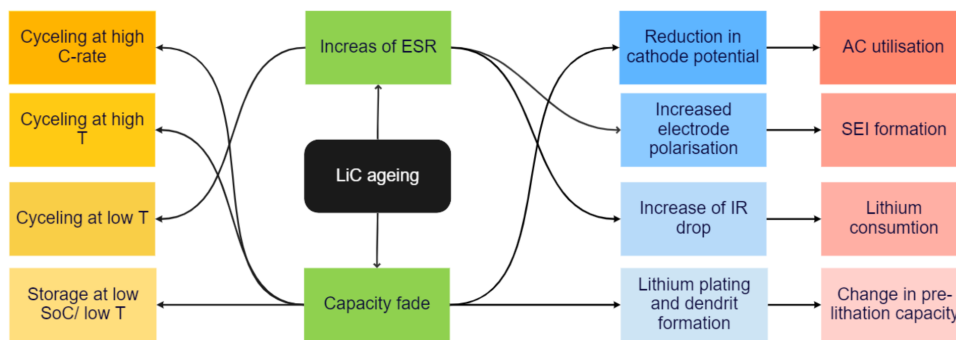


Figure 4.7: *Different effects of ageing mechanisms for a lithium-ion capacitor*[51]

Cycle ageing occurs during charge and discharge cycles. Where cycle number, temperature, depth of discharge (DOD) and C-rate all plays a critical role in determining the ageing process. A continuous line of charging and discharging leads to stress on the battery. The ions that are being moved between the anode and cathode can cause them to swell and contract. In time, this will cause degradation of the battery [52].

The C-rate affects the internal resistance, which in turn dictates the heat production and affect the lifetime of the cell. The continuous fading of the LiC's capacity is due to reduced utilization of AC material as the products of electrolyte decomposition can lower the accessibility of the pores, in addition to the formation of SEI film at the anode [53].

Several state assessment methods for lifetime model ageing evaluation, or state of health (SOH) monitoring, is necessary to ensure a LiC system with a long and safe lifespan. Monitoring of the reduction of the capacity and the increase in the equivalent series resistance (ESR) gives an approximation of the overall degradation, and is often used to determine the end-of-life for a LiC. This corresponds to a 20% reduction of the capacity and/or a 100% increase in the ESR. Several models for predicting the ageing behavior have been presented. Soltain and Ronsmans presented a comprehensive lifetime model able to predict the end-of-life for different calendar and cycling tests at different conditions [51]. This model concluded with that the DOD had no effect on the degradation of the LiC. The model has been validated and compared to experimental result and presented a relative error of less than 5%.

4.3 Similar technologies

In order to better understand the properties and performance of Beyonder's lithium-ion capacitor one must look at similar technologies. The most relevant technologies which can be compared to Beyonder's LiC are supercapacitors and different types of LiBs. These technologies are briefly described below and then compared to Beyonder's technology in tables and figures.

4.3.1 Lithium-ion batteries

Lithium-ion batteries can be used in a wide array of applications from electric vehicles to grid-scale applications. They are based on charge and discharge reactions between lithiated metal oxide and a graphite anode. The term lithium-ion can however refer to several different chemistries. The two most common lithium-ion chemistries are Nickel Manganese Cobalt (NMC) and Lithium Iron Phosphate (LFP) which are further elaborated below. Lithium Titanate Oxide batteries (LTO) are also further elaborated since they are the closest to LiC's when it comes to performance of high power.

Lithium iron phosphate battery

LFP batteries use lithium iron phosphate as the cathode material which is a natural mineral of the olivine family. These batteries have a generally lower energy density than similar lithium-ion batteries, but because of its many advantages it has gained considerable market acceptance. LFPs are some of the most chemically and thermally stable LiBs on the market today, with a lower chance of thermal runaway than its competitors. The production does not require use of precious and expensive materials such as cobalt and nickel. Other advantages include a long lifespan and better cycle stability characteristic, competitive prices and high efficiencies. The biggest drawback of LFPs is however their low energy density which is an important trait in most applications. Due to its cost, lifespan, safety and low weight, suitable applications include home energy storage, transportation and solar-powered lighting systems [54, 55].

Lithium nickel manganese cobalt oxide battery

NMCs have a cathode combined of nickel, manganese and cobalt. The battery delivers an overall strong performance with a high specific energy density and a low self-heating rate. Nickel is widely used in batteries because of its high energy density. However it has a low and poor stability. Manganese has the benefit of forming a spinel structure to achieve low internal resistance but offers a low specific energy. In NMCs these two metals are combined at the cathode where they enhance each other's strengths. Although NMC powder can refer to a variety of blends, the most common is a 1-1-1 blend which refers to one-third nickel, one-third manganese and one-third cobalt. This blend is the most used for mass production and offers a lower cost due to the reduced use of cobalt. Typical applications for NMCs include power tools, electric bikes and other electric powertrains [56–58].

Lithium titanate oxide battery

LTOs are modified from LiBs. The graphite in the anode has been replaced by lithium-titanate crystals which provides a surface area of 100 m^2 per gram compared to 3 m^2 for LiBs. This allows for more rapid transfer of electrons which constitutes faster recharging and a longer lifetime. The cell has a nominal voltage of 2.4 V and releases a high discharge current, 10 times that of other LiBs. LTOs have many possible applications, but is most suitable for applications which focuses on high speed charging and energy storage. Given the battery's properties is has a large potential for integration with energy storage solutions, bridging the gap between battery energy storage and grid power. The battery allows for a synergy between solar and wind power, battery storage and the grid. It has a great potential for contributing to grid stabilisation, creating a renewable energy source more sustainable than any other previous alternatives [59].

4.3.2 Supercapacitor

A supercapacitor (SC) differs from a regular capacitor in that it has a higher capacitance. There are three types of capacitors: electrostatic capacitor, electrolytic capacitor and the supercapacitor. What makes the supercapacitor special is its high capacitance and ability to undergo rapid charge and discharge cycles at high current and short duration. Noteworthy disadvantages of the supercapacitor is its low specific energy, which is 10-50 times less than Li-ion batteries. In addition during discharge the voltage decreases on a linear scale reducing the usable power spectrum, whereas electrochemical batteries delivers a steady voltage [60]. Since supercapacitors store electricity in a static state they are better at rapidly charging and discharging energy. Typical applications therefore include various means of transport where they are used for short term storage, regenerative braking or burst mode power-delivery. Smaller units are used as backup power systems for static random-access memory (SRAM). In large-scale applications supercapacitors are commonly used in wind turbines. Here, they help to stabilize the intermittent power supplied by the wind [61].

4.3.3 STATCOM

A static synchronous compensator (STATCOM) is a fast-acting device capable of absorbing or providing reactive power. Electrical loads in the grid both absorb and generate reactive power. The transmitted load often has big fluctuations which means that the reactive power in the grid varies a lot as well. This can lead to unacceptable voltage-variations including voltage depression or even voltage collapse. By installing a STATCOM in a suitable point of connection to a power grid, the power transfer capability will increase. The reason being the STATCOM's ability to regulate the voltage, keeping it at a stable profile under different network conditions. It can also be useful for improving the power quality because of its ability to perform active filtering. STATCOMs can also provide power factor correction, reactive power control, reducing low-frequency power oscillations and flicker mitigation. Typical applications are in sectors where voltage stability and power quality are crucial. Examples of employment are in the electric power transmission, electrical networks of heavy industrial plants, electric power distribution and in electric systems. STATCOMs can also be integrated in wind power systems where they can maintain the active power, reactive power and terminal voltage as constant [62–64].

4.3.4 Technical comparison

Regarding energy storage devices, there is an ever-increasing number of different technologies on the market. These technologies varies from energy dense batteries, to capacitors which can supply a high power output, where Beyonder's LiC is as mentioned a combination between these two. The following section will provide a detailed comparison of the technologies mentioned above. STATCOM have not been included in the comparison since it is not an energy storage device.

The characteristics of the different technologies is shown in table 4.1. The cell voltage is quite even for the different technologies. Some of the biggest differences is found in the power and energy density. The power density is 10 and 100 times higher in the capacitor and LiC than in the LiB. With respect to energy densities it is Beyonder's LiC that is closest to the density of a LiB. Regarding calendar and cycle life, the supercapacitor by far has the longest lifetime with 8-15 years and 1 million cycles. Even though the supercapacitors lifetime is a plus, its self-discharge rate is the highest of the different technologies, at 50% over two weeks.

One major difference in the technologies is the risk of creating a thermal runaway, which is when the Li-ion cell enters an uncontrollable, self-heating state. The usage of activated carbon instead of metal oxide in the LiC removes the risk of oxygen gassing inside the cells at high temperatures. This means that there is no oxygen on the inside of the cell that can support an internal fire.

Table 4.1: Comparison of key performance parameters of commercial and proposed energy storage devices

Characteristics	LiB [65, 66]	Supercapacitor [67]	Beyonder's LiC [68]
Cell voltage	3.6-3.7	2.7-3.0	2.0-4.0
Power density kW/kg	0.1	1.953	10
Energy density Wh/kg	100	5.1	80
C-rate 1/h	1	360-3600	20
Calendar life	10-15 years	8-15 years	15 years
Cycle stability	3000	1 million	100k cycles
Self-Discharge	.35% to 2.5% per month	50% over 2 weeks	<5% over 3 months
Thermal runaway	Yes	No	No
Temperature range	-20C to +60C	-40C to + 65C	-40C to +70C
Price \$/kWh	77-110 [69]	10 000 [60]	1 000 [68]

In order to compare the different LiB-technologies (LFP, NMC and LTO), snapshots of their performance have been obtained and illustrated in Figure 4.8, 4.9 and 4.10. All of the batteries are widely used and they all have their pros and cons. However since their performances are somewhat different, they are used in dissimilar applications. When investigating their costs it is evident that the LTO battery is the cheapest per kWh compared to a cost of 110\$ for the NMC and 77\$ for the LFP [69].

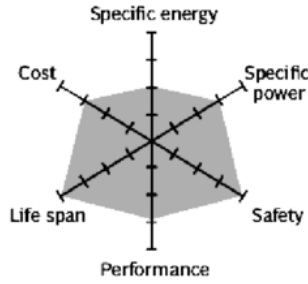


Figure 4.8: *Snapshot of the performance of a LFP battery [70]*

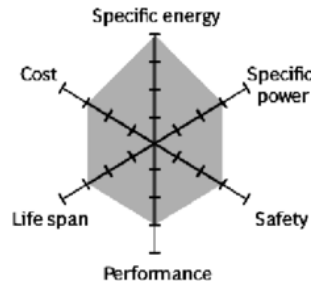


Figure 4.9: *Snapshot of the performance of a NMC battery [70]*

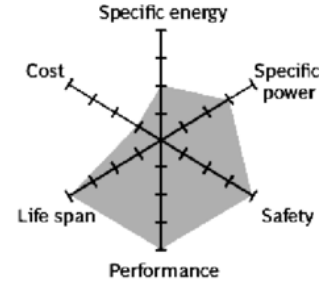


Figure 4.10: *Snapshot of the performance of a LTO battery [70]*

The price per kWh for the LiC is a lot higher compared to that of the different LiBs. However, a LiC is mostly made to be able to have a high power density in addition to having some storage capacity. Equation 4.7 shows how the required C-rate depends on the total discharge time for the storage device where shorter discharge times results in higher C-rates.

$$C\text{-rate}_{\text{required}} = \frac{60\text{min}}{\text{Discharge time}} \quad (4.7)$$

$$\text{Price per unit power} = \frac{1}{C\text{-rate}_{\text{required}}} \cdot \text{Price per unit energy} \quad (4.8)$$

Equation 4.8 displays the correlation between price per unit power, C-rate and the price per Wh. If the cost per unit power is compared between the different technologies, the result differentiates from earlier. Since the LiB only delivers power at unity C-rate, it can never be discharged completely in less than one hour. That is, if it is desirable to deliver 100 kW in 30 minutes, the LiB needs a capacity of 100 kWh to not exceed its C-rate. The LiC however, could have a capacity of 50 kWh and still only be subject to a C-rate of 2. If it is desirable to deliver the same power during 3 minutes, the LiC capacity could be reduced to 5 kWh corresponding to a C-rate of 20, whereas a LiB would still require a capacity of 100 kWh to stay within its C-rate limitation. Equation 4.7 and 4.8 presents a correlation between C-rate and price per unit of power and is an important aspect to consider when comparing investment costs. The equations show how the price per unit power is reduced in applications where high C-rates are required.

4.4 Controlling and dimensioning of energy storage

When stabilizing the power from IRES with storage systems it is essential to have correct control and management systems, in addition to proper dimensioning. This builds on different theories and strategies to obtain the desired result. This section presents the equation for a control strategy based on a moving average and the change in power between the average and the actual power.

$$SMA_k = \frac{1}{k} \sum_{i=n-k+1}^n P_i \quad (4.9)$$

Equation 4.9 calculates a simple moving average or SMA. The window size is represented by k and n is the number of observed values. P is in this case power. By comparing the P_{i+1} to the last recorded average value, P_i , and recording the difference, Δp , the amount of power charged or discharged from the storage system can be calculated.

$$I_{ss} = \frac{P_{in} - P_{avg}}{U} \quad (4.10)$$

From SMA the storage system current (I_{ss}) can be expressed as the difference in power divided by voltage (U) as shown in equation 4.10.

$$P_{ss} = I_{ss} \cdot U_{ss} \quad (4.11)$$

The power of the storage device is then represented as P_{ss} which is the product of the storage system's current (I_{ss}) and voltage (U_{ss}).

$$P_{out} = P_{in} - P_{ss} \quad (4.12)$$

The output power is then defined as the power in, minus the power from the storage device. This strategy will result in a more stable power profile similar to the average power. To obtain the desired result the storage system needs to be adequate dimensioned to cope with the power and energy demand while at the same time not be over dimensioned.

Dimensioning of energy storage

$$R_{equivalent} = R_1 + R_2 + R_3 + \dots \quad (4.13)$$

$$\frac{1}{R_{equivalent}} = \frac{1}{R_1} + \frac{1}{R_2} + \frac{1}{R_3} + \dots \quad (4.14)$$

In equation 4.13 and 4.14 the equivalent resistances of respectively series and parallel connections is shown. For series connections, the resistances is added together to get the equivalent. Meanwhile regarding parallel connections, the inverse of the resistances is added together resulting in the inverse of the equivalent resistance.

$$OCV = U_{nominal} \cdot n_{series} \quad (4.15)$$

The equation for open-circuit voltage (OCV) is shown in 4.15. The OCV is a product of the nominal voltage multiplied with the number of components in series. It shows the difference of the electrical potential between two terminals when it is disconnected from a circuit.

$$Q_{Total} = Q_{nominal} \cdot n_{series} \cdot n_{parallel} \quad (4.16)$$

The total capacity (Q_{Total}) is shown in equation 4.16. This is a product of the nominal capacity multiplied with the number of components connected in both series and parallel connections.

$$SoC = SoC_{t_0} + \frac{1}{Q_{rated}} \int_0^t (I_b - I_{loss}) dt \quad (4.17)$$

State of charge, or SoC, is defined in equation 4.17. There are several ways of estimating the state of charge, whereas the Coulomb counting method is one of the most commonly used. This method integrates the flowing current over time so that the total sum of energy entering or leaving the battery is derived. SoC_{t_0} is the initial SoC, I_b is the battery current and I_{loss} is the current consumed by the loss reactions. The integral is multiplied with the inverse of the rated capacity (Q_{rated}) of the battery, which results in the estimated SoC. A change in SoC affects both the overall cycle ageing, and the C-rate. The overall capacity determines how the SoC changes over time, which in turn affects the C-rate. This is therefore crucial to bear in mind when dimensioning the storage system.

$$C\text{-rate} = \frac{I}{Q} \quad (4.18)$$

$$C\text{-rate} = \frac{dSoC}{dt} \quad (4.19)$$

The calculation of the C-rate is shown in two different ways in equation 4.18 and 4.19. In the first equation the C-rate is defined by the current, I , divided by the capacity (Q). The second definition is the change in SoC divided by the change in time.

5 Simulation Methodology

The following section describes in detail the processes completed in order to perform various simulations. A number of different components including a LiC, LiB, battery controller and cycle counter had to be constructed in order to perform the simulations. The BESS technologies also had to be properly dimensioned after the construction was completed. A total of three simulations have been performed;

1. LiC, used for power stabilization, integrated in full-scale wind power plant
2. LiC, used for power stabilization, integrated in full-scale solar power plant
3. LiC, used for power stabilization, integrated in preexisting energy shifting-system containing a LiB. (Solar power plant)

Even though the lithium-ion capacitor is most suitable for applications in wind power, it was also simulated for solar power as it is also subject to varying power production. These simulations had a main focus of stabilizing the power output. Lastly the LiC was integrated in an already existing power system consisting of a LiB integrated in a solar power plant for the purpose of energy shifting. In order to perform such complex simulations the programming and numeric computing platform MATLAB was used.

5.1 Software

The software used to complete the simulations was MATLAB, version R2020b. Integrated in MATLAB is Simulink which is a block diagram environment for Model-Based design and multidomain simulation. It supports system-level simulation, design, code generation and verification of embedded systems. Simulink provides customizable block libraries, a graphical editor, and solvers for simulating and modeling systems. Since the program is integrated with MATLAB, it enables usage of MATLAB codes and algorithms into models and exportation of simulation results to MATLAB for analysis.

5.2 Assumptions

In order to accomplish the mentioned simulations, several assumptions had to be made;

- Due to the importance of high-resolution data, solar irradiation data was collected from a site in Quebec, Canada. This dataset was later converted from irradiance [W/m^2] to power [W] by multiplying with an area in order to simulate an actual solar power plant.
- The line loss, which refers to the quantity that is lost during transmission and distribution of electricity across the electric grid, was neglected. This assumption was made due to lacking importance and lacking knowledge of the length of the transmission lines.
- The setup used for the different simulations in Simulink all consisted of several blocks. Many of these blocks had their own assumptions such as steady state or ideal behaviour already built in.

- SoC was collected from the Simulink software, however it was not elementary how this value was determined (Coulomb counting, current integration, Kalman filtering, etc.) It was thus assumed that this value gave an accurate representation of the SoC of the storage device.
- Several assumptions were made considering the table-based battery used in the simulations. Firstly, the entered parameters for resistance, capacity and voltage were not tabulated over temperature. Realistically battery properties changes with changing temperature, with for example capacity loss at low temperatures and increased self-discharge at high temperatures. Secondly the self-discharge of the battery was disabled. In real life self-discharge occurs due to internal chemical reactions which reduces the charge of the battery. Both these assumptions were made in order to simplify the simulation process.
- The designed systems did not take auxiliary systems into account. Devices such as transformers, inverters and rectifiers was left out, portraying a simplified system.
- The wind power data and the solar irradiation data, which originally contained data for respectively one hour and one day, was assumed to be a representative for the entire year. In order to reduce the sources of error corresponding to this assumption a capacity factor for respectively wind and solar power was taken into account.
- The voltage of 690 V, used in the dimensioning process, corresponding to the low voltage side of the transformer at Lista renewable energy park was also assumed to be the voltage at the solar power plant. This is because the solar power plant was scaled down to be within the same magnitude as the wind power plant.
- The simulated systems does not consider a three-phase alternating current with 120 electrical degrees phase shift, but rather power as a single input signal.

5.3 Design of battery energy storage system

The complete setup of the battery energy storage systems used in the simulations consists of various components. These include the LiC and LiB itself with their belonging design parameters, along with an input signal, battery controller and cycle counter.

5.3.1 Lithium-ion capacitor

Construction

The LiC was built up by a number of components, which is shown in Figure 5.1. Starting with a table based battery, where no-load voltage was calculated as a function of optional temperature and charge level. A controlled current source was added to secure that the current was maintained at the preferred level. Both a current and voltage sensor were implemented, of which the voltage sensor were connected in parallel to the current source. The sensors were added to convert the measured values into physical signals proportional to the voltage and current. To be able to run the simulations, a solver configuration had to be added to specify the needed solver parameters for the model. Finally a powergui was added, where a certain method to solve the circuit was chosen. The method for the powergui was chosen to be "Continuous" which uses a variable-step solver from Simulink.

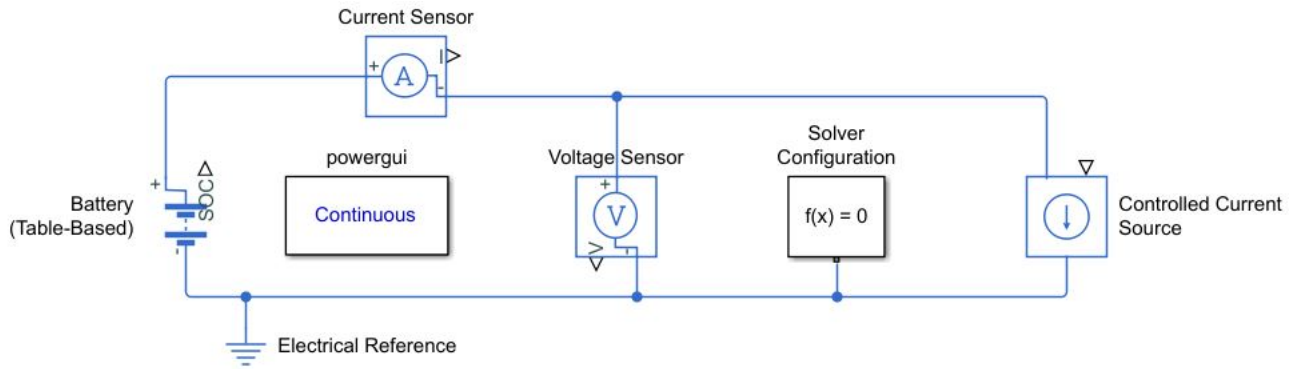


Figure 5.1: *Simulink illustration; Complete construction of lithium-ion capacitor in Simulink containing a battery, controlled current source, current sensor and voltage sensor*

Dimensioning

The LiC was dimensioned using the same method for all of the simulations. It was primarily dimensioned using voltage data, but it was also dimensioned based on energy and power extracted from the datasets from Lista and Quebec illustrated in the Case Study section. In addition to this, the C-rate and cycle stability was taken into account in order to ensure a sustainable solution. As mentioned in section 4.2.2 the LiC can deliver power at a maximum of 20 C and has a cycle stability of 100 000 cycles which should correspond to a lifetime of minimum 10 years.

Firstly the excel-spreadsheet from Beyonder, based on equations from the theory and shown in appendix A.2 and A.3, containing data on a LiC cell was used. These cells were connected in series in order to increase the voltage and form a rack in accordance with equation 4.15 from the theory section. The nominal voltage of the rack was set to be 690V, equal to the one at Lista renewable energy park, corresponding to the low voltage side of the transformer. Secondly the production data was analysed to find the greatest power peak and energy demand. In order to cope with the relevant demand, the capacity of the LiC was altered by connecting several racks in parallel to form a pack. Lastly the capacity was increased by increasing the number of packs in parallel to ensure that the C-rate and cycle stability was within the mentioned boundaries using equation 4.16 to 4.19.

Design parameters

After the LiC had been properly dimensioned using the cell data shown in table 5.1, several values were extracted from the excel-spreadsheet. These include values for the open cell voltage, internal resistance and capacity at different state of charge-values. The values was then entered in the table-based battery in the circuit shown in Figure 5.1 to imitate a functioning lithium-ion capacitor.

Table 5.1: *The complete data for a single LiC cell including the capacity and voltage values. The values are obtained from the excel-spreadsheet sent from Beyonder, shown in appendix A.2*

Capacity [kWh]	Nominal voltage [V]	Max voltage [V]	Min voltage [V]
0.032	3.00	3.80	2.20

5.3.2 Lithium ion battery

The design process of the LiB was executed in almost the exact same way as for the LiC. The construction setup is the same as the one showed in Figure 5.1 and the dimensioning process followed the same steps. However the cell data and therefore the design parameters entered into the table-based battery were different. Additionally the LiB can deliver power at a maximum of 1C and has a cycle stability of 3000 cycles. A NMC battery was selected to simulate the LiB due to its high specific energy. A large LiB pack was selected, with a capacity of 83 MWh, this pack was able to store all the excess energy with no curtailment and the LiC's impact could be analyzed to its fullest. The cell data for this battery is shown in Figure 5.2.

Table 5.2: *The complete data for a single NMC cell including the capacity and voltage values [71, 72]*

Capacity [kWh]	Nominal voltage [V]	Max voltage [V]	Min voltage [V]
0.2322	3.60	4.20	2.75

5.3.3 High resolution power input signal

In order to illustrate a working wind and solar power plant several power input signals were obtained. High resolution datasets with frequent measurements were used in order to represent the simulated systems accurately. For a wind power plant the power signal for one hour from Lista, shown in Figure 3.3, was used. This signal was multiplied by a factor of 31 since Lista renewable energy park consists of 31 wind turbines. The input signal is illustrated in Figure 5.2 along with a moving average with a window size of 600 points, created with equation 4.9, used as a reference signal. For the solar power plant, solar irradiation was gathered from a cite in Quebec, Canada, which contained measurements every half second. The data was collected by the CanmetENERGY laboratory in Varennes, as part of a High-Resolution Solar Radiation Time Series Generation project. This data was than scaled up to lay a basis for comparison with the wind data. The same solar data, shown in Figure 5.3, was used for both the power stabilisation

and energy shifting cases. The figure also illustrates a moving average, created with equation 4.9, with a window size of 600 used as a reference signal. These power signals and moving averages were then added to a signal input block in Simulink and connected to a BESS controller.

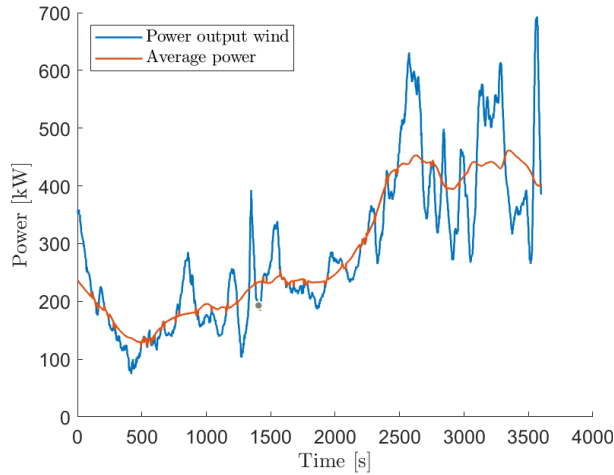


Figure 5.2: Wind power production and a moving average for one hour from Lista

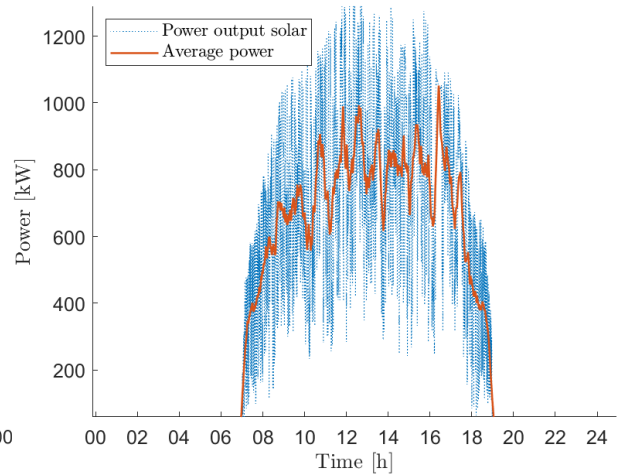


Figure 5.3: Solar power production combined with a moving average during one day in Quebec

5.3.4 BESS controller

In order to dictate the behaviour of the BESS, a controller was constructed as a function in MATLAB. It provides the BESS with information on when to charge, discharge or do nothing. The controller was constructed based on power data and equations 4.9 to 4.12 from the theory section. Firstly a reference value was created using the power data collected and equation 4.9 with a window size of 600. The product from the equation is an array with a moving average power. By creating this average value the same amount of energy will enter and leave the BESS during the relevant time period. The actual and average power are plotted and illustrated in Figure 5.2.

$$I_{ss} = \begin{cases} > 0 \rightarrow Charge \\ < 0 \rightarrow Discharge \end{cases} \quad (5.1)$$

These two values along with the state of charge from the BESS was then used as inputs for the MATLAB function. The function firstly checks the SoC of the LiC. If the SoC is between 10% and 100% the function investigates if the difference between the actual and average power is positive or negative. Then it decides if the BESS should charge or discharge. The BESS charges/discharges with a current relevant to the difference between the actual and average power. If however the SoC is lower than 10% the BESS either charges or does nothing. The function produces information regarding the magnitude and sign of the current. As a reference, a positive sign is set to be charge while a negative sign is discharge shown in equation 5.1. A flowchart explaining the function is illustrated in Figure 5.4, while the actual MATLAB script is illustrated in appendix B.1. The finished function, containing both positive and negative currents, was then used as an input for the controlled current source in the circuit shown in Figure 5.1.

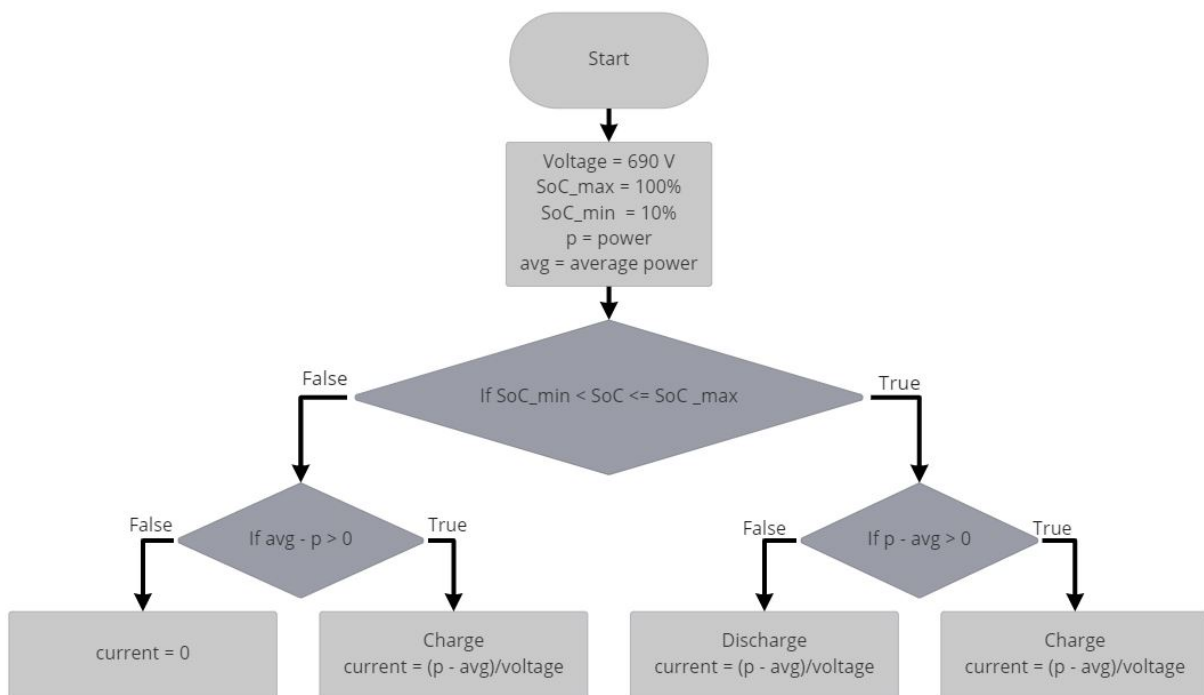


Figure 5.4: Flow chart illustrating a BESS controller with power, average power and SoC as inputs, and current as output.

5.3.5 Cycle counter

In order to measure the number of cycles a grid connected BESS subject to micro-cycles runs through, a cycle counter, based on theory by Gundogdu, B. and Gladwin, D.T was constructed [73]. By scaling up the results from the cycle counter and comparing them to the maximum cycle stability of the BESS, it was possible to estimate its lifetime. A flow chart of the cycle counter is shown in Figure 5.5, and the MATLAB script is illustrated in appendix B.3.

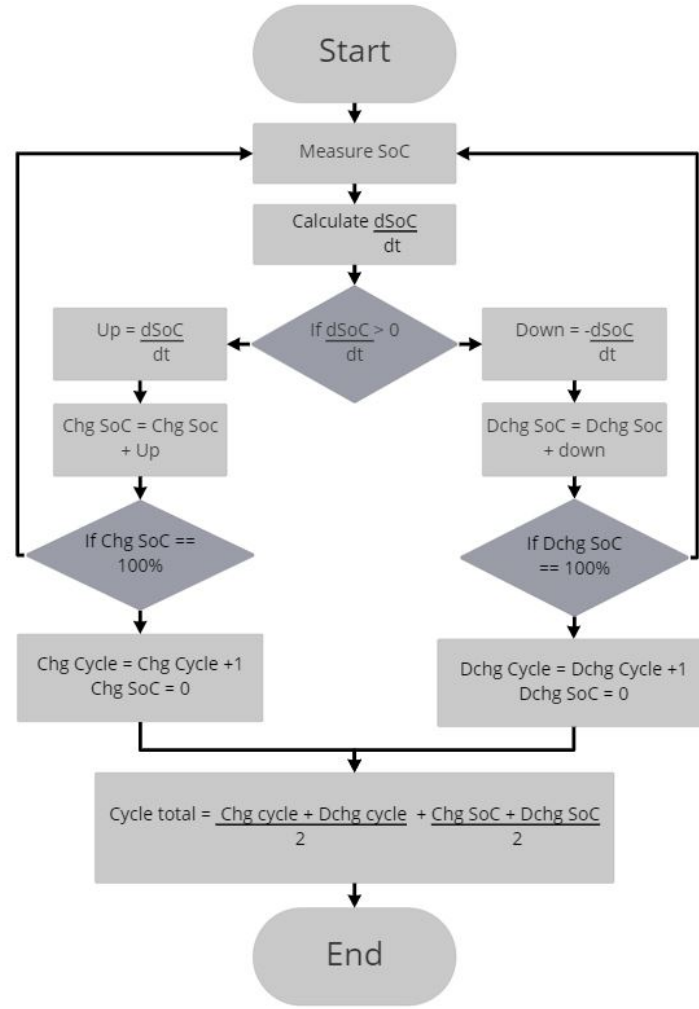


Figure 5.5: Flowchart illustrating the cycle counter based on ΔSoC for grid tide BESS subject to microcycles.[73]

The cycle counter was based on SoC and the relative change with respect to time, $\frac{d\text{SoC}}{dt}$. By recording the SoC continuously and calculating its derivative, one half-cycle was added when ΔSoC had reached 100%. The counter considered both negative and positive ΔSoC , i.e. both discharge and charge cycles before adding them together and dividing them by two to achieve the number of full cycles. To calculate the estimated lifetime, firstly a capacity factor was taken into account. This factor considers how often the energy system produces energy or in other words, the ratio between actual produced energy and the maximum possible energy production. It was estimated a capacity factor at 0.4 for wind power and 0.25 for solar production. Secondly, number of cycles was scaled up to get cycles/years. Thereby dividing total number of cycles in a lifetime by cycles/years to obtain estimated lifetime in years as shown in equation 5.2.

$$\text{Lifetime} = \frac{\text{Cycles}_{\max}}{\frac{\text{cycles}}{\text{hour}} \cdot \frac{\text{hours}}{\text{year}}} \quad (5.2)$$

5.4 LiC integrated in renewable energy production plant

Figure 5.6 shows the construction of the LiC integrated in a wind and solar power plant. The construction displayed in the figure is simplified for visual purposes, whereas the actual construction used can be seen in appendix C.1. It is similar to the construction displayed in Figure 5.1 with a few more components. An input signal was added, containing the actual and average power data. The input signal along with the state of charge-values from the battery were used as inputs to the BESS controller. The controller was then connected to the controlled current source. In addition, the cycle counter was included to keep track of the BESS lifetime.

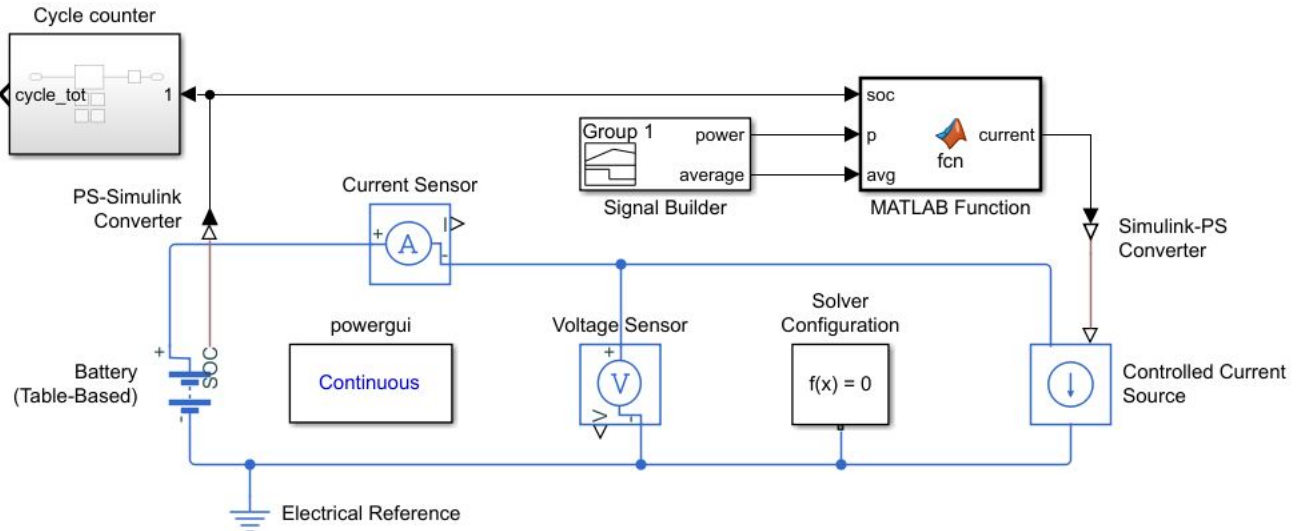


Figure 5.6: Simulink illustration; The complete construction of a lithium-ion capacitor integrated in a wind power plant in Simulink containing a signal builder, cycle counter and BESS controller. The figure is simplified for visual purposes

5.5 LiC integrated in energy shifting-system for a solar power plant

The combination of LiC and LiB for energy shifting was investigated further. Due to the LiC's exceptional power density and LiB's energy density the combination of the two had desirable characteristics. Both the LiC and the LiB was constructed as the modules above, although the control strategy was altered. It was altered in a way that played to the advantages of each component. By assigning most of the energy demand and the slow power variations to the LiB while the LiC still covered the fastest power variations, a desired result could be obtained.

As before, the control strategy was based on a moving average of the input power, however in this case the grid demand was taken into account. If the production exceeded the grid demand, the LiB accommodated by the LiC would store the energy and shift it to when the demand exceeded the production. This strategy led to a production curve similar to the grid consumption. To control the symbiotic interaction between the LiC and the LiB, a control algorithm was prepared, but first a reference system was created.

5.5.1 Creating a reference system, LiB in solar

To fully express the impact of LiC integration in an energy shifting-system, firstly a reference system was created. The reference system was set to consider the solar production power, its average and the grid demand in addition to a constant base production. If the power production was above the demand, the LiB would store the energy between \pm a constant value of the average, which could later be released during peak-load periods. To protect the LiB from rapid power variations and high C-rates it was set not to consider the highest peaks, but only the energy in between the \pm average range. This led to a more gentle charge characteristic, however some of the energy was then lost due to the LiB's insufficient power characteristic. Lastly the LiC was introduced in the system allowing the comparison between the reference system and the combination system. The setup can be seen in Figure 5.7, which displays a large system containing the LiC and LiB constructions as smaller systems. This system has been simplified for visual purposes, whereas the actual system used can be seen in appendix C.2.

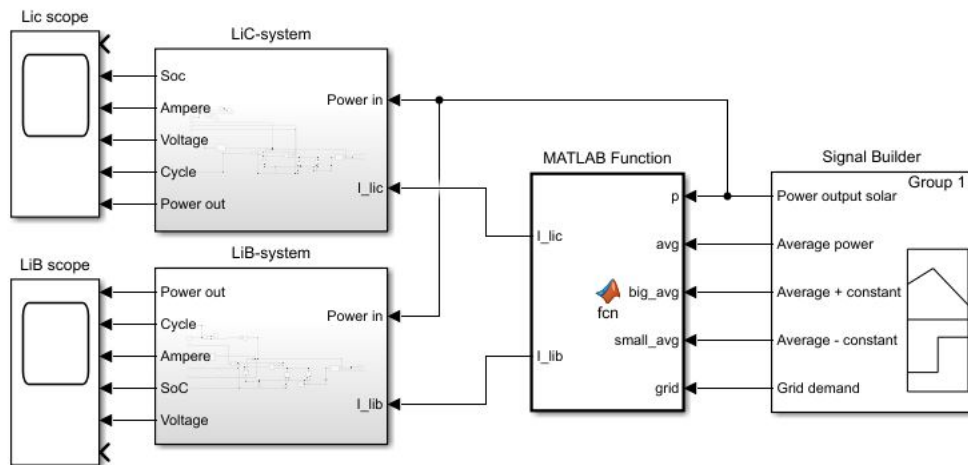


Figure 5.7: Simulink illustration; LiC and LiB systems integrated in an energy shifting-system for a solar power plant. The system is simplified for visual purposes

The LiC and the LiB where both, as explained above, assigned different tasks. The LiB was designed to cover the values within a range of ± 100 kW of the average power. That is, if the power was between ± 100 kW of the average power, the LiB would handle the stabilizing and storing single-handedly. 100 kW was selected as this gave a desirable ratio between the LiC and LiB capacity while still respecting the inferior power characteristics of the LiB. On the other side, if the measured power was above ± 100 kW of the average, the LiC would work in combination with the LiB. A MATLAB script containing the controller code can be seen in appendix B.2. The input signal and the average values was later scaled by a factor of 10 000 to simulate a full scale solar power plant. In addition to shaving the peaks, the LiC also supplied the Lib with power in the event of a sudden power drop in the solar production. This led to a beneficial charge characteristic within the C-rate limitations of the LiB. Hopefully it would both protect the LiB and increase its longevity. The LiC was dimensioned by following the same methodology as in the previous solar power case whereas the LiB was dimensioned after the required energy amount. The solar power, the calculated average with ± 100 kW and an estimated grid demand is shown in Figure 5.8. This figure also contains a base production constantly at 300 kW, representing power production from sources such as hydropower or thermal power.

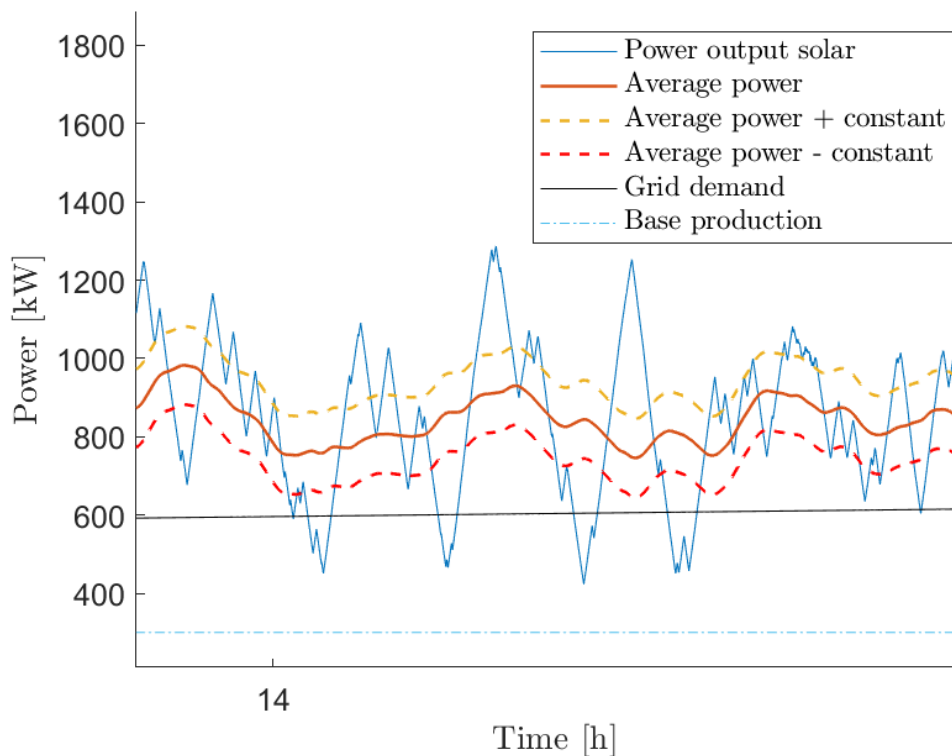


Figure 5.8: *Solar power production, calculated average with a \pm constant, estimated grid demand and base production*

6 Results and Discussion

The following section will present detailed results both from the design process and the simulations themselves. Additionally economical aspects will be included in order to evaluate the profitability of the technology. The results will then be discussed in sections following different categories. At the end, the sustainability and footprint of the LiC will be discussed.

6.1 Design of BESS

Included in the results of the BESS design are the design parameters obtained after the dimensioning process was completed. The detailed design parameters of the LiB is not included due to the focus of the rapport being on the LiC-technology.

6.1.1 Design and dimensioning process

The dimensioning process focused on connecting single LiC-cells in series and parallel based on the requirements described in the methodology section. For the wind power plant application, 230 cells were connected in series to form a rack and then 30 of these racks were connected in parallel to obtain the desired capacity. For the solar power plant the rack was constructed to be the same size, but then 90 were connected in parallel due to a higher capacity demand. For the energy shifting-system the same number of cells were connected in series, but 63 were connected in parallel. When the LiC cells was connected in such a way it was possible to extract the desired design parameters from the excel-spreadsheet. These design parameters include the capacity, resistance and open cell voltage for different SoC-values and are presented in table 6.1. The values were entered into the table-based battery for the simulations. As seen from the tables, the LiC has the same OCV-values in all the applications. This is because the same amount of cells were connected in series to obtain a voltage of 690 V, corresponding to the low voltage side of the transformer in the wind power plant. However, the resistance and capacity values are different due to different capacity-demands for the applications.

Table 6.1: *Design parameters of LiC integrated in different systems, including values for the resistance, capacity and open cell voltage at different state of charge-values*

LiC integrated in:	Wind power plant				Solar power plant				ES-system			
Capacity [kWh]	220.8				662.4				463.7			
Resistance [Ω]	0.0021				0.0007				0.001			
SoC [%]	0	10	20	30	40	50	60	70	80	90	100	
OCV [V]	460.0	531.8	571.4	613.4	659.5	714.5	760.4	797.1	830.7	876.3	920.0	

As seen from the table the installed capacity is smaller in the energy shifting-system than in the solar power plant, even though the LiC is implemented in the same solar power plant. The reason being that the energy shifting-system also contains a LiB. The LiB handles the middle portion of the power fluctuations which means that the amount of energy the LiC has to handle is smaller and the capacity is therefore reduced.

The voltage of 690 V from Lista was assumed to be representative for the solar power plant as well, even though it is not accurate. It is reasonable to assume a higher voltage value for the solar power plant due to its larger size. However the solar power plant was scaled down to be within the same magnitude as the wind power plant, so the difference between the assumed and actual voltage value is not of great significance.

Several simplifications, which may have impacted the results of the simulations, were made regarding the design of the LiC and LiB. Firstly, the parameters entered into the table-based battery were only given for 11 different SoC-values. Additionally the battery parameters were not tabulated over temperature. In real life, battery characteristics are altered with changing temperatures. The battery behaviour would have been more accurate with an increased number of values for the OCV and if the battery characteristics considered the surrounding temperature. However these assumptions were made in order to complete the simulations in reasonable time, additionally the desired results were possible to obtain regardless.

The line loss between different components in the simulations were neglected. Realistically there would have been line losses in the transmission lines between the power source and the storage technology and from the storage technology to the regional grid. It would have been easy to take the line loss into account by calculating it and then reducing the amount of power that was transferred between the different components in the simulations. However the length of these lines would have been hard to find seeing that the simulations are of imaginary systems. In addition to this, other components usually found in such complex systems, were also neglected. Electric power systems usually contain components such as transformers, rectifiers, voltage regulators and loads. If these components were to be included, the simulated system would have been much larger and much more complex. Even though including these components would have portrayed a more realistic system, they were neglected due to restricted time and resources.

6.2 LiC integrated in renewable energy production plant

The LiC was integrated in two different renewable energy production plants; a wind power plant and a solar power plant. In addition, it was integrated in a solar power plant already containing a LiB used for energy shifting.

6.2.1 Wind power plant

Figure 6.1 shows the power output from 31 wind turbines at Lista and the stabilized power output after implementing a 220.8 kWh LiC. The original power varies from about 2MW to 23 MW within the hour with several rapid power fluctuations, whereas the output power after the LiC was implemented varies significantly less (3-16 MW). The MATLAB-script shown in appendix B.4 calculated that the number of fluctuations exceeding 20 kW/s was reduced by 47% after the LiC implementation. This amount of fluctuation in the power output is decided by the capacity of the LiC, in addition to the control algorithm, which could be adjusted to some extent to fit the current requirements. The data points are gathered at an arbitrary day and is set to represent a standard production hour at the wind power plant. Although the fluctuation in production could vary from day to day, from some days with more stable production, to days with larger variations. The total production variation is somewhat taken into account by the capacity factor used in calculating the cycle stability.

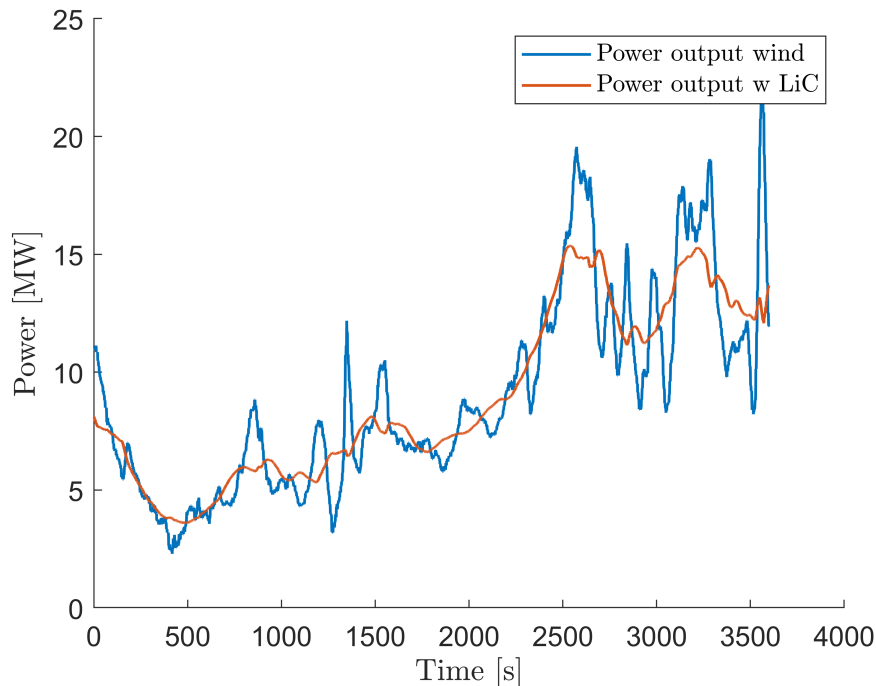


Figure 6.1: Wind power output and power output in MW after implementing the LiC-system during one hour

Figure 6.2, shows the number of cycles the LiC is subject to due to several micro-cycles. The cycle counter increase almost linearly with some variations at points where the power fluctuation are the greatest. The figure depicts the relationship between capacity and number of cycles

by presenting three different capacities, rated capacity and $\pm 30\%$ of rated capacity. At rated capacity the LiC is subject to roughly 1.1 cycles per hour corresponding to a lifetime of 10.4 years as shown below in equation 6.1. A capacity of $\pm 30\%$ corresponds to respectively 0.8 and 1.5 cycles per hour and a lifetime of 14.3 and 7.61 years.

$$\text{Lifetime} = \frac{\text{Cycles}_{\text{max}}}{\frac{\text{cycles}}{\text{hour}} \cdot \frac{\text{hours}}{\text{year}}} = \frac{100\,000}{1.1 \cdot 8760} = 10.4 \text{ years} \quad (6.1)$$

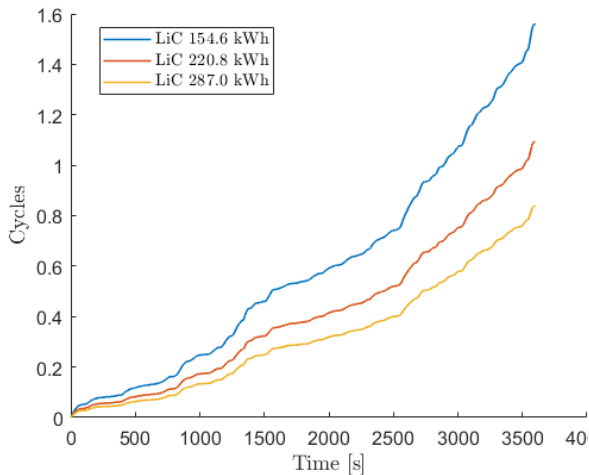


Figure 6.2: Numbers of cycles for LiC due to micro cycles at three different capacities while stabilizing one hour wind production

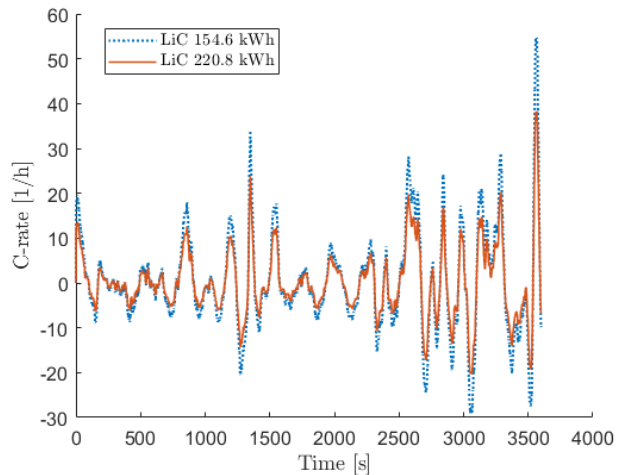


Figure 6.3: C-rate for two different LiC capacities during stabilizing of one hour wind production

Figure 6.3 shows the C-rate at which the LiC is charged and discharged during stabilizing of wind power. The figure shows the C-rate for two different capacities, one at rated capacity (220.8 kWh) and one at 70% of rated capacity (154.6 kWh). At rated capacity the absolute value of the C-rate is rarely above 20, however at a lower capacity the C-rate increases. Negative values represent the C-rate during discharge while positive represent charging. It is evident that the variation in C-rate is closely related to the fluctuations in the wind power.

From Figure 6.1 it is evident that the introduction of LiC in wind power generation is beneficial for stabilizing the power output. The LiC was dimensioned and programmed to obtain this exact result. By minor adjustments to the control algorithm and a different LiC capacity, both a more and less stable power output could be obtained if desirable. This would in some cases be beneficial since the degree of stabilization needed is dependent on the penetration depth of IRES in the energy system. By taking this into account, both over and under dimensioning could be avoided. This perspective is not within the scope of this paper, however considering the penetration level of IRE in the energy system is an important aspect when implementing and dimensioning the LiC and will be further discussed below in section 6.3, "Improving power quality". This paper only considers if LiC is a viable solution and not to what extent.

When dimensioning, the procedure presented in the methodology was followed. After the voltage level, power and energy capacity was within the required range it was found that the C-rate and number of cycles was the limiting factor. As shown in Figure 6.2 and 6.3 the lifetime is influenced by a reduction in the capacity. Not only due to more cycles per hour but also a higher C-rate which goes beyond the rated value. This is due to both the C-rate and the cycle counter's dependency on ΔSoC which is opposite proportional to the capacity. As shown in Figure 6.2 and equation 6.1, the number of cycles is used to estimate the lifetime of the LiC. This estimation is solely based on Beyonder's projected lifespan and cycle stability obtained from their testing facilities and research process. The cycle stability of 100 000 cycles could therefore be subject to estimations not accounted for by this paper. Since the dimensioning process was defined by the cycle stability it is crucial, for a correct result, that this value is correct, as well as the cycle counter itself. It is assumed that the cycle stability accounts for various variables such as cycle and calendar ageing, lithium plating and SEI formation as presented in "Ageing mechanisms" in section 4.2.2. However the cycle counter itself could be a source of error. This algorithm is heavily based on ΔSoC with respect to time which is given directly from the battery block in Simulink, leading to uncertainties with obtaining the SoC value. Although it could be argued that this method, despite of it's imperfections could give a rather accurate estimation of the LiC's lifetime.

The C-rate is, as the cycle counter, also dependent on the change in SoC with respect to time. The C-rate is a property of the LiC and exceeding it could cause irreversible damage to the storage device and affect its lifetime. The control algorithm does not take the C-rate into account, and the LiC is therefore dimensioned thereafter. Here, the algorithm could be changed to account for high C-rates, protecting the LiC and preventing over-dimensioning. If the control algorithm detects rapid variations in SoC leading to high C-rates, it could disconnect and spare the LiC. This would on the other hand cause a power spike in the production, leading to issues in the power grid. To avoid this, the LiC has to be dimensioned to handle the utmost fluctuations during the entire year. However, this may not be justified as dimensioning the storage device for the worst case scenario will leave the LiC poorly utilized a vast majority of the time. It could therefore be argued that it would be beneficial to introduce a fail-safe to enhance the longevity of the storage device.

6.2.2 Solar power plant

Figure 6.4 shows the solar production and the stabilized power output after implementing the LiC at rated capacity (662.4 kWh) and at 70% of rated capacity (463.7 kWh) between 7am and 7pm, while Figure 6.5 displays a more detailed version of the same result. It is evident that the fluctuation in power output increases with the decrease of the LiC's capacity. At rated capacity only a few spikes is left behind, however at a capacity of 463.7 kWh, multiple spikes and dips pass through. Nonetheless, this result is still a major improvement. The MATLAB-script shown in appendix B.4 calculated that the number of fluctuations exceeding 20 kW/s was reduced by 92% after the LiC implementation. This result is, as for the wind power case, also dependent on the control algorithm and the dimensioning of the LiC. The solar power can, at a given hour, fluctuate between 12 MW and 4 MW. By introducing the LiC, the fluctuations are reduced to a fraction of the previous case. Also in this case it is assumed that the fluctuations presented below is representative for an entire year, however a capacity factor of 0.25 is accounted for when calculating the lifetime.

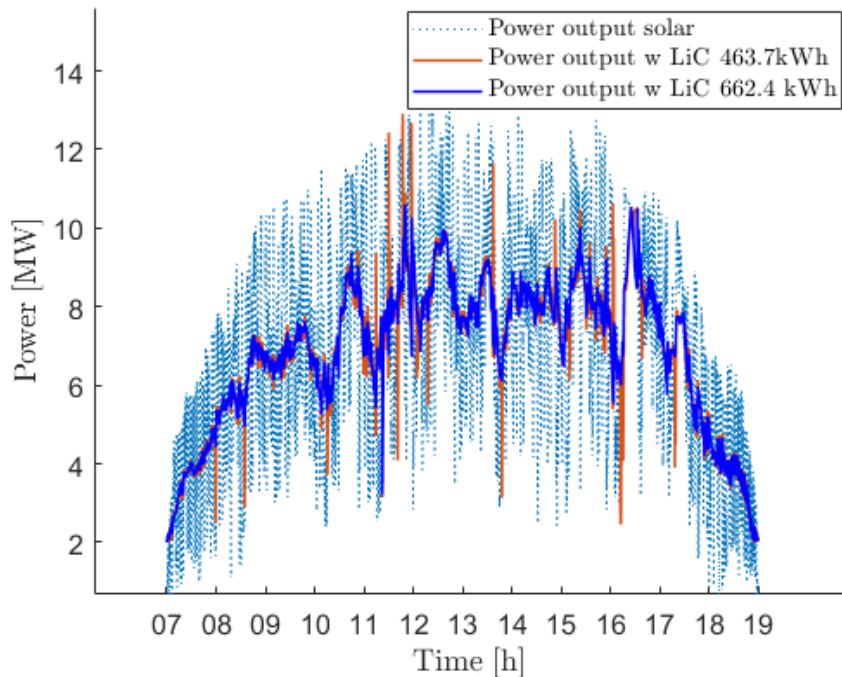


Figure 6.4: *Solar power and power out after stabilizing with LiC at two different capacities*

Figure 6.6 displays the SoC during two hours at midday at two different capacities. It is evident that at a smaller capacity the LiC maximizes its SoC more frequently and is beyond this point not able to further stabilize the power output. The LiC is set to stay within 0.1 and 1, or 10% and 100% SoC.

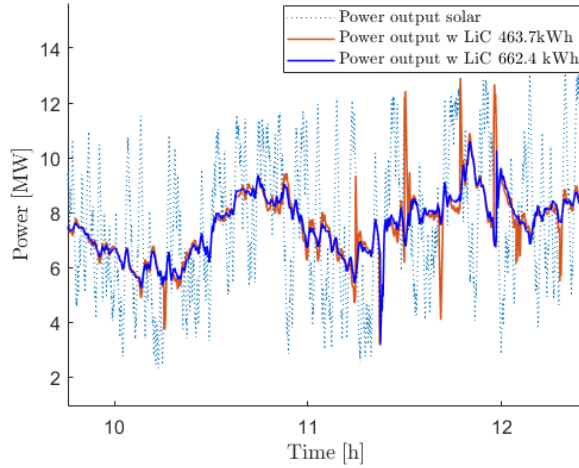


Figure 6.5: Solar power and power output after stabilizing with LiC at two different capacities, magnified

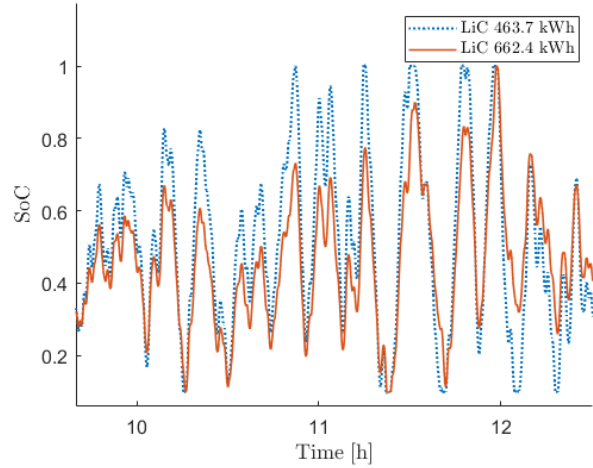


Figure 6.6: SoC for LiC while stabilizing solar power at two different capacities

Figure 6.7 shows number of cycles the LiC is subject to due to several micro-cycles during the 12 hours of solar production. Three capacities are shown, one at rated capacity of 662.4 kWh and two at $\pm 30\%$ of the rated capacity. The smallest LiC is subject to about 10 full cycles corresponding to a lifetime of 27 years, while the largest is subject to 5.5 cycles corresponding to 50 years. The LiC at rated capacity has a lifetime of 40 years.

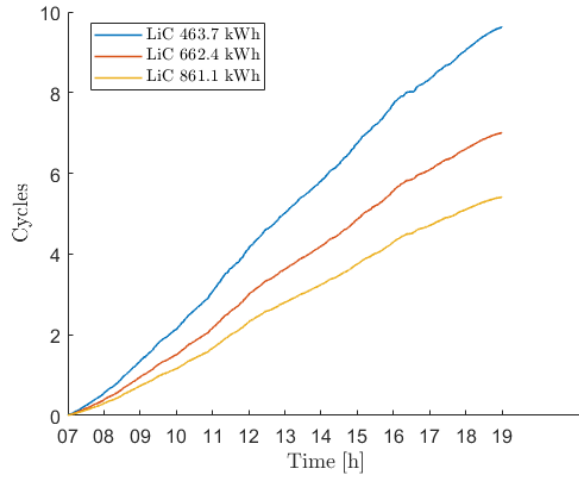


Figure 6.7: Numbers of cycles for LiC due to micro cycles at three different capacities

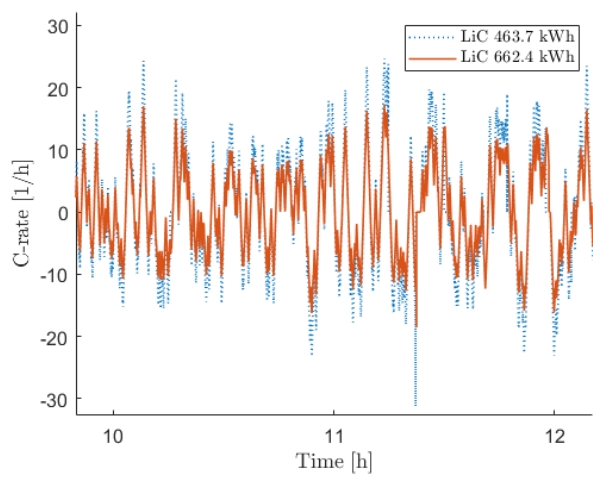


Figure 6.8: C-rate for two different LiC capacities during stabilizing of solar production

Figure 6.8 demonstrates the C-rate during charging and discharging over a period of about two hours midday for two different capacities. Negative values represent the C-rate during discharge while positive represent charging. At rated capacity the C-rate stays within a C-rate of ± 20 , however some deviation from this may be found if the LiC's capacity is reduced by 30%.

As in the wind power case, the solar power converges around a moving average as Figure 6.4 shows. However, in this case, especially at lower capacities, the power output contains several dips and spikes. This is due to the fact that the LiC maximizes its SoC as shown in Figure 6.6, making it unable to further stabilize the power. Since solar power does not contain as rapid fluctuations as wind power, the peaks consists of a larger amount of energy. This amount of energy is also the reason for why the capacity of the LiC has increased with a factor of three from the wind power case, even though both cases delivers output power at roughly the same magnitude. The LiC was in this case not dimensioned based on C-rate and cycle stability, but rather the amount of energy the LiC was required to maintain. If a smaller capacity would be desirable, it could be obtained by altering the control algorithm and minimize the window size of the moving average. This would lead to a more fluctuating power output closer to the actual power, but it reduces the size of the LiC.

In contrast to case 1 where cycle stability and C-rate were predominant factors in the dimensioning process, they did not affect the capacity in case 2. This can be seen in Figure 6.7 and 6.8 as number of cycles corresponds to a lifetime of 27-50 years for the different capacities, and the C-rate is within the limit. However at smaller capacities the C-rate limit of ± 20 is to some extent exceeded. This is most likely due to the fact that the LiC has a much higher capacity in this case. I.e if the algorithm was altered to give a less stable output signal and the capacity was reduced it is likely that it would result in the same cycle stability as in case 1.

The lifetime of 27-50 years, for the different capacities, derived from the simulation is a lot higher then what Beyonder suggested. The reason being that the LiC had to be dimensioned with a high capacity in order to cope with the large energy amounts associated with the solar power production. When the capacity is very high, the LiC does not undergo as many cycles during a day as it would do with a smaller capacity. However the LiC in this case will not survive 27-50 years as the lifetime is decided by the limiting factor either being the calendar life of 15 years or the cycle stability of 100 000 cycles. In this case the LiC reaches the calendar lifetime limit first, meaning that it will have to be replaced after 15 years.

6.2.3 Energy shifting-system (solar power plant)

Figure 6.9 and 6.10 shows the amount of power assigned to both the LiC and the LiB respectively throughout the day. From the magnified figure it is evident that the LiC is assigned the high peaks and the low valleys while the LiB handles the power in between. The LiC is then responsible for protecting the LiB from rapid power variations giving it a more beneficial charge and discharge characteristic.

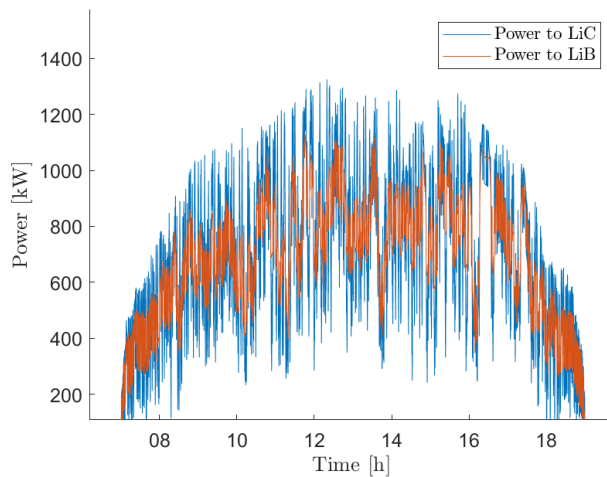


Figure 6.9: *Power assigned to LiC and LiB respectively for the entire day*

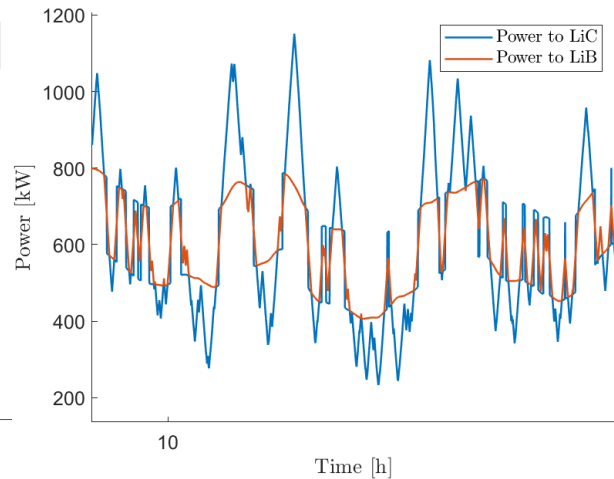


Figure 6.10: *Power assigned to LiC and LiB respectively, magnified*

Figure 6.11 and 6.12 shows the energy shifting reference system and the same system after the introduction of a 463.7 kWh LiC. The blue curve represents the solar power whereas the black curve simulates an estimated grid demand. Meanwhile, the red curve shows the power output delivered to the grid after the introduction of the ESS. In Figure 6.11 it is evident that some of the energy is not shifted due to the LiB's insufficient power density. This causes the power curve to dip off earlier in the evening, compared to the case with LiC and LiB in combination. It is also shown that the power output fluctuates to a substantial extent when the LiB is single-handedly responsible for the energy shifting, whereas a large degree of these fluctuations are filtered out when the LiC is introduced.

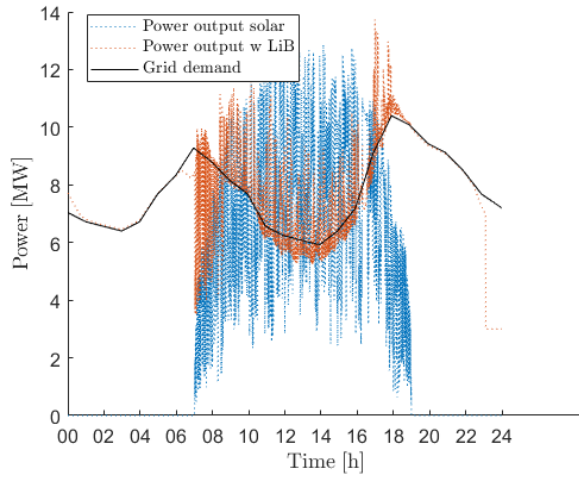


Figure 6.11: Power output from LiB with solar output power and grid demand

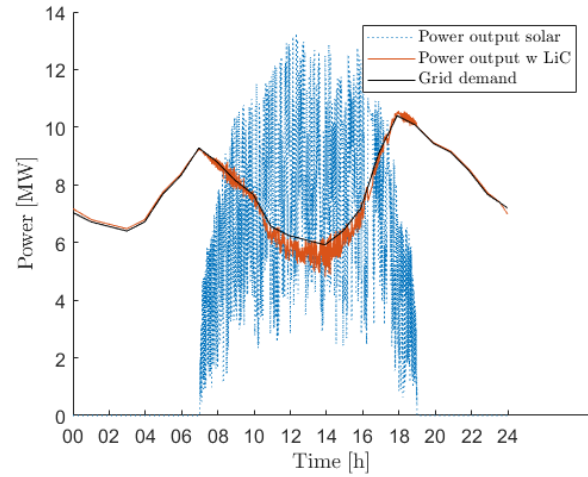


Figure 6.12: Power output from LiC and LiB with solar output power and grid demand

Figure 6.13 shows the number of cycles the LiB is subject to as a result of shifting the solar production to cover the peak demand. When not accommodated by the LiC, the LiB runs through approximately 1.4 cycles whereas this number is reduced to 1.15 after the LiC introduction. It is evident that the two scenarios follow the same charge and discharge pattern as there is a close correlation between the two curves.

In Figure 6.14 the C-rate for the LiB is presented, both with and without the LiC's assistance. In both scenarios the C-rate stayed well within the maximum C-rate of 1C, however the C-rate for the reference system has larger fluctuations at a greater magnitude than the scenario with the LiC. The figure only contains values between 7 am and 7 pm as the daylight hours are of highest interest. The C-rate for the LiC fluctuates between ± 15 , this result was however not plotted.

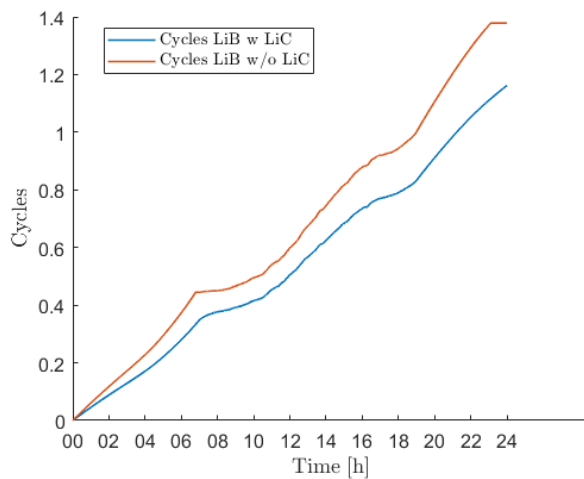


Figure 6.13: Number of cycles for LiB at two different capacities during energy shifting

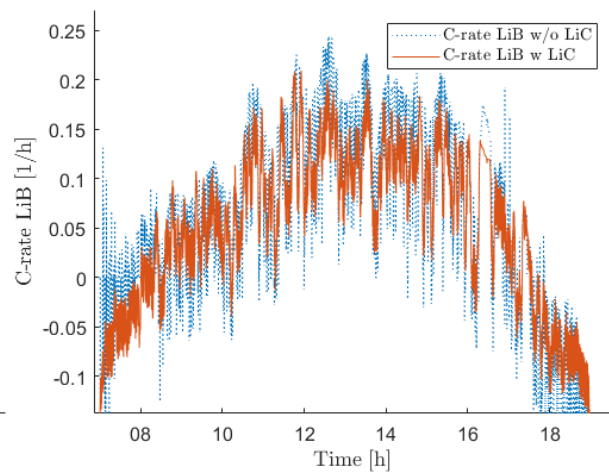


Figure 6.14: C-rate for LiB at two different capacities during energy shifting

In contrast to case 1 and 2, case 3 is not only set to handle the fluctuating power output from IRES but also to shift the energy to match the prevailing energy demand. Figure 6.9 shows how the energy is distributed between the LiC and the LiB. This distribution is based on a moving average where the LiB covers the area between ± 100 kW of the average. This value is dependent on the power characteristics of the LiB in addition to the capacity of the LiC in proportion to the LiB. The value gave a desirable ratio between the LiC and LiB capacity while still respecting the inferior power characteristics of the LiB. It is noteworthy that these compositions could be altered to better fit the need of each power system. By looking at the need for energy storage and the amount of fluctuations in a power system, a tailored storage system with an adjacent control algorithm could be obtained.

The control algorithm for the LiC is similar to the algorithm for the previous cases, however it only considers the energy above and below the \pm average mark. The LiB algorithm is set to consider the grid demand and the total energy production, consisting of a base production and the solar production. In this case the grid demand is only constructed for illustrative purposes where the main objective is to make the production match the consumption curve. The algorithm of the reference system was constructed in similar manner to the final scenario. However in the final scenario the LiC provided the LiB with power in case of a sudden power drop in the solar production, causing a gentler charging characteristic. In the reference system the LiB had to handle these dips single-handedly, whereas the high peaks was ignored by the LiB in order to not exceed its C-rate and power limitations and to avoid over-dimensioning. The fact that this led to an insufficient energy shifting is discussed below. A thorough dimensioning process of the LiB system is not within the scope of this paper, where rather the effect of the introduction of the LiC is emphasised. With this in mind the LiB was dimensioned to be able to handle the energy requirements between the grid demand and the power production. The solar input signal was as for case 2, assumed to be representative for the entire period when the capacity factor was accounted for. However, in the word of Nicholas Etherden and Math H. J. Bollen:

As a prolonged period of overproduction will fill even the largest energy storage, it is in practice not justified to dimension the energy storage for the worst case as its capacity would be poorly utilized the vast majority of the time [74].

The LiC was dimensioned to handle the energy amount, however in contrast to case 2 the energy amount was not the limiting factor. This is mainly due to the symbiotic interaction between the LiB and the LiC. In this case, the C-rate was the limiting factor. The LiC was then scaled to where the C-rate did not exceed its limitations. Section 4.2.2 in the theory section enlightens how the C-rate affects the internal resistance, and thereby the heat production in the cell. This can lead to a fading of the capacity, which is due to the increase of charge transfer resistance at the SEI.

By introducing the LiC to the system, the LiB did not have to cope with the largest power variations. In order to handle these, the LiB would have to be dimensioned an extensive amount since it has a relatively low power density. Reducing these variations means a reduced amount of stress on the battery. As mentioned in the theory section, too much stress can lead to a faster degradation of the battery caused by the ions being moved between the cathode and anode. This pushing and pulling can lead to battery failure before the calendar lifetime would dictate.

Diminishing the degree of degradation leads to the batteries not having to be replaced as frequently. Not having to reinvest multiple times, means less batteries in circulation. To neither have to produce nor recycle as many devices, will help in reducing greenhouse gas emissions over time.

Figure 6.11 displays the reference system where a LiB is the only energy storage used. The red graph in the figure deviates significantly from the grid demand, when the variations in solar radiation is at its greatest. Since the LiB is not able to embody all the variations, this energy will not be exploited. This means that a potentially large amount of energy is lost, leading to a loss of income accordingly. Not only will the energy not be utilized but the rapid power fluctuations are not stabilized and can create imbalances and problems in the grid.

As displayed in Figure 6.13, introduction of the LiC reduces the number of cycles from 1.4 to 1.15 per day. This results in a decrease of 18% from the reference system to case 3. The cycle counter is as previously explained, dependent on several factors. Since the LiB is, in contrast to the reference system, able to store and shift more energy when combined with the LiC, it required a somewhat higher capacity. If the capacity had been held constant the SoC would reach its maximum several times. This would again lead to an insufficient energy shifting with several spikes and dips at the point where the SoC reaches its max and min value. The control algorithm does not incorporate this aspect, which in turn could lead to an inaccurate result due to the re-dimension process. To avoid these inaccuracies the control algorithm could be altered to incorporate some form of prognostic data or statistics to better utilize the battery's capacity throughout the day. However it is assumed that the increase in capacity from the reference system to the final scenario is to some extent annulled by the increase in shifted power. It could therefore be argued that the decrease in number of cycles could be legitimate. Although, this decrease may not be adequate to justify the investment cost of the LiC. Beyond estimated that the LiC could potentially double the LiB's lifetime, however this was not obtained in the presented results. It could be discussed that by altering the control algorithm and the LiC's capacity a greater effect on the LiB's lifetime might be observed. If the LiC covered a greater portion of the power by curtailing the area covered by the LiB, i.e., reducing the LiB capacity, the LiC could have a greater influence on the total lifetime. As the LiC is nowhere near its maximum cycle stability it has the ability to assist the LiB more, however the C-rate and energy amount must still be taken into account to assure a safe and sustainable operational life.

6.3 Improving power quality

The above results accumulates in several mutual aspects. Mainly concerning stabilizing of power fluctuations leading to increased power quality. As presented in the theory section "Reliability of supply: power, voltage, and frequency" (4.1) the power quality is an important aspect of the modern power system and the reliability of supply. All cases, case 1 and 2 in particular argues that a more stable power output leads to better power quality. The power quality is composed of voltage quality and the variations in frequency. By utilizing equation 6.2 it is evident that the variations in voltage and then also the voltage quality is dependent on the produced power. However, as briefly discussed in section 6.2.1, the control algorithm and dimensioning process could easily be altered to fulfill the need at different systems. This need is dependent on several factors such as the IRES penetration which is discussed below, and the consumption pattern. This makes it difficult to quantify the stabilization required to maintain an adequate power and voltage quality. The frequency on the other hand is less dependent on the fluctuation in power production and more dependent on the difference between production and consumption. However, it is harder to match a fluctuating production to the consumption, therefore a more stable production will also be beneficial for the power system and less prone to frequency variations. It could be argued that a system designed to improve the power quality should be a function of voltage quality and frequency itself, however, this would be utmost difficult as several simplifications were made to the system. Such as not considering the power generation as a three-phase, alternating current system, but only as a power signal and its magnitude. The concept is however anchored in theory and simplified for simulation purposes, but this simplification makes it hard to include voltage quality and frequency as numeric values. It is therefore only argued that a decrease in power fluctuations leads to an increase in power quality although there are several influential factors left out.

$$\Delta U = \frac{RP + XQ}{U_{PCC}} + j \frac{PX + QR}{U_{PCC}} \quad (6.2)$$

There are several benefits with a stable IRE production apart from higher power quality. A less fluctuating production could lead to a more optimal production from base-load plants, as these would not have to respond to peak demands in the case of sudden power drop from IRES or an imbalance between the production and the consumption. However this fast response or frequency response is not usually the area of responsibility for base-load production but rather fast-responding plants or peak plants. These plants initiates the initial response and the primary control stage explained in the theory section "Frequency" (4.1.3) to compensate for the imbalances. If these peak-power plants are fossil-based, one can obtain a reduction in CO₂ emissions by introducing more stable intermittent power production. This result could also be obtained by matching the production to the consumption. By introducing energy storage and energy shifting one could diminish the need for peak power plants and obtain an overall better power quality and an increased reliability of supply making it easier to increase the IRES penetration.

6.4 IRES penetration

By implementing a LiC to the power grid, a larger percentage of the energy from IRES gets exploited. Regarding wind and solar power production, the stabilized power output reduces energy lost caused by low quality voltage and frequency. For the last case, with energy shifting, energy loss was reduced compared to using a LiB alone. Since a LiB has too low of a power density, it is not able to store all of the greatest fluctuations in the solar irradiation. As a result of this, some of the energy and thereby income is lost. With the LiC implemented, the amount of lost energy is almost completely diminished. This reduction in energy loss points to a reduction in the need of non renewable energy sources as well.

The advantage of non renewable energy sources is its flexibility to fit the grid demand, which does not apply to IRES being directly connected to the grid. Being able to stabilize the production from IRES opens up for an increased degree of implementation. The higher percentage of implementation, the higher the need for a stable, high quality power output. For instance a system with 40% IRES penetration would require a more stable output power to obtain the same power quality and energy security as a system with only 20% IRES penetration. By other means, in order to implement a higher percentage of IRES, a stabilizing technology is needed to maintain a high delivery security. This necessity is ever increasing with the current electrification of the society. An increased implementation of stabilised energy production from IRES will be an important step into phasing out non renewable energy sources. With a technology like Beyonder's, this will not happen at the expense of the security of supply. The solution will not only help with environmental, but also financial savings. A better utilization of the IRES increases the power producers income which furthermore reduces the consumers electricity price, however to achieve this a substantial investment cost is required.

6.5 Economical aspects

The implementation of lithium-ion capacitors in full-scale renewable production plants entails large investment costs which are dependent on the installed capacity. The total investment cost, for different applications, was calculated by multiplying the installed capacity with the prices per kWh presented in table 4.1. Table 6.2 shows a total investment cost of 220 800 \$ and 662 400 \$ for respectively a wind and solar power plant. The installed capacities corresponds to a LiC-pack with a total weight of 2.8 tonnes for the wind power plant and 8.3 tonnes for the solar power plant. With regards to the energy-shifting system the total investment cost is 463 700 \$, which is smaller than for the solar power plant even though the solar power plant is the same size in both simulations. This is because the energy shifting-system also contains a LiB which handles a portion of the energy.

Table 6.2: *Installed capacity, price and weight of LiC-system for three different applications*

Application	Installed capacity	\$/kWh	Total price	Total weight
LiC in Wind	220.8 kWh	1000	220 800 \$	2 760 kg
LiC in Solar	662.4 kWh	1000	662 400 \$	8 280 kg
LiC in ES-system	463.7 kWh	1000	463 700 \$	5 796 kg

When comparing the investment cost of a LiC to that of different lithium-ion batteries it can be seen that it is much higher. This applies to all of the different LiBs, including LFP, NMC and LTO. On the other hand the investment cost for a LiC is only a tenth compared to a supercapacitor as presented in table 4.1. The price differences are easily justified when taking the calendar life and cycle stability into account, whereas the price increases with increasing life time. On the other side lithium-ion batteries and supercapacitors have different properties and therefore applications, and can not fill the same demands as a LiC. Since there is a correlation between C-rate and price per unit of power, and the LiB has a lower power density and a lower C-rate, it would require an over-dimensioned system in order to produce the same results as a LiC. In that way a LiB would have a higher investment cost than a LiC even though the price per kWh is lower. Nevertheless if power over a longer period of time is desirable, the LiB is a more economical sustainable solution. As explained in the theory section and equation 4.7, the LiC, with a C-rate of 20, becomes less expensive per unit of power the higher the required C-rate is. At even shorter times (<20 sec) and higher C-rates the supercapacitor enters its domain with a C-rate between 360-3600 [60].

Whether or not the investment cost of the LiC can be justified, it is necessary to size it up against the cost of the production plant it will be implemented in. The simulated wind power plant had an installed capacity of 71.3 MW. The total cost of installing a wind in Norway is about 1325 \$/kW which equals a total investment cost of almost 95 000 000 \$ [75]. By comparing the investment cost of 220 800 \$ for the LiC-system for this application it can be seen that it makes up only 0.23% of the total cost. The same can be seen for the solar power plant which has an investment cost of around 950 \$/kW [76]. However the lifetime of the LiC-system is a lot shorter than the lifetime of the renewable energy production plants. The LiC-system

is simulated to last about 10.4 years, while the normal life expectancy of a wind and solar power plant is respectively 20-25 years and 30-40 years. This means that the investment cost associated with the LiC-system have to be made 2-3 times for the wind power plant and 3-4 times for the solar power plant. On the other hand, looking at the wind power plant, the LiC investment percentage compared to the total investment cost only increases from 0.23% to 0.70%.

The results from case 1 and 2 shows that a LiC is a great contributor to stabilize the power production. Utilizing more of the wind and solar power entails an increase in income for the power producers, which furthermore helps defending the LiC investment. In contrast to case 1 and 2, the investment cost in case 3 could bring forth several moments of uncertainties. The introduction of the LiC led to a somewhat longer lifetime in the LiB reducing the need for maintenance and replacements. Implementing the LiC also led to a better utilization of the prevailing energy. These results constitutes economical benefits for the power producers, however Beyond expected a doubling of the LiB's lifetime whereas this was not found in the presented results. As discussed in section 6.2.3 above, there could be several reasons for this deviation. Nevertheless it could be argued the shortcomings in prolonging the LiB's longevity would make it difficult to justify the LiC's investment cost.

As explained in section 4.1.1 there exists several guidelines for equipment manufacture, operation and installation. Although power providers are not federally obligated to adopt these standards for the time being, they may be in the future. If such measures become federally mandated, power providers may receive fines and be otherwise penalized which can lead to large financial burdens. As seen from the previous results the power quality was gravely improved with the implementation of a LiC-system. Since the voltage and frequency quality is closely related to the power quality it is reasonable to assume that those were improved as well. By implementing power conditioning equipment like a LiC-system, power providers may steer clear of such financial burdens in the future. Secondly the implementation of a LiC-system, and therefore improved power quality, points to reduced voltage and frequency deviations and reduced losses. Reduced losses means that the power provider has more electricity to sell, which again leads to higher incomes.

6.6 Sustainability and footprint

Since Beyonder's LiC is a somewhat new type of technology, the amount of emissions connected to its production process are somewhat uncertain. As with all types of BESS, there will be emissions from different sectors. However, Beyonder claims to have created a more eco-friendly, energy efficient and safer battery. It is made using renewable energy sources as well as ecological materials such as sand and sawdust [77]. Beyonder creates super activated carbon from forestry residue of both spruce and pine with a patented activation method. Furthermore the LiC has a relatively long lifetime compared to similar technologies, meaning that it does not have to be replaced as often. In this way emissions regarding production, transport and installation can be avoided.

6.6.1 Exclusion of critical materials

In a standard lithium-ion battery, heavy metals like nickel, cadmium and cobalt are commonly used materials. These metals are usually recovered from countries with poor working conditions, before being shipped great distances. Having materials being produced in Norway from recycled resources, is a contributor to both reducing emissions and preventing exploitation of humans.

In addition to saving emissions from recovery and shipping, the recycling process is considerably easier and more environmental friendly for Beyonder's LiC. The activated carbon is possible to recycle from the batteries after their lifetime has expired. However, in rare cases where the material cannot be reactivated, the deposition of the LiC is a lot less toxic for the environment than for a regular battery. All together this means that there is a great potential for saving the environment from toxicity using this technology [78].

6.6.2 Reduced CO₂ emissions

As showed in the theory section, the composition of a LiC is somewhat different from a LiB. The production of the cathode materials in a LiB entails the largest portion of CO₂ emissions at 28.5 kgCO₂eq/kWh [79]. Since these materials are replaced with recycled sawdust in Beyonder's LiC, the emissions from their production are thereby eliminated. Although the cathode materials in a LiC entails their own emission, they are significantly smaller.

With regards to the energy shifting simulation in case 3, the implementation of a LiC increased the lifetime of the LiB. The production of a typical LiB has a CO₂ emission of 73 kgCO₂eq/kWh considering a cradle to gate analysis [79]. Since the LiB lifetime was increased, the battery pack would not have to be replaced as many times. In that way the production emission of 73 kgCO₂eq/kWh would not occur as often.

6.6.3 Geographical production area

The production area of Beyonder's lithium-ion capacitor is localized in Norway which is a big driving factor for its sustainability. The material production for the LiC is a energy-intensive process and is supported by a Norwegian power mix. Norway is in an unique position where hydropower constitutes over 90% of the national power supply, while the rest of Europe still

relies on thermal power often driven by fossil fuels. Hydropower is considered a renewable energy source and have zero emissions during production. Another feature of the Norwegian hydropower is its ability to store power. Half of Europe’s magazine capacity is located in Norway and over 75% of the Norwegian production capacity is adjustable. The global power production makes up 30% of the total greenhouse gas emissions which makes a Norwegian-based production a sustainable choice. The average Norwegian carbon intensity is at around 28 gCO₂/kWh, which is only a fraction of EU’s at 231 gCO₂/kWh. Figure 6.15 and 6.16 below shows a comparison of the power production in Norway versus Japan, which are one of the biggest battery-producers in the world. The figure illustrates that a Norwegian-based production is the more sustainable choice [80–82].

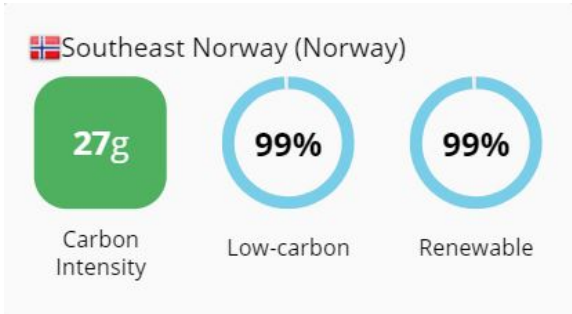


Figure 6.15: *Carbon Intensity, share of low carbon power production and share of renewable power production in southeast Norway [82]*

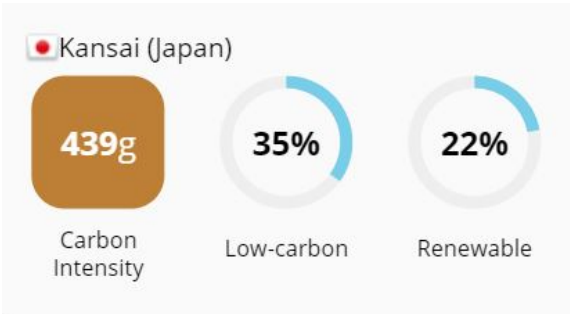


Figure 6.16: *Carbon Intensity, share of low carbon power production and share of renewable power production in Kansai, Japan [82]*

Another important factor for the sustainability of Beyonder’s LiC is that many of the materials used comes from within the country. The traditionally long and complex value chain in production is shortened. Hence Beyonder can enter long term contracts with the various suppliers which allows for better cooperation regarding environmental improvements. The use of local resources will, as mentioned earlier, also reduce emissions related to transport and allow for a more environmentally friendly excavation.

6.7 Limitations and future work

The thesis was affected by several limitations, which are presented in the list below. The list also contains suggestions on what the future work of the project would include.

- *Lack of prior research studies on the topic.* Beyonder's LiC is a fairly new technology and there exists a limited amount of available information about the technology. In addition the market is very competitive, meaning that producers of similar technologies withholds information about their own product. A limited amount of available data have had a moderate impact on the report. The simulation results are affected by the accuracy of the LiC cell parameters used. In addition the economical results are directly impacted by the price per kWh found for the LiC.

Future work would include more research and data collection on the LiC (conducting laboratory tests) as well as contacting production companies for more information.

- *Restricted bachelor thesis.* This bachelor thesis represents a first look at the implementation of LiC technology in relevant IRES and is therefore restricted to only contain simplified analyses. As a consequence of this several simplifications of the simulated systems had to be made.

Future work would include building a more accurate and complex system in the simulations. This system would take into account the line loss, auxiliary systems, temperature-tabulated battery parameters and perhaps a three-phase alternating current system in order to express sinusoidal voltage and frequency variations in real time. Additionally, more detailed market, economical (TCO) and emission analyses would be desirable.

- *Data collection.* Data collection was necessary in order to complete the simulations and to write several parts of the report. Regarding the simulation of case 2, power output data from a working full-scale solar power plant in Norway was not available. For that reason solar irradiation data from a cite in Quebec, Canada, was used. The impact of this limitation is minimal since the solar irradiation data accurately illustrates the production curve for an actual solar power plant and the data was scaled down to an appropriate size.

Future work would include obtaining high resolution datasets for an actual solar power plant, including power, voltage and frequency data. Additionally larger datasets, extending over several days, would give a better understanding of how the LiC-system operates.

- *Trade secrets.* Since Beyonder's LiC is a relatively new technology, they are somewhat reluctant to share detailed information about its construction, chemistry and emissions. For that reason the sustainability of the technology could not be assessed and compared to similar technologies.

Future work would include obtaining more detailed information regarding the LiC construction in addition to a life cycle assessment.

7 Conclusion

The requirement for storage technology is ever rising, especially due to the increasing implementation of IRES. This paper addressed the implementation of lithium-ion capacitors and its ability to optimize wind and solar power, with regards to power, voltage and frequency quality. The combination of LiC and LiB was further examined and the LiC's impact on several systems was analysed.

The simulations in case 1 and 2, which emphasised the impact a LiC has on a fluctuating power profile, resulted in a beneficial power characteristic. For both wind and solar power, the power output was a lot more stable constituting an improved power quality. This resulted in that, if dimensioned properly, the LiC could reach a sustainable lifetime in both cases while still performing adequately. Furthermore, this can lead to a higher possible penetration of IRES and an overall reduction in CO₂ emissions. From the simulations it is evident that the LiC, both regarding economical aspects and sustainability, is a viable solution.

In case 3 the aspects of a LiC in combination with a LiB for energy shifting was investigated. The results portrayed that the LiC induced a longer lifetime in the LiB by presenting a more beneficial charge and discharge characteristic. A prolonged lifetime insinuates that the batteries does not have to be replaced as often, leading to a more sustainable storage system. The energy was utilized in a better manner and set to match the consumption in order to eliminate several inconveniences with IRES. However the increase in the LiB's lifetime was a lot smaller than what was desired. For that reason the benefits of the LiC integration in this case did not outweigh the associated investment cost.

Although the production, transport and installation of Beyonder's LiC all have associated emissions, the technology has many environmental benefits compared to its competitors. The LiC is made using ecological materials and excludes the use of heavy metals. Additionally, the energy-intensive production process is supported by a Norwegian power mix, consisting mostly of hydropower. All things considered Beyonder has created an eco-friendly and energy efficient technology.

As a result of the current electrification of the society, and the climate crisis the world is facing, there is a desperate need of technologies that can utilize the produced electricity as efficiently as possible. Implementing a LiC-system will contribute to exploit more of the available wind and solar power, while at the same time facilitate a higher IRES penetration. In this regard the LiC technology can be a great contributor to reach the all-embracing climate goals.

References

- [1] Hannah Ritchie and Max Roser. “CO and Greenhouse Gas Emissions”. In: *Our World in Data* (May 2020). URL: <https://ourworldindata.org/co2-and-other-greenhouse-gas-emissions> (visited on 01/20/2022).
- [2] — *SDG Indicators*. URL: https://unstats.un.org/sdgs/report/2021/?fbclid=IwAR20q45I328r1H_9gi0eX5FRPVTs81-alSMJ1Hq0IeCxCHoYnz_992edbak (visited on 01/20/2022).
- [3] DNV. *Energy transition outlook 2021*. file:///Users/eliene/Downloads/DNV_ETO_2021_Main_Report%20(1).pdf. 2021.
- [4] *Personal communication with Beyonder*.
- [5] S.M. Lambert et al. “Comparison of supercapacitor and lithium-ion capacitor technologies for power electronics applications”. In: *5th IET International Conference on Power Electronics, Machines and Drives (PEMD 2010)*. Apr. 2010, pp. 1–5. DOI: 10.1049/cp.2010.0115.
- [6] *Why is energy consumption increasing?* en-GB. URL: <https://www.internetgeography.net/home-2/> (visited on 01/19/2022).
- [7] *Surging electricity demand is putting power systems under strain around the world - News*. en-GB. URL: <https://www.iea.org/news/surging-electricity-demand-is-putting-power-systems-under-strain-around-the-world> (visited on 01/19/2022).
- [8] *Causes of Climate Change*. en. URL: https://www.wwf.org.nz/what_we_do/climateaction/causes_of_climate_change/ (visited on 01/19/2022).
- [9] Martin. *Climate Change*. en-US. URL: <https://www.un.org/sustainabledevelopment/climate-change/> (visited on 01/19/2022).
- [10] *Energy Transition Outlook 2017*. en. URL: <https://eto.dnv.com/2017> (visited on 05/06/2022).
- [11] DNV. *Pathway to net zero emissions, Energy Transition Outlook 2021*. *DNV_pathway_to_net_zero_2021_single_highres.pdf*. 2021.
- [12] Goran Mandic et al. “Lithium-Ion Capacitor Energy Storage Integrated With Variable Speed Wind Turbines for Power Smoothing”. In: *IEEE Journal of Emerging and Selected Topics in Power Electronics* 1.4 (Dec. 2013). Conference Name: IEEE Journal of Emerging and Selected Topics in Power Electronics, pp. 287–295. ISSN: 2168-6785. DOI: 10.1109/JESTPE.2013.2284356.
- [13] simionauc. *Battery storage: The answer to renewable energy intermittency*. en. Apr. 2018. URL: <https://auclimate.wordpress.com/2018/04/17/battery-storage-the-answer-to-renewable-energy-intermittency/> (visited on 05/01/2022).
- [14] *We want to meet the global need for eco-friendly energy storage solutions for industrial use*. en-US. URL: <https://www.beyonder.no/markets> (visited on 05/02/2022).
- [15] *Trenger raskere utbygging av strømmettet*. no. URL: <https://www.energinorge.no/nyheter/2021/trenger-raskere-utbygging-av-stromnett/> (visited on 02/17/2022).
- [16] *Ruster opp kraftnettet for milliarder: – Et historisk høyt nivå*. nb. URL: <https://e24.no/i/gPm10B> (visited on 02/17/2022).

- [17] T R Ayodele et al. “Challenges of Grid Integration of Wind Power on Power System Grid Integrity: A Review”. en. In: (2012), p. 9.
- [18] *KILE – kvalitetsjusterte inntektsrammer ved ikke-levert energi - NVE*. URL: <https://www.nve.no/reguleringsmyndigheten/regulering/nettvirksomhet/okonomisk-regulering-av-nettselskap/om-den-okonomiske-reguleringen/kile-kvalitetsjusterte-inntektsrammer-ved-ikke-levert-energi/> (visited on 02/18/2022).
- [19] *Hva er NorFlex? | NorFlex-prosjektet | Fornyelse | Vår virksomhet*. no. URL: <https://www.ae.no/var-virksomhet/fornyelse/norflex-prosjektet2/hva-er-norflex/> (visited on 05/06/2022).
- [20] *Personal communication with Lista renewable energy park*.
- [21] *Power BI*. URL: <https://app.powerbi.com/home?fbclid=IwAR0xjmluJeyyxIafq6iq-ZstFYCh172As3XD5HT13B2aGP1GoRTbo88n8vI> (visited on 05/01/2022).
- [22] Natural Resources Canada. *High-Resolution Solar Radiation Datasets*. eng. Last Modified: 2020-02-18 Publisher: Natural Resources Canada. Apr. 2016. URL: <https://www.nrcan.gc.ca/energy/renewable-electricity/solar-photovoltaic/18409> (visited on 04/25/2022).
- [23] *The electricity grid*. en. URL: <https://energifaktanorge.no/en/norsk-energiforsyning/kraftnett/> (visited on 02/18/2022).
- [24] *Security of electricity supply*. en. URL: <https://energifaktanorge.no/en/norsk-energiforsyning/forsyningsikkerhet/> (visited on 02/18/2022).
- [25] *Grid-Connected Renewable Energy Systems*. en. URL: <https://www.energy.gov/energysaver/grid-connected-renewable-energy-systems> (visited on 04/25/2022).
- [26] NVE. *Opprustning av kraftnettet for å redusere energitapet*. https://publikasjoner.nve.no/rapport/2004/rapport2004_01.pdf. 2004.
- [27] *A modern and digital power supply system*. en. URL: <https://energifaktanorge.no/en/norsk-energibruk/ny-teknologi-i-kraftsystemet/> (visited on 02/18/2022).
- [28] *Introduction to Power Quality - ScienceDirect*. URL: <https://www.sciencedirect.com/science/article/pii/B9780128007822000014?via%3Dihub> (visited on 04/25/2022).
- [29] *Håndbok spenningskvalitet*. no. URL: <https://www.sintef.no/ekspertise/sintef-energi/spenningskvalitet2/handbok-spenningkvalitet/> (visited on 02/18/2022).
- [30] *Distributed Generation - ScienceDirect*. URL: <https://www.sciencedirect.com/science/article/pii/B9780128032169000080?via%3Dihub> (visited on 04/25/2022).
- [31] *Frequency Control in a Power System - Technical Articles*. en. URL: <https://eepower.com/technical-articles/frequency-control-in-a-power-system/> (visited on 02/18/2022).
- [32] *Tertiary Control - an overview | ScienceDirect Topics*. URL: <https://www.sciencedirect.com/topics/engineering/tertiary-control> (visited on 02/18/2022).
- [33] Bruce Dunn, Haresh Kamath, and Jean-Marie Tarascon. “Electrical Energy Storage for the Grid: A Battery of Choices”. EN. In: *Science* (Nov. 2011). Publisher: American Association for the Advancement of Science. DOI: 10.1126/science.1212741. URL: <https://www.science.org/doi/abs/10.1126/science.1212741> (visited on 02/02/2022).

- [34] Anurag Chauhan and R. P. Saini. “A review on Integrated Renewable Energy System based power generation for stand-alone applications: Configurations, storage options, sizing methodologies and control”. en. In: *Renewable and Sustainable Energy Reviews* 38 (Oct. 2014), pp. 99–120. ISSN: 1364-0321. DOI: 10.1016/j.rser.2014.05.079. URL: <https://www.sciencedirect.com/science/article/pii/S1364032114004043> (visited on 02/02/2022).
- [35] Naoki Nitta et al. “Li-ion battery materials: present and future”. en. In: *Materials Today* 18.5 (June 2015), pp. 252–264. ISSN: 1369-7021. DOI: 10.1016/j.mattod.2014.10.040. URL: <https://www.sciencedirect.com/science/article/pii/S1369702114004118> (visited on 02/02/2022).
- [36] Li Li Zhang and X. S. Zhao. “Carbon-based materials as supercapacitor electrodes”. en. In: *Chemical Society Reviews* 38.9 (Aug. 2009). Publisher: The Royal Society of Chemistry, pp. 2520–2531. ISSN: 1460-4744. DOI: 10.1039/B813846J. URL: <https://pubs.rsc.org/en/content/articlelanding/2009/cs/b813846j> (visited on 02/18/2022).
- [37] Ajay Jagadale et al. “Lithium ion capacitors (LICs): Development of the materials”. en. In: *Energy Storage Materials* 19 (May 2019), pp. 314–329. ISSN: 2405-8297. DOI: 10.1016/j.ensm.2019.02.031. URL: <https://www.sciencedirect.com/science/article/pii/S2405829718315174> (visited on 02/02/2022).
- [38] Mahdi Soltani and S. Hamidreza Beheshti. “A comprehensive review of lithium ion capacitor: development, modelling, thermal management and applications”. en. In: *Journal of Energy Storage* 34 (Feb. 2021), p. 102019. ISSN: 2352-152X. DOI: 10.1016/j.est.2020.102019. URL: <https://www.sciencedirect.com/science/article/pii/S2352152X20318545> (visited on 02/02/2022).
- [39] Jin Zhang et al. “Different types of pre-lithiated hard carbon as negative electrode material for lithium-ion capacitors”. en. In: *Electrochimica Acta* 187 (Jan. 2016), pp. 134–142. ISSN: 0013-4686. DOI: 10.1016/j.electacta.2015.11.055. URL: <https://www.sciencedirect.com/science/article/pii/S001346861530829X> (visited on 02/02/2022).
- [40] *Review of Hybrid Ion Capacitors: From Aqueous to Lithium to Sodium | Chemical Reviews*. URL: <https://pubs.acs.org/doi/10.1021/acs.chemrev.8b00116> (visited on 02/02/2022).
- [41] Rajesh Kumar et al. “Recent progress in the synthesis of graphene and derived materials for next generation electrodes of high performance lithium ion batteries”. en. In: *Progress in Energy and Combustion Science* 75 (Nov. 2019), p. 100786. ISSN: 0360-1285. DOI: 10.1016/j.pecs.2019.100786. URL: <https://www.sciencedirect.com/science/article/pii/S0360128519300619> (visited on 02/02/2022).
- [42] Rajesh Kumar et al. “A review on synthesis of graphene, h-BN and MoS2 for energy storage applications: Recent progress and perspectives”. en. In: *Nano Research* 12.11 (Nov. 2019), pp. 2655–2694. ISSN: 1998-0000. DOI: 10.1007/s12274-019-2467-8. URL: <https://doi.org/10.1007/s12274-019-2467-8> (visited on 02/02/2022).
- [43] *Graphene-Based Materials for Lithium-Ion Hybrid Supercapacitors - Ma - 2015 - Advanced Materials - Wiley Online Library*. URL: <https://onlinelibrary.wiley.com/doi/10.1002/adma.201501622> (visited on 02/02/2022).

- [44] Jae-Hun Kim et al. “Effect of carbon types on the electrochemical properties of negative electrodes for Li-ion capacitors”. en. In: *Journal of Power Sources* 196.23 (Dec. 2011), pp. 10490–10495. ISSN: 0378-7753. DOI: 10.1016/j.jpowsour.2011.08.081. URL: <https://www.sciencedirect.com/science/article/pii/S0378775311016272> (visited on 04/26/2022).
- [45] Seong Jin An et al. “The state of understanding of the lithium-ion-battery graphite solid electrolyte interphase (SEI) and its relationship to formation cycling”. en. In: *Carbon* 105 (Aug. 2016), pp. 52–76. ISSN: 0008-6223. DOI: 10.1016/j.carbon.2016.04.008. URL: <https://www.sciencedirect.com/science/article/pii/S0008622316302676> (visited on 02/02/2022).
- [46] Ya-Bin An et al. “Improving anode performances of lithium-ion capacitors employing carbon–Si composites”. en. In: *Rare Metals* 38.12 (Dec. 2019), pp. 1113–1123. ISSN: 1867-7185. DOI: 10.1007/s12598-019-01328-w. URL: <https://doi.org/10.1007/s12598-019-01328-w> (visited on 02/21/2022).
- [47] Y. Firouz et al. “Lithium-ion capacitor – Characterization and development of new electrical model”. en. In: *Energy* 83.C (2015). Publisher: Elsevier, pp. 597–613. URL: <https://ideas.repec.org/a/eee/energy/v83y2015icp597-613.html> (visited on 02/21/2022).
- [48] *Advanced electrolyte/additive for lithium-ion batteries with silicon anode - ScienceDirect*. URL: <https://www.sciencedirect.com/science/article/abs/pii/S2211339816300454?via%3Dihub> (visited on 02/21/2022).
- [49] Xianzhong Sun et al. “Electrochemical performances and capacity fading behaviors of activated carbon/hard carbon lithium ion capacitor”. en. In: *Electrochimica Acta* 235 (May 2017), pp. 158–166. ISSN: 0013-4686. DOI: 10.1016/j.electacta.2017.03.110. URL: <https://www.sciencedirect.com/science/article/pii/S001346861730590X> (visited on 02/22/2022).
- [50] W. J. Cao et al. “Development and characterization of Li-ion capacitor pouch cells”. en. In: *Journal of Power Sources* 257 (July 2014), pp. 388–393. ISSN: 0378-7753. DOI: 10.1016/j.jpowsour.2014.01.087. URL: <https://www.sciencedirect.com/science/article/pii/S0378775314001116> (visited on 02/22/2022).
- [51] Mahdi Soltani, Jan Ronsmans, and Joeri Van Mierlo. “Cycle life and calendar life model for lithium-ion capacitor technology in a wide temperature range”. en. In: *Journal of Energy Storage* 31 (Oct. 2020), p. 101659. ISSN: 2352-152X. DOI: 10.1016/j.est.2020.101659. URL: <https://www.sciencedirect.com/science/article/pii/S2352152X20314961> (visited on 03/28/2022).
- [52] Jonathan M. Larson et al. “Pascalammety with operando microbattery probes: Sensing high stress in solid-state batteries”. en. In: *Science Advances* 4.6 (June 2018), eaas8927. ISSN: 2375-2548. DOI: 10.1126/sciadv.aas8927. URL: <https://www.science.org/doi/10.1126/sciadv.aas8927> (visited on 04/26/2022).
- [53] *Causes of supercapacitors ageing in organic electrolyte - ScienceDirect*. URL: <https://www.sciencedirect.com/science/article/abs/pii/S0378775307014760?via%3Dihub> (visited on 02/22/2022).

- [54] *Lithium iron phosphate battery*. en. Page Version ID: 1072821184. Feb. 2022. URL: https://en.wikipedia.org/w/index.php?title=Lithium_iron_phosphate_battery&oldid=1072821184 (visited on 02/22/2022).
- [55] *Benefits of Lithium Iron Phosphate batteries (LiFePO₄)*. URL: <https://www.superb.com/en/lithium-iron-phosphate-batteries/benefits-lithium-batteries> (visited on 02/22/2022).
- [56] *NMC Battery Material for Li-ion Cells (LiNiMnCoO₂)*. en-US. URL: <https://www.targray.com/li-ion-battery/cathode-materials/nmc> (visited on 02/22/2022).
- [57] *BU-205: Types of Lithium-ion*. en. Sept. 2010. URL: <https://batteryuniversity.com/article/bu-205-types-of-lithium-ion> (visited on 02/22/2022).
- [58] *Nickel Manganese Cobalt Battery vs. Lithium Ion-Difference and Replacement_ Greenway battery | E-BIKE Battery-Custom Lithium Battery Pack*. URL: <https://m.greenway-battery.com/news/Nickel-Manganese-Cobalt-Battery-vs.-Lithium-Ion-Difference-and-Replacement-263.html> (visited on 02/22/2022).
- [59] *Lithium Titanate (LTO) Cells - Technical Advantages | shop.GWL.eu*. URL: <https://shop.gwl.eu/LTO-Tech/> (visited on 04/28/2022).
- [60] *BU-209: How does a Supercapacitor Work?* en. Sept. 2010. URL: <https://batteryuniversity.com/article/bu-209-how-does-a-supercapacitor-work> (visited on 02/22/2022).
- [61] Erika Granath. *Supercapacitor: Workings and applications*. en. URL: <https://www.power-and-beyond.com/supercapacitor-workings-and-applications-a-922367/> (visited on 02/22/2022).
- [62] *Power quality improvement in grid connected wind energy system using STATCOM | IEEE Conference Publication | IEEE Xplore*. URL: https://ieeexplore.ieee.org/abstract/document/6203878?casa_token=Aq4Y8YF0cwYAAAAA:lWNOBT4GKw2gkb1J-EYS5FZP9r1FTe8CPdFa-ysqfVLtsLL_RVy7Kf0GaVKvqJvpNN-kVJ90IA&fbclid=IwAR0_1ePQmiMCB3va0-Uq8AEgDVSPijIoo8EvUzR55p6ebZJq0LfHkHYa3no (visited on 02/22/2022).
- [63] *STATCOM | Hitachi Energy*. en. URL: <https://www.hitachienergy.com/offering/product-and-system/facts/statcom> (visited on 02/22/2022).
- [64] *Static Synchronous Compensator (STATCOM) - ENTSO-E*. URL: <https://www.entsoe.eu/Technopedia/techsheets/static-synchronous-compensator-statcom> (visited on 02/22/2022).
- [65] LICAP Industries. *Lithium Ion Capacitors*. 2021.
- [66] LÍgia da Silva Lima et al. "Life cycle assessment of lithium-ion batteries and vanadium redox flow batteries-based renewable energy storage systems". en. In: *Sustainable Energy Technologies and Assessments* 46 (Aug. 2021), p. 101286. ISSN: 2213-1388. DOI: 10.1016/j.seta.2021.101286. URL: <https://www.sciencedirect.com/science/article/pii/S2213138821002964> (visited on 05/09/2022).
- [67] LICAP. *LICAP Ultra Capacitor*. en. URL: https://assets.website-files.com/5dc8ead8c19d433eb7097216/60862a9f081981828ace417f_LICAP_SC0370-270-RSS-Datasheet_102120.pdf (visited on 04/28/2022).


- [68] Beyonder AS. *Datasheet Gen 3*. <https://beyonderas.sharepoint.com/:b:/r/sites/NTNUBachelorGroup2-BESSforWind/Shared%20Documents/General/Dokumenter%20fra%20Beyonder/Datasheet%20Gen%203.pdf?csf=1&web=1&e=MlIIwe>. 2021.
- [69] *Battery Pack Prices Fall to an Average of \$132/kWh, But Rising Commodity Prices Start to Bite*. en-US. Section: Press Release. Nov. 2021. URL: <https://about.bnef.com/blog/battery-pack-prices-fall-to-an-average-of-132-kwh-but-rising-commodity-prices-start-to-bite/> (visited on 04/20/2022).
- [70] *Fig. 1. A comparison between main lithium ion battery chemistries 4*. en. URL: https://www.researchgate.net/figure/A-comparison-between-main-lithium-ion-battery-chemistries-4_fig1_273257298 (visited on 03/29/2022).
- [71] *Understanding a Lithium-ion cell datasheet • EVreporter*. URL: <https://evreporter.com/understanding-a-lithium-ion-cell-datasheet/> (visited on 04/26/2022).
- [72] *E66A*. en-US. URL: <https://www.batemo.de/products/batemo-cell-library/e66a/> (visited on 04/26/2022).
- [73] Burcu Gundogdu and Daniel Thomas Gladwin. “A Fast Battery Cycle Counting Method for Grid-Tied Battery Energy Storage System Subjected to Microcycles”. In: *2018 International Electrical Engineering Congress (iEECON)*. Mar. 2018, pp. 1–4. DOI: 10.1109/IEECON.2018.8712263.
- [74] Nicholas Etherden and Math H. J. Bollen. “Dimensioning of Energy Storage for Increased Integration of Wind Power”. In: *IEEE Transactions on Sustainable Energy* 4.3 (July 2013). Conference Name: IEEE Transactions on Sustainable Energy, pp. 546–553. ISSN: 1949-3037. DOI: 10.1109/TSTE.2012.2228244.
- [75] *Investment costs*. URL: <https://www.wind-energy-the-facts.org/index-43.html> (visited on 04/25/2022).
- [76] *What is a solar farm? Costs, land needs & more*. en. URL: <https://www.solarreviews.com/content/blog/what-is-a-solar-farm-do-i-need-one> (visited on 04/25/2022).
- [77] *Technology*. en-US. URL: <https://www.beyonder.no/technology> (visited on 01/27/2022).
- [78] *Recycling and reactivation of activated carbon | Desotec*. URL: <https://www.desotec.com/en/solutions/recycling-and-reativation-activated-carbon> (visited on 02/22/2022).
- [79] Hans Eric Melin. “Analysis of the climate impact of lithium-ion batteries and how to measure it”. en. In: (), p. 17.
- [80] Mathias Klingenberg. *Den svenske monsterfabrikken skal produsere verdens grønneste batterier*. no. May 2020. URL: <https://www.tu.no/artikler/den-svenske-monsterfabrikken-skal-produsere-verdens-gronneste-batterier/490502> (visited on 02/22/2022).
- [81] *Kraftproduksjon*. nb. URL: <https://energifaktanorge.no/norsk-energiforsyning/kraftforsyningen/> (visited on 02/22/2022).
- [82] *Live-data: Strøm og CO2 | Kart: Kraftproduksjon og CO2-utslipp*. URL: https://energiogklima.no/klimavakten/live-data-strom-og-co2/?fbclid=IwAR0d8iADSe7VgMZ9HZCMkVWkpkqCmpeVTx_VKdkA7bDoti2vnjqTnZehnM0 (visited on 02/22/2022).

Appendix


A Data from Beyonder

A.1 Datasheet LiC Gen. 3


BEYONDER™




**High power,
moderate energy**




**No cobalt, nickel
or other heavy
metals**



**Fast charge &
discharge time,
~ 2 min**



**Based on sustainable
forestry residue**



**Rechargeable up
to 100 000 times**

SPECIFICATIONS

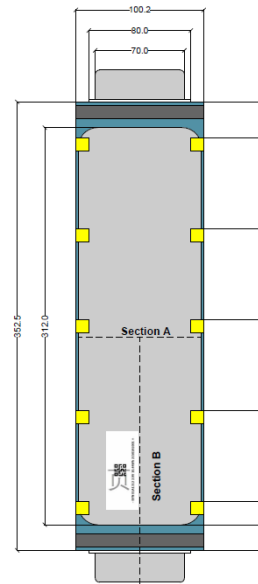
C-rate	Continuous	
Capacitance	Rated, C *	11000F
	Tolerance	0-20%
Voltage	Rated minimum (V _r) – Rated maximum (V _s)	2.00-4.00 V
	Maximum voltage (not repeated -and for no longer than 1 second)	4.20 V
ESR DC	Typical *	0.4 mΩ
Current	Maximum peak (1 second)	350A
	Volumetric energy density, E _v *	160 Wh/L
Energy	Gravimetric specific energy, E _m *	80 Wh/kg
	Stored energy, E *	35 Wh
	Power density, P _v **	10 kW/L
Power	Specific power, P _m **	10 kW/kg

CHARACTERISTICS AND SERVICE LIFETIME

Lifespan (hours at rated voltage and maximum operating temperature)	Projected life span (storage time)	15 years
	Projected cycle stability (cycles) **	100 000
	Floating performance **	>2000
	Self-discharge (voltage reduction by 5% at 5°C)	3 months

FUNCTIONALITIES, SAFETY AND STANDARDS

Temperature	Ambient, operational	-20 - 40 °C
	Storage (discharged condition) range	-40 - 70 °C
Standards and certifications	*IEC 62391-1, ** IEC 62391-2, UN-3508	



DIMENSIONS

Dimensions	LxWxD	352.50x100.20x6.85mm
	Tabs (Al)	23.25x70.00x0.50mm
	(Ni)	23.25x70.00x0.30mm
	Volume	0.214L
Weight		0.426kg

The information herein is solely provided for reference only and is subject to modification without notice.

@ post@beyonder.no

www.beyonder.no

Stokkamyrveien 30, 4313 Sandnes

© Beyonder 2021

Company number: 917 015 961

A.2 Excel spreadsheet for connecting cells

Cell parameter						LIC_cell_data			
OCV	R_int	R_1	R_2	C_1	C_2	Byonder 2.G cell			
2	2.68E-04	2.68E-04	2.68E-04	200	200	LIC_rack_Capcity	0.032	Kwh	
2.3121	2.68E-04	2.68E-04	2.68E-04	190	190	LIC_max_Voltage	3.8	VDC	
2.4842	2.68E-04	2.68E-04	2.68E-04	180	180	LIC_min_Voltage	2.2	VDC	
2.6671	2.68E-04	2.68E-04	2.68E-04	170	170	LIC_Nom_Voltage	3	VDC	
2.8673	2.68E-04	2.68E-04	2.68E-04	160	160				
3.1066	2.68E-04	2.68E-04	2.68E-04	150	150				
3.3059	2.68E-04	2.68E-04	2.68E-04	140	140				
3.4655	2.68E-04	2.68E-04	2.68E-04	130	130				
3.6116	2.68E-04	2.68E-04	2.68E-04	120	120				
3.81	2.68E-04	2.68E-04	2.68E-04	110	110				
4	2.68E-04	2.68E-04	2.68E-04	100	100				
Module						LIC_Module_data			
OCV	R_int	R_1	R_2	C_1	C_2	12	S	4	P
24.0	0.001	0.001	0.001	66.7	66.7	Capcity	1.5	Kwh	
27.7	0.001	0.001	0.001	63.3	63.3	Max_Voltage	45.6	VDC	
29.8	0.001	0.001	0.001	60.0	60.0	Min_Voltage	26.4	VDC	
32.0	0.001	0.001	0.001	56.7	56.7	Nom_Voltage	36	VDC	
34.4	0.001	0.001	0.001	53.3	53.3				
37.3	0.001	0.001	0.001	50.0	50.0				
39.7	0.001	0.001	0.001	46.7	46.7				
41.6	0.001	0.001	0.001	43.3	43.3				
43.3	0.001	0.001	0.001	40.0	40.0				
45.7	0.001	0.001	0.001	36.7	36.7				
48.0	0.001	0.001	0.001	33.3	33.3				
Rack						LIC_Rack_data			
OCV	R_int	R_1	R_2	C_1	C_2	22	S	1	P
528.0	0.0177	0.0177	0.0177	3.0	3.0	Capcity	33.8	Kwh	
610.4	0.0177	0.0177	0.0177	2.9	2.9	Max_Voltage	1003.2	VDC	
655.8	0.0177	0.0177	0.0177	2.7	2.7	Min_Voltage	580.8	VDC	
704.1	0.0177	0.0177	0.0177	2.6	2.6	Nom_Voltage	792	VDC	
757.0	0.0177	0.0177	0.0177	2.4	2.4				
820.1	0.0177	0.0177	0.0177	2.3	2.3				
872.8	0.0177	0.0177	0.0177	2.1	2.1				
914.9	0.0177	0.0177	0.0177	2.0	2.0				
953.5	0.0177	0.0177	0.0177	1.8	1.8				
1005.8	0.0177	0.0177	0.0177	1.7	1.7				
1056.0	0.0177	0.0177	0.0177	1.5	1.5				
Pack						LIC_pack_data			
OCV	R_int	R_1	R_2	C_1	C_2	1	S	14	P
528.0	0.0013	0.0013	0.0013	42.4	42.4	Capcity	0.47	Mwh	
610.4	0.0013	0.0013	0.0013	40.3	40.3	Max_Voltage	1003.2	VDC	
655.8	0.0013	0.0013	0.0013	38.2	38.2	Min_Voltage	580.8	VDC	
704.1	0.0013	0.0013	0.0013	36.1	36.1	Nom_Voltage	792	VDC	
757.0	0.0013	0.0013	0.0013	33.9	33.9				
820.1	0.0013	0.0013	0.0013	31.8	31.8				
872.8	0.0013	0.0013	0.0013	29.7	29.7				
914.9	0.0013	0.0013	0.0013	27.6	27.6				
953.5	0.0013	0.0013	0.0013	25.5	25.5				
1005.8	0.0013	0.0013	0.0013	23.3	23.3				
1056.0	0.0013	0.0013	0.0013	21.2	21.2				

A.3 Excel spreadsheet for connecting cells w/ functions

	A	B	G	H	I	J
1	Cell parameter		LIC_cell_data			
2	OCV	R int	Byonder 2.G cell			
3	2	0.0002681	LIC_rack_Capcity	0.032		Kwh
4	2.3121	0.0002681	LIC_max_Voltage	3.8		VDC
5	2.4842	0.0002681	LIC_min_Voltage	2.2		VDC
6	2.6671	0.0002681	LIC_Nom_Voltage	3		VDC
7	2.8673	0.0002681				
8	3.1066	0.0002681				
9	3.3059	0.0002681				
10	3.4655	0.0002681				
11	3.6116	0.0002681				
12	3.81	0.0002681				
13	4	0.0002681				
14	Module		LIC_Module_data			
15	OCV	R int	230	S	1	P
16	=A3*G\$15	=(B3*G\$15)/I\$15	Capacity	=I15*I3*G15		Kwh
17	=A4*G\$15	=(B4*G\$15)/I\$15	Max_Voltage	=AVRUND.OPP		VDC
18	=A5*G\$15	=(B5*G\$15)/I\$15	Min_Voltage	=G15*I5		VDC
19	=A6*G\$15	=(B6*G\$15)/I\$15	Nom_Voltage	=G15*I6		VDC
20	=A7*G\$15	=(B7*G\$15)/I\$15				
21	=A8*G\$15	=(B8*G\$15)/I\$15				
22	=A9*G\$15	=(B9*G\$15)/I\$15				
23	=A10*G\$15	=(B10*G\$15)/I\$15				
24	=A11*G\$15	=(B11*G\$15)/I\$15				
25	=A12*G\$15	=(B12*G\$15)/I\$15				
26	=A13*G\$15	=(B13*G\$15)/I\$15				
27	Rack		LIC_Rack_data			
28	OCV	R int	1	S	80	P
29	=A16*G\$28	=(B16*G\$28)/I\$28	Capacity	=I28*I16*G28		Kwh
30	=A17*G\$28	=(B17*G\$28)/I\$28	Max_Voltage	=I17*G28		VDC
31	=A18*G\$28	=(B18*G\$28)/I\$28	Min_Voltage	=I18*G28		VDC
32	=A19*G\$28	=(B19*G\$28)/I\$28	Nom_Voltage	=I19*G28		VDC
33	=A20*G\$28	=(B20*G\$28)/I\$28				
34	=A21*G\$28	=(B21*G\$28)/I\$28				
35	=A22*G\$28	=(B22*G\$28)/I\$28				
36	=A23*G\$28	=(B23*G\$28)/I\$28				
37	=A24*G\$28	=(B24*G\$28)/I\$28				
38	=A25*G\$28	=(B25*G\$28)/I\$28				
39	=A26*G\$28	=(B26*G\$28)/I\$28				
40	Pack		LIC_pack_data			
41	OCV	R int	1	S	3	P
42	=A29*G\$41	=(B29*G\$41)/I\$41	Capacity	=I29*G41*I41		kwh
43	=A30*G\$41	=(B30*G\$41)/I\$41	Max_Voltage	=I30*G41		VDC
44	=A31*G\$41	=(B31*G\$41)/I\$41	Min_Voltage	=I31*G41		VDC
45	=A32*G\$41	=(B32*G\$41)/I\$41	Nom_Voltage	=I32*G41		VDC
46	=A33*G\$41	=(B33*G\$41)/I\$41				
47	=A34*G\$41	=(B34*G\$41)/I\$41				
48	=A35*G\$41	=(B35*G\$41)/I\$41				
49	=A36*G\$41	=(B36*G\$41)/I\$41				
50	=A37*G\$41	=(B37*G\$41)/I\$41				
51	=A38*G\$41	=(B38*G\$41)/I\$41				
52	=A39*G\$41	=(B39*G\$41)/I\$41				

B MATLAB Scripts

B.1 BESS-controller wind/solar power plant

```
function current = fcn(soc, p, avg)      %Input parameters for function

voltage = 690;                          %Defining parameters [V]
soc_min = 0.1;                          %Defining parameters [%]
soc_max = 1;                            %Defining parameters [%]

if (soc > soc_min) && (soc < soc_max)    %Soc is between allowed limits
    if p - avg                          %Charge
        current = ((p - avg)/voltage); %Magnitude of current to charge
    elseif avg - p                      %Discharge
        current = ((p - avg)/voltage); %Magnitude of current to discharge
    else                                %p = avg
        current = 0;                   %Do nothing
    end
elseif soc <= soc_min                  %Soc is below allowed limit
    if p - avg                          %Charge
        current = ((p - avg)/voltage); %Magnitude of current to charge
    else                                %p = avg or p < avg
        current = 0;                   %Do nothing
    end
else                                    %Soc = soc_max
    if avg - p                          %Discharge
        current = ((p - avg)/voltage); %Magnitude of current to discharge
    else                                %Soc < soc_max
        current = 0;                   %Do nothing
    end
end
end
```


B.3 Cycle counter

```
function cycle_tot = fcn(dsoc) %Input variable for function
global A; %Soc charge
global B; %Cycle charge
global C; %Soc change in charge
global D; %Cycle change in charge
if dsoc > 0; %Change in soc > 0
    up = dsoc; %Up = increase in soc
    A = A + up; %A increases
    if A > 1; %A > 1
        B = B + 1; %B increases
        A = 0; %A is set to zero
    else %A =< 1
        B = B; %B remains the same
    end
else %Change in soc =< 0
    down = - dsoc; %Down = decrease in soc
    C = C + down; %C decreases
    if C > 1; %C > 1
        D = D + 1; %D increases
        C = 0; %C is set to zero
    else %C =< 1
        D = D; %D remains the same
    end
end
cycle_tot = ((B + D)/2) + (A + C)/2; %Number of cycles is calculated
end
```


C.2 LiC integrated in energy shifting-system

